

Федеральное государственное автономное образовательное учреждение  
высшего образования «Уральский федеральный университет имени первого  
Президента России Б. Н. Ельцина»  
Химико-технологический институт  
Кафедра химической технологии топлива и промышленной экологии  
Кафедра органической и биомолекулярной химии  
Лаборатория перспективных материалов, зеленых методов и биотехнологий  
Научно-образовательного и инновационного центра химико-  
фармацевтических технологий

На правах рукописи

**Аль-Саммаррайи Иман Шакир Авад**

**ПОЛУЧЕНИЕ НОВЫХ ВИДОВ ПЛОСКИХ  
УЛЬТРАФИЛЬТРАЦИОННЫХ МЕМБРАН НА ОСНОВЕ  
ПОЛИВИНИЛХЛОРИДА И ЕГО  
МОДИФИЦИРОВАННЫХ СТРУКТУР**

2.6.10. Технология органических веществ

2.6.12. Химическая технология топлива и высокоэнергетических веществ

Диссертация на соискание учёной степени  
кандидата технических наук

Научные руководители:

Сабинова Тамара Михайловна, д.т.н. доцент

Зырянов Григорий Васильевич, д.х.н. профессор РАН

Екатеринбург – 2024

Federal state autonomous educational institution of higher education "Ural federal university named after the first President of Russia B.N. Yeltsin"

Institute of Chemical Technology

Department of Chemical Technology of Fuel and Industrial Ecology

Department of Organic and Biomolecular Chemistry

Laboratory of Advanced Materials, Green Methods and Biotechnologies  
Scientific, Educational and Innovation Center for Chemical and Pharmaceutical  
Technologies

*As a manuscript*

**Al-Sammarraie Eman Shakir Awad**

**PREPARATION OF NEW TYPES OF FLAT ULTRAFILTRATION  
MEMBRANES BASED ON POLYVINYL CHLORIDE AND  
ITS MODIFIED STRUCTURES**

2.6.10. Technology of organic compounds

2.6.12. Chemical technology of fuels and high-energy substances

Dissertation for the degree of Ph. Candidate of Technical Sciences

Academic Supervisors:

Sabirova Tamara Mikhailovna, Doctor of  
Technical Sciences, professor

Zyryanov Grigory Vasilyevich, Doctor of  
Chemical Sciences, professor of the RAS

Ekaterinburg – 2024

## CONTENT

<b>INTRODUCTION.....</b>	<b>5</b>
<b>Chapter 1. Literature review of Methods for the modification of PVC and the preparation of PVC-based membranes.....</b>	<b>13</b>
1.1 Polyvinylchloride (PVC) .....	13
1.2 Nucleophilic substitution reactions.....	13
1.3 Functionalization of PVC by PVC-C coupling by alkylation.....	15
1.3.1 General provisions.....	15
1.3.2 Cross-combination reactions of polyvinyl chloride .....	16
1.4 PVC-N bond functionalization .....	17
1.4.1 Heterocyclic functionalization of polyvinyl chloride.....	17
1.4.2 Azidation of polyvinyl chloride .....	19
1.5 PVC-S bond functionalization .....	19
1.6 PVC-O bond functionalization .....	21
1.7 Prospects of mechanochemical approaches to PVC modification.....	24
1.8 Application of Modified PVC.....	25
1.9 Membrane techniques .....	29
1.9.1 Membrane Filtration Types.....	29
1.9.2 Configurations and Operations of Membranes .....	30
1.9.3 Materials and Properties of Membranes.....	31
1.9.4 Preparation and Synthesis of Membranes .....	33
1.9.5 Membrane in carwash wastewater .....	33
1.9.6 Review of membrane techniques in carwash sector (Commercial and modified membrane techniques) .....	37
Conclusion to chapter 1 .....	40
<b>Chapter 2. Experimental Studies of The Synthesis of Functionalized PVC Derivatives ..</b>	<b>42</b>
2.1 Features of Post-Modification of Polymers .....	42
2.1 Laboratory support for experimental research.....	42
2.2 Description of Methods and Characteristics for Synthesis of PVC Derivatives Modified by N- and S- Nucleophiles .....	44
2.4 Investigation of the possibility of modification of PVC with fragments of N- and S-nucleophiles .....	45
2.4.1 The effect of ball grinding on the PVC structure .....	45
2.4.2 Study of PVC functionalization with N-nucleophile fragments .....	47
2.4.3 Study of the interaction of PVC with some O-nucleophiles .....	51
2.4.4 Study of PVC functionalization with S-nucleophile fragments.....	51
2.4.5 Results of analysis of post-modification PVC derivatives.....	57
Conclusion to the chapter 2.....	63
<b>Chapter 3. Investigation of the possibility of manufacturing UF membranes based on PVC and its modified structures.....</b>	<b>64</b>
3.1 Laboratory support for experimental research .....	64
3.2 Description of laboratory techniques for the manufacture of UF membranes based on PVC and its modified structures.....	67

3.3 Studying the Membrane Characterizations Measurements.....	72
3.4 Studying the Permeability and Rejection of CWW by Obtained UF Membranes .....	73
3.5 Results of the study of permeability and rejection of car wash WW by obtained membranes 74	
3.5.1 Membranes prepared from non-modified PVC.....	74
3.5.2 Membranes prepared from Post modified-PVC derivatives .....	76
3.5.3 Membranes prepared from PVC Modified with Silicon Dioxide NPs-SDS.....	77
Conclusions to chapter 3.....	78
<b>Chapter 4. Discussion of the Results.....</b>	<b>79</b>
4.1 Non-Modified PVC Membranes.....	79
4.1.1 The Morfology, Topology and other characteristics.....	79
4.1.2 PVC membranes performance evaluation for carwash treatment.....	84
4.2 Post- Modified PVC Derivatives Membranes .....	89
4.2.1 Characterizations and Performance Evaluation of PM PVC Membranes.....	89
4.3 Nanocomposite PVC Membranes.....	94
4.3.1 Characterizations of Nanocomposite Membranes.....	94
4.3.2 Membrane Performance Evaluation for Carwash Treatment.....	104
4.4 Discussion and Explanation of the Obtained Results of Experimental Studies Based on the Data Analysis of the Prepared Membranes.....	110
4.5 Investigation and Evaluation of Biodegradation of Pollutants from Car Washes Contained in The Retentate of Used UF Membranes.....	113
Conclusion to the chapter 4.....	114
<b>CONCLUSION.....</b>	<b>115</b>
<b>LIST OF ABBREVIATIONS AND CONVENTIONS .....</b>	<b>118</b>
<b>REFERENCES.....</b>	<b>121</b>
<b>APPENDIX (A).....</b>	<b>136</b>
<b>IR-Spectra for obtained post modified PVC derivatives.....</b>	<b>136</b>

## INTRODUCTION

**Relevance of the research topic.** In the context of the growth of the use of motor vehicles both in the industrial sector and for personal needs, the share of water and detergent consumption for their cleaning in various types of car washes is increasing. At present, the volume of wastewater (WW) generated by numerous car washes, characterized by the presence of a number of toxic pollutants (suspended solids; petroleum products in the form of oils, lubricants and energy fuels; detergents, etc.), has become comparable to the volume of wastewater generated by a large industrial enterprise in the city. Despite this, due attention is not paid to the completeness of their cleaning, which causes significant damage to the natural environment.

Taking into account the fact that modern technologies increasingly focus on the use of high-cost membrane methods, including those for wastewater treatment of various compositions, the development of new, economically feasible and environmentally friendly types of materials for the manufacture of effective ultrafiltration (UF) membranes is one of the urgent modern tasks.

Ultrafiltration (UF) is both one of the most important intermediate stages of water treatment of UF membranes for desalination (the pore size of UF membranes varies from 0.01 to 0.1  $\mu\text{m}$ ), and the main stage with sufficient purification of WW from particles and molecules of colloidal size. Of the well-known polymers, polyvinyl chloride (PVC) is of the greatest interest for research into the production of new modified structures—commercially available, cheap, resistant to acids, alkalis and oils, with a unique ability to accept and retain plasticizers of different chemical composition and molecular size material.

At present, low toxic forms of rigid (vinyl plastic) and flexible (plastic) PVC have been developed and used for the production of numerous PVC-based products. However, the high prevalence of biodegradable PVC creates a serious problem due to its accumulation in nature and the need to dispose of waste materials and products based on it. In recent years, the so-called "green methods" have become in demand in laboratory and industrial conditions, i.e. synthesis processes that consist in minimizing the number

of reaction steps, taking place at room temperature, in the absence of solvent and catalysts based on transition metals, etc. It has been proven that mechanosynthesis/mechanical grinding using a ball mill can serve as a method of modification, including chemical modification, of a wide range of materials. Including (co-)polymers and composites. For example, the effectiveness of such processes for changing the crystal structure and microtexture of polymers, increasing their mechanical properties, improving the compatibility of polymer mixtures, as well as for realizing the wide possibilities of chemical reactions of grafting was previously shown.

**The degree of development of the research topic.** The development and implementation of ultrafiltration began in the 80s of the twentieth century on the basis of the experience of manufacturing and using anisotropic reverse osmosis membranes from cellulose acetate, obtained by S. Loeb and S. Sourirayajan (USA). The methodological basis of the dissertation research in terms of modification and manufacture of UF polymer membranes by the phase-inversion method is the works widely known in world practice, including those carried out with the participation of Professor Qusay F. Alsalhy (Iraq). The method of mechanosynthesis of polymers, used in this work for post-polymerization functionalization (post-modification) of PVC, was developed in the works of academicians V.A. Kargin and N.A. Plate in the early 1960s. Abroad, the mechanosynthesis of polymers and composites based on them is carried out by research groups with the participation of professors S. Gratz and L. Borchard (Germany), J. G. Kim (Korea), and T. Fricsich (England).

**The subject of the study.** Commercial PVC polymers and UF membranes produced using post-modified and modified PVC structures.

**The object of the study.** Mechanosynthesis of post-modified (PM) derivatives based on PVC and *N*- and *S*-nucleophilic reagents; phase-inversion method of production: UF membranes based on PVC (vinyl plastic) and its structures modified with thiophenols and silicon dioxide nanoparticles.

**The aim of the dissertation.** The aim of the dissertation work is in the expansion of the range of available, cost-effective, effective and environmentally acceptable flat UF

membranes for cleaning WW of car washes containing oil products and suspended solids, due to the use of modified structures in the process of manufacturing PVC membranes.

**To achieve this goal, a set of the following theoretical, scientific, technical and experimental tasks was solved:**

1. Literature review:

- State, importance and development of membrane methods in world practice, including for cleaning WW of car washes;

- Materials, methods of manufacturing and modification of the structure of UF membranes to improve their performance characteristics with justification for the choice of the initial polymer material for experimental studies;

- Well-known methods of chemical post-modification of polymers, including PVC;

- Characteristics and properties of the main pollutants of car washes.

2. Experimental studies including:

- Study of the possibility of obtaining new PVC derivatives by its chemical modification with reagents of various nature under conditions of mechanosynthesis or other methods;

- Production of UF membranes by phase-inversion method based on commercial PVC, its post-modified derivatives and PVC modified with silicon dioxide nanoparticles.

3. Instrumental study of the composition and structure of new PVC derivatives obtained by mechanosynthesis. Selection of synthesized PVC polymer derivatives for the production of UF membranes.

4. Study, evaluation and comparison of structural, morphological and operational characteristics of new types of membranes, including the efficiency of cleaning WW of car washes from the main pollutants.

**Scientific novelty and theoretical significance:**

1. For the first time, chemical modification of PVC under conditions of mechanosynthesis was carried out.

2. With the help of  $^1\text{H}$  NMR and IR spectroscopy, as well as gel-penetrating chromatography (GPC), the possibility of chemical interaction of PVC with *N*- and *S*-

nucleophilic reagents under conditions of mechanochemistry - contact grinding of reagents in a ball mill was proved.

3. For the first time, new derivatives of PVC post-modified with fragments of *N*- and *S*-nucleophiles have been obtained, namely PVC modified with fragments of: azoloazines;  $\alpha$ -aminomethyl-phosphonates; Schiff bases and aza-triptycene.

4. For the first time, the method of wet molding (phase inversion) resulted in composite flat-sheet UF membranes based on PVC modified with 1) its functionalized derivatives and 2) silicon dioxide nanoparticles.

5. With the help of SEM and AFM, it has been proved that an increase in the concentration of PVC in the casting solution of membranes from 14 to 16 % leads to: a decrease in the size of macro voids and an increase in the thickness of membranes; reduction of their permeability and deterioration of antifouling properties of membranes used for cleaning WW of car washes.

6. It has been proved that the limiting factors influencing the structure and properties of UF membranes are the concentrations of commercial and modified PVC, as well as the dose of silicon dioxide nanoparticles additive in PVC casting solutions.

7. Using the SEM method and special calculations, it was established that the morphology of UF membranes (including differences in the form of finger-like structures, porosity and pore size) directly depends on the amount of modified silica nanoparticles (0.05, 0.1, 0.15, 0.2, 0.25 wt.%) which added to the casting solution for preparing UF membranes.

8. It has been proved that the addition of PVC casting solutions to its structures modified with three types of thiophenols (4-*tert*-octylthiophenol, 4-*tert*-butylthiophenol and thiophenol), as well as modified silicon dioxide nanoparticles, contributes to the improvement of their operational characteristics, which is expressed in an increase in the efficiency of retention of pollutants in car washes, including suspended solids and petroleum products, compared to PVC membranes without additives.

**The practical value of the work** lies in the development of relatively simple and effective technological methods for the production of PVC derivatives modified with



fragments of *N*- and *S*-nucleophiles under mechanosynthesis; in the production of new types of composite UF membranes made on the basis of PVC modified with its functionalized derivatives and silicon dioxide nanoparticles, effective for cleaning WW of car washes.

**The author's personal contribution** consisted in the search, analysis and systematization of literature data, taking into account the purpose and objectives of the work; in the formation of an analytical review of the literature on their basis; in the planning, implementation and description of experimental studies on the synthesis of new PVC derivatives, as well as in the manufacture of UF membranes; in the analysis of the qualitative composition of WW before and after purification in UF membranes; in the processing and discussion of the results of experiments; in the interpretation of the results of research on new structures of synthesized materials and UF membranes obtained using the necessary set of instrumental methods; preparing publications based on them, as well as presenting these results at conferences.

**The methodology and methods of the dissertation research** were as follows:

1) search and development of approaches to the chemical synthesis of new PVC derivatives containing *N*- and *S*-fragments, as well as other methods of PVC modification;

2) production of new types of UF membranes by phase-inversion: a) PVC; b) on the basis of chemically modified PVC derivatives obtained by mechanosynthesis; c) based on PVC modified with silicon dioxide nanoparticles;

3) in the application of the necessary set of instrumental and computational and analytical methods: to determine the composition of new PVC derivatives; to assess the structural and morphological characteristics of UF membranes and their effectiveness for cleaning the WW of car washes;

4) in the use of reagents that are commercially available or obtained using known or optimized techniques.

**The reliability and validity of the work** is ensured by: in terms of proving the structure and composition of the obtained new PVC derivatives – by the use of the necessary set of instrumental methods, namely:  $^1\text{H}$  NMR and IR-spectroscopy, elemental

analysis, gel-penetrating chromatography; in terms of obtaining UF membranes – by using methods of scanning electron microscopy (SEM), atomic force microscopy (AFM); Fourier transform infrared spectroscopy (FTIR); the use of methods from the state register of APHA to determine the content of typical impurities in the WW of car washes. The experimental part of the work was carried out using the equipment of the Department of Organic and Biomolecular Chemistry, the Department of Chemical Fuel Technology and Industrial Ecology, as well as the Scientific, Educational and Innovative Center for Chemical and Pharmaceutical Technologies (SE and ICCPT) of the Chemical Technology Institute (CTI) of the Ural Federal University. Instrumental studies were carried out in specialized laboratories based on the equipment of the Federal State Educational Institution of Higher Education "UrFU".

**The following provisions are submitted for defense:**

1. Substantiation of the choice of the starting material (PVC) for experimental studies of the production of new types of PVC and UF membrane derivatives on its basis.
2. Mechano-synthesis of new PVC derivatives modified with fragments of *N*- and *S*-nucleophiles. Results of instrumental determination of their structure and composition.
3. Production of new structures of UF membranes by wet molding (phase inversion): based on PVC; based on PVC modified with functionalized derivatives and silicon dioxide nanoparticles.
4. Results and Interpretation of Instrumental Study of Structural and Morphological Characteristics of UF Membranes Obtained. Evaluation parameters of UF membranes.
5. Results of an experimental study of the effectiveness of the obtained UF membranes for cleaning the WW of car washes from the main pollutants. Evaluation of the influence of membrane structure and morphology on the efficiency of WW purification.

**Approbation of the work.** The main results of this dissertation research are presented and discussed at the following Russian and international conferences: Sino-

Russian ASRTU Forum Ecology and Environmental Sciences (Yekaterinburg, 2020); the 9th Jordan International Chemical Engineering Conference (Aman, Jordan, 2021); IY All-Russian Scientific and Practical Conference with the Participation of Young Scientists "Current Trends in the Development of Chemical Technology, Industrial Ecology and Environmental Safety" (St. Petersburg, 2022); XVI International Scientific and Practical Conference SUEB (Yekaterinburg, 2022); International Scientific and Practical Conference "Fundamental and Applied Research in the Field of Chemistry and Ecology" (Kursk, 2023); XII International Scientific and Practical Conference "Current Aspects of the Development of Science and Society in the Era of Digital Transformation" (Moscow, 2023); LIX International Scientific and Practical Conference "Advances in Science and Technology" (Moscow, 2024); International Scientific and Practical Conference "Problems of Scientific and Practical Activity. Search and Selection of Innovative Solutions" (Yekaterinburg, 2024); VIII International Scientific and Practical Conference "BULATOV READINGS" (Krasnodar, 2024).

**Publications.** The main results of the dissertation work are presented in 12 publications, including 4 articles published in peer-reviewed scientific journals and publications determined by the Higher Attestation Commission of the Russian Federation and the Attestation Council of UrFU, and, among them, 3 articles are indexed in the international citation databases, such as Scopus.

**Structure and scope of work.** The dissertation work with a total volume of 140 pages consists of four main chapters, including an analytical review of the literature, an experimental part (2 chapters) and a discussion of the results; as well as a table of contents, introduction, conclusion, list of references and abbreviations and notations. The work contains 141 references to literary sources, 18 tables and 86 figures.

**Acknowledgments.** The author expresses his heartfelt gratitude and deepest gratitude for the scientific guidance and support to the supervisors of the dissertation work, Doctor of Technical Sciences, Professor T.M. Sabirova and Doctor of Chemical Sciences, Professor of the RAS G.V. Zyryanov, to Professor Qusai F. Alsalhi (Iraq) –

for great consulting assistance and support in carrying out the work; as well as other specialists and services that facilitate the conduct and completion of dissertation research: Ph.D. Al-Ithawi V.K.A. (Iraq), Ph.D. Nikonov I.L., Ph.D. Khasanov A.F., Baklykov A.V., Trofimov A.A., Platonov V.A., Nadtochii V.V., Ph.D. Gorkovenko A.N., Doctor of Chemical Sciences Kopchuk D.S., Ph.D. Kovalev I.S., Ph.D. Eltsov O.S. and the team of the Laboratory of Spectral Analysis Methods; Director of Institute of Chemical Technology of UrFU Doctor of Chemical Sciences Associate Professor Varaksin M.V.; Director of SE and ICCPT of Institute of Chemical Technology of UrFU, Doctor of Chemical Sciences, Professor Kozitsina A.N.; Head of the Department of Organic and Biomolecular Chemistry of Institute of Chemical Technology of UrFU, Doctor of Chemical Sciences, Professor, Corresponding Member of the RAS Rusinov V. L., Doctor of Chemical Sciences Professor, Academician of the RAS Charushin V. N., Doctor of Chemical Sciences, Professor, Academician of the RAS Chupakhin O. N., research teams of: Laboratory of Structural Research and Physico-Chemical Methods of Analysis of Institute of Chemical Technology of UrFU; Departments of Chemical Technology of Fuel & Industrial Ecology and Organic and Biomolecular Chemistry of Institute of Chemical Technology of UrFU; Laboratory of Green Methods, Advanced Materials and Biotechnologies, SE and ICCPT of Institute of Chemical Technology of UrFU, other members of Institute of Chemical Technology of UrFU and Institute of Organic Synthesis of Ural Branch of the RAS.

This work was carried out within the framework of the Megagrant of the Ministry of Science and Higher Education of the Russian Federation (Agreement No. 075-15-2022-1118 dated June 29<sup>th</sup> 2022).

# Chapter 1. Literature review of Methods for the modification of PVC and the preparation of PVC-based membranes

## 1.1 Polyvinylchloride (PVC)

Polyvinyl chloride (PVC) has been a significant polymer for over a century, but its production has some structural defects. To address these, heat stabilizers and light-absorbing dyes are used. However, new approaches to obtaining PVC have been proposed, such as chemical modification through dechlorination, nucleophilic and radical reactions, elimination or dehydrochlorination, and inoculation polymerization. These modifications result in functionalization reactions of the carbon atom of PVC with atoms of various elements, offering a wider range of applications and membrane systems. Chemical components like plasticizers and stabilizers are added to PVC to enhance its properties, such as heat resistance and strength.

Currently, *p*-isopropenylcalixarenes is being investigated to increase the effectiveness of these stabilizers [1]. PVC's dehydrochlorination issue is due to its labile chlorine atoms, which can cause production issues [2, 3]. However, chemical modifications can address this issue by adding molecular and macromolecular substituents through organic reactions. These modifications are used in various fields, such as ion-selective membrane electrodes, membrane sensors, and metal separation columns. The polymerization method, developed over half a century ago, is particularly effective for surface modification of PVC and other polymers.

## 1.2 Nucleophilic substitution reactions

Modified polyvinyl chloride can be obtained by nucleophilic modification, among which all chemical transformations of PVC contributed to its dechlorination; common chemical reaction pathways such as substitution, elimination, reduction, grafting, crosslinking and decomposition were used.

Kameda and co-authors [4] noted the study of nucleophilic reactions of PVC **L1** postmodification by dechlorination with five nucleophiles:  $I^-$ ,  $OH^-$ ,  $SCN^-$ , phthalimide anion and  $N_3^-$ , in EG (ethylene glycol) and DMF (*N,N*-dimethylformamide) as solvents, to obtain compounds **L2**, **L3**, **L4**, **L5**, **L6** accordingly (Figure 1.1), as a result,

dechlorination occurred faster for  $N_3^-$  and  $OH^-$ , however, the highest degree of dechlorination was observed for  $SCN^-$  and  $I^-$ .

Carey and Sundberg in their work [5, 6] noted the most pronounced nucleophilic properties marked  $I^-$ . In addition, Moulay and Zeffouni reported that the best medium for activation of substitution is the THF/acetone solvent system based on the results of the reaction of polyvinyl chloride with  $I^-$ . Yoshinaga et al. Reported [7] on the successful reaction of polyvinyl chloride with nucleophile  $OH^-$  in THF (tetrahydrofuran), DMSO (dimethyl sulfoxide), as well as in the dioxane–water system. Moulay in his research [8] reports that PVC with Schiff bases as chelating fragments capable of forming complexes with heavy metal ions can be obtained by the reaction of azidated polyvinyl chloride with salicylaldehyde. In addition, the authors note that PVC- $NH_2$  (compound **L7**) can be obtained in two ways: by reduction of  $LiAlH_4$  azidate and as a result of the reaction of iminophosphorus-containing PVC **L8** with ammonium hydroxide, which in turn is formed by applying the Staudinger reaction to PVC- $N_3$  using triphenylphosphine.

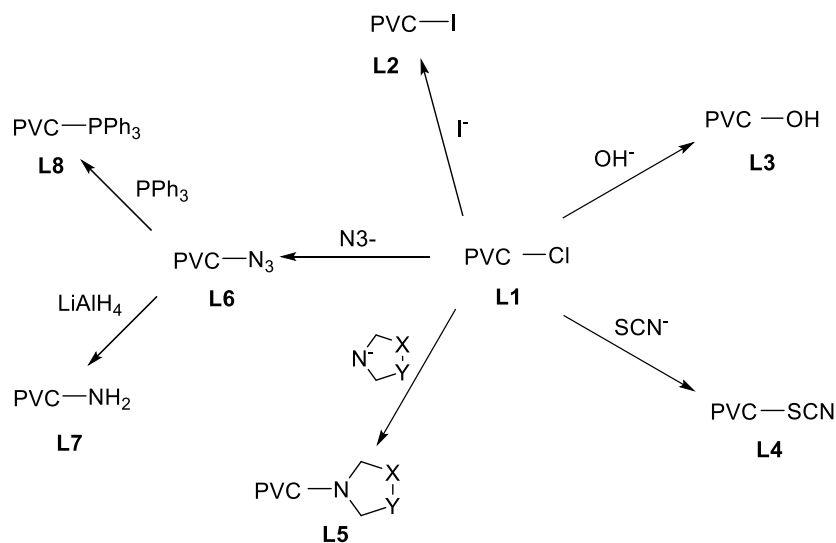


Figure 1.1 - Scheme of functionalization of polyvinyl chloride by nucleophilic substitution

Much attention was paid to the selection of a solvent for the functionalization of polyvinyl chloride. So, the reaction was carried out using THF/acetone, noting the advantages of this system for nucleophilic substitution (dechlorination of PVC). A study was also conducted using the DMSO/water system (9:1), the degree of dechlorination

was also significant (99%), at a lower temperature (80 °C) and after a shorter time (3 hours).

### 1.3 Functionalization of PVC by PVC-C coupling by alkylation

#### 1.3.1 General provisions

Kennedy and Pi [9] patented the alkylation process of PVC **L1** to produce allyl-PVC **L9**. Allyltrialkylsilane **L10** was used for quantitative alkylation in the presence of Friedel-Crafts acids such as  $\text{AlEt}_2\text{Cl}$  and  $\text{TiCl}_4$  (Figure 1.2). The number of allyl groups included in the PVC chain was **L1–L3**. Thermal analysis of allylated PVC revealed a significant improvement in its thermal stability. Further epoxidation of allyl groups in compound **L9** using *m*-chlorobenzoic acid (*m*-CPBA) in 1,2-dichloroethane resulted in the production of epoxy-PVC **L11**.

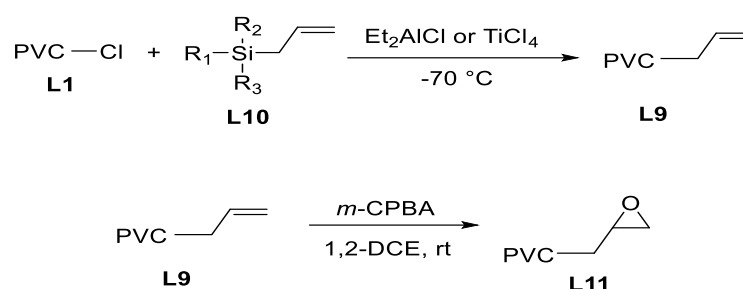


Figure 1.2 – Scheme of alkylation process of PVC

Percec described the first example of the preparation of telechelic dihydroxy PVC **L12** by reacting iodine-substituted PVC **L13** with 2-allyloxyethanol **L14** [10]. The reaction was carried out in dimethyl sulfoxide at 70 °C and catalyzed by sodium dithionite/ sodium bicarbonate (Figure 1.3). The modification includes the addition of two active chloro-methyl chain ends to 2-allyloxyethanol **L14**.

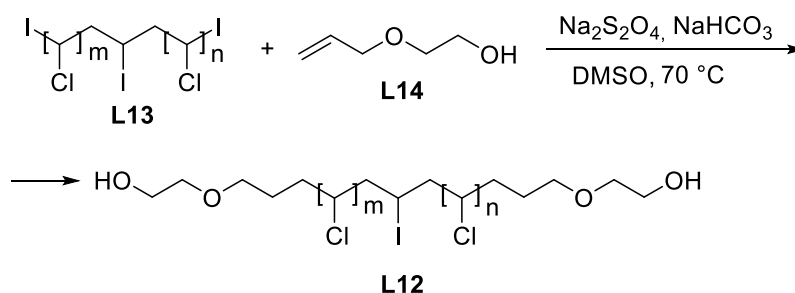


Figure 1.3 – preparation of telechelic dihydroxy PVC

### 1.3.2 Cross-combination reactions of polyvinyl chloride

As part of the Bicak and Karagoz study [11] used PVC material **L1** to produce rubber balls of cross-linked PVC **L15** (Figure 1.4). Their strategy was to achieve unsaturation (up to 40–50 %) in the PVC matrix. Such unsaturation was necessary for further administration of benzyl chloride **L16** by reaction with unsaturated groups in the presence of acid. This led to the formation of spherical granules of benzyl chlorinated PVC **L17**. The Diels-Alder reaction between unsaturated chains of the PVC matrix was used to stitch PVC balls **L15**.

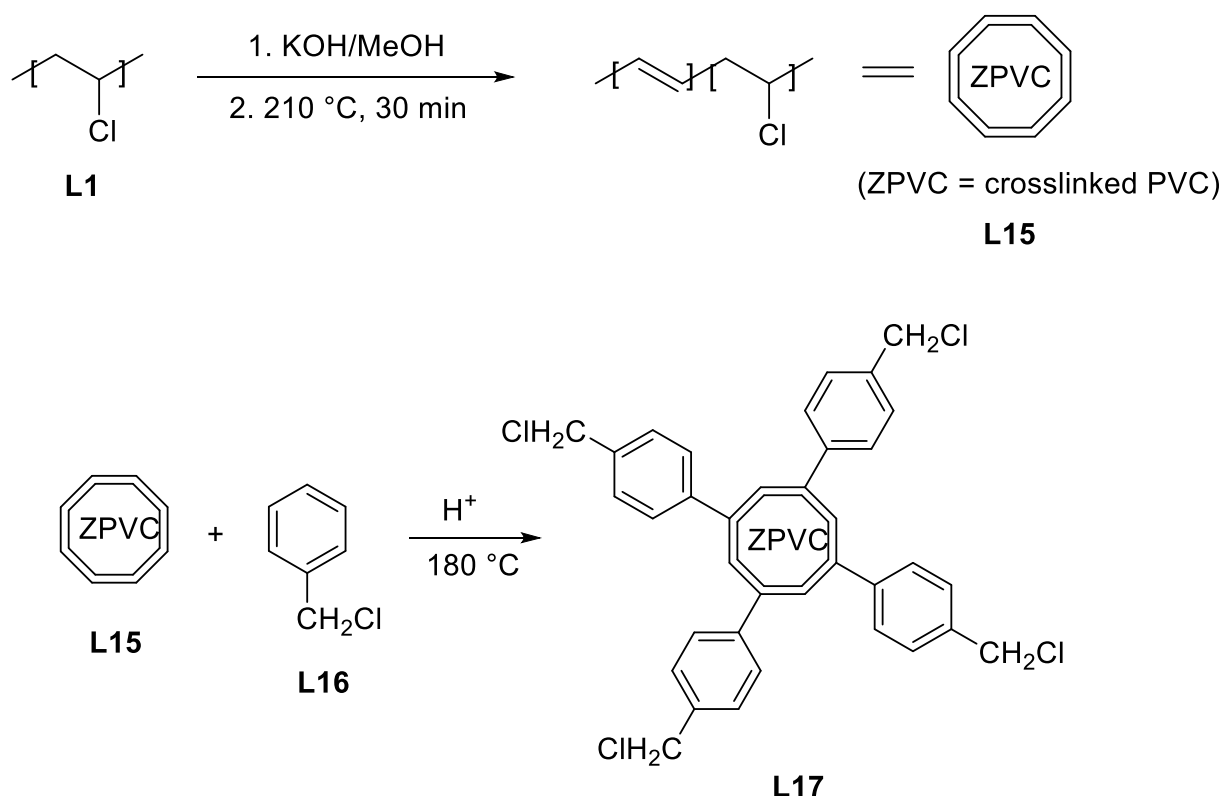


Figure 1.4 – Scheme of produce rubber balls of cross-linked PVC

In another study, Shmakova and co-authors [12] studied the irradiation product of a mixture of PVC and triallyl cyanurate (TAC). After careful annealing of the mixture, the film was irradiated with  $^{60}\text{Co}$  rays with a dose rate of 5 or 45 kGy/h. The resulting material was cross-linked PVC with TAC, while polymerization of the vinyl sections of TAC took place. It was noted that the rate of polymerization of TAC after such an introduction was higher than that of free TAC, which indicates the stimulating effect of HCl formed during dehydrochlorination during irradiation.



## 1.4 PVC-N bond functionalization

### 1.4.1 Heterocyclic functionalization of polyvinyl chloride

Abdelaal and Sobahi [13], reported on options for the functionalization of polyvinyl chloride **L1**, through heterocyclic modifications to produce PVC associated with oxazoles **L19** and triazoles **L18** by attaching *p*-phenylenediamine **L21** to form anilated PVC **L20**, the primary amino group of which was diazotized, and then hippuric acid was added to obtain oxazole PVC **L19** with a degree of modification of 64%. Triazole-containing polyvinyl chlorides **L18**, in turn, were obtained by reacting oxazole-polyvinyl chloride with anilines **L22** (Figure 1.5) with high yields (67, 71 and 78 % for R = *o*-NH<sub>2</sub>, *p*-NH<sub>2</sub> and *p*-OH, respectively). Moreover, the obtained derivatives of polyvinyl chloride **L18**, **L19**, **L20** were investigated for the absorption of copper (II) ions, the chelating ability of these compounds was proved by IR spectroscopy.

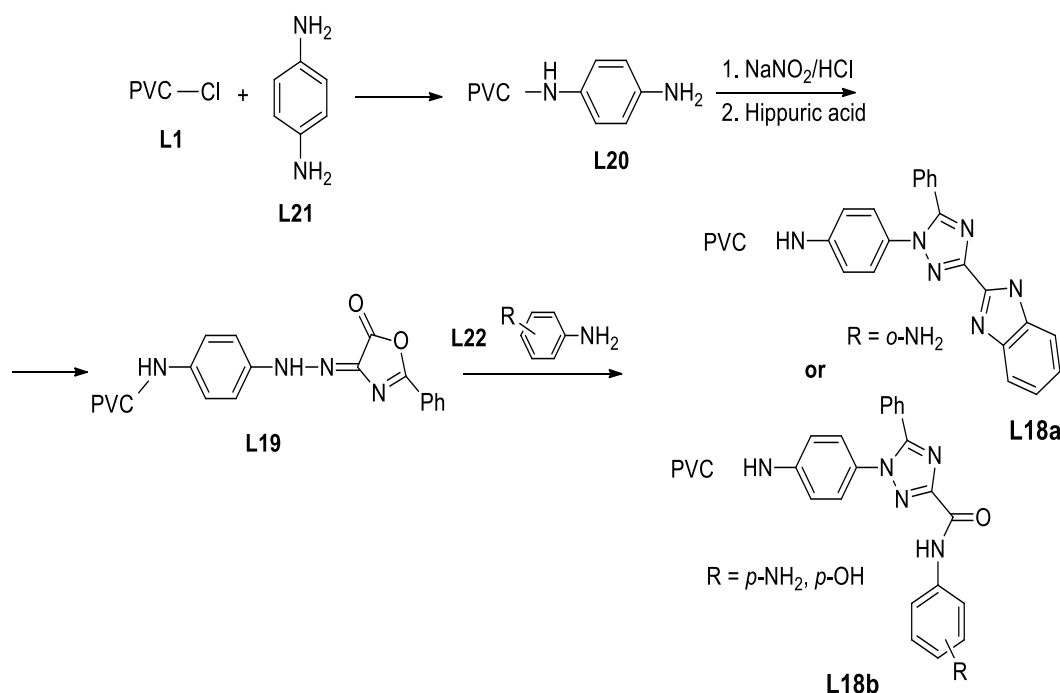


Figure 1.5 – Scheme of Heterocyclic modifications of polyvinyl chloride

Kruglova and co-authors [14] investigated the possibility of attaching azole units (triazole **L25** and tetrazole **L26**) to the PVC **L1** matrix (Figure 1.6). The reactions of PVC with metal salts of tetrazole X-Tet (where X= Na, K, Li) and 1,2,3-triazole were studied, leading to the formation of 1,2,3-triazole-PVC **L23** and tetrazole-PVC **L24**.

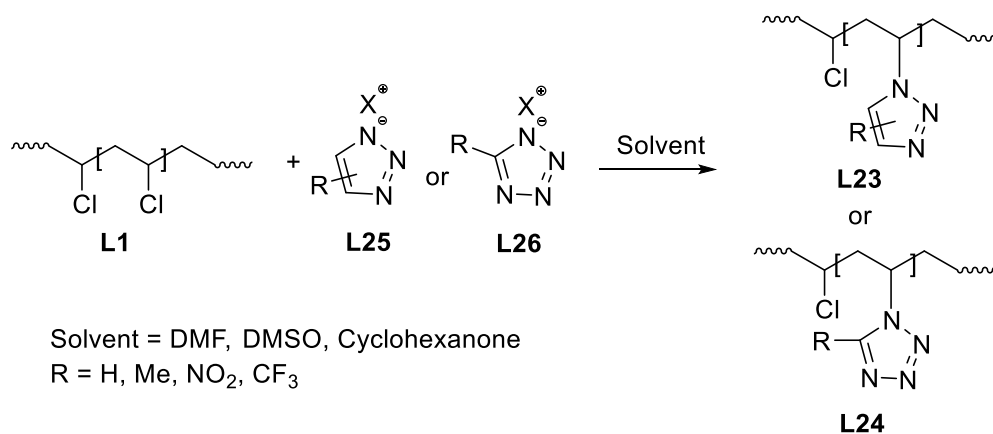


Figure 1.6 – Scheme of functionalization of polyvinyl chloride by reaction with tetrazole / 1,2,3-triazole

The modified PVC was influenced by solvent nature, anti-ionic alkaline ion X<sup>+</sup>, [VC units]/[X-Tet], reaction temperature, and reaction time. The optimal substitution was 72 % for Na-Tet under DMFA or *N*-methylpyrrolidone, 90 °C, 27 hours, and 1:2 ratio [VC]/[X-Tr]. DMSO was the worst solvent due to low substitution. Temperatures above 90 °C caused blackening and resin-gelation due to dehydrochlorination. PVC functionalization reactions occurred at higher temperatures and for shorter time. The degree of substitution in azole links depends on the substituent's nature. Methylated triazoles increase substitution to 88 %, while nitro derivatives reduce it to 25 %. Trifluoromethyl group on tetrazole accelerates reaction at 160°C. Azole fragments improve PVC thermal properties.

Shaglaeva and co-authors [15] recently proposed a methodology for nucleophilic substitution of polyvinyl chloride **L1** with pyrazole (Pz) and dimethylpyrazole (dmPz) **L27** (Figure 1.7). The modification reaction was carried out in DMFA, DMSO and cyclohexanone at temperatures from 0 to 45°C. The yields of **L28** products ranged from 14 to 24 %.

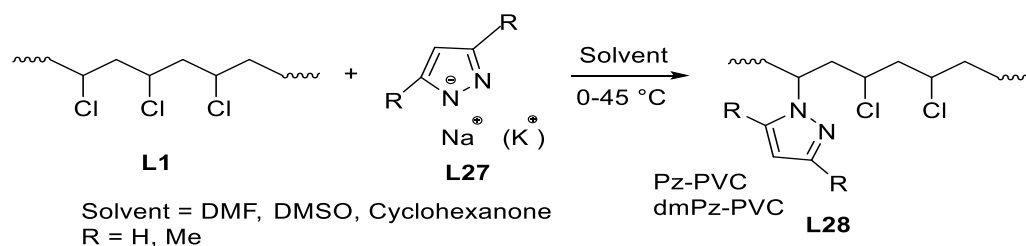


Figure 1.7 – Scheme of functionalization of polyvinyl chloride with pyrazole (Pz) and dimethylpyrazole (dmPz)

### 1.4.2 Azidation of polyvinyl chloride

Reinecke and his team [16] conducted a study on the azidation of PVC films using two approaches: cross thermal clustering (PTC) and a solvent/insoluble agent system. The optimal level of azidation was reached at 6 mol.% after 50 hours under PTC conditions, but the films lost transparency and smoothness due to partial polymer crystallization. The solvent/insoluble agent system involved water proportion, film thickness, and temperature. The study found that higher solvent-to-insoluble ratio led to greater swelling and more significant film modification. The conversion increased over time, with 5.5 mol.% conversion at 60 °C for 200 hours and 6 mol.% at 52 °C for 50 hours. The thickness of the film did not affect the degree of azidation.

In addition, Lakshmi and colleagues [17] studied the adhesion of *Staphylococcus aureus* and *E. coli* strains to plasticized PVC surfaces after azidation using sodium. The surfaces became hydrophilic, with a lower wetting angle compared to unmodified PVC. The azidated surface showed significantly lower bacterial adhesion to microorganisms, with levels for *S. aureus* (100 %), N<sub>3</sub>-PVC (15 %), and crossed PVC (92 %), and *E. coli* (100 %), N<sub>3</sub>-PVC (10%), and crossed PVC (115 %). Thus, the azidation of PVC films in a solution/insoluble system has proven to be an effective modification method that preserves the transparency and surface properties of the films, as well as reduces bacterial adhesion.

### 1.5 PVC-S bond functionalization

A study conducted by a group of Grohens and co-authors [18] is devoted to the study of the adhesion of bacteria responsible for potential nosocomial infections to chemically modified PVC films obtained from untreated PVC **L1**. In particular, two types of bacteria are considered - *E. coli* and *S. aureus*. To obtain functionalized PVC **L29** and **L30** using reactions, two types of modifiers were used: containing a mobile hydrogen atom (HS-Ar<sub>1</sub>) **L31** and without it (HS-Ar<sub>2</sub>) **L32** (Figure 1.8). The determination of bacterial adhesion to solid PVC and modified samples was carried out by measuring wettability, measurements related to the time of bubble formation, as well as static adhesion tests.

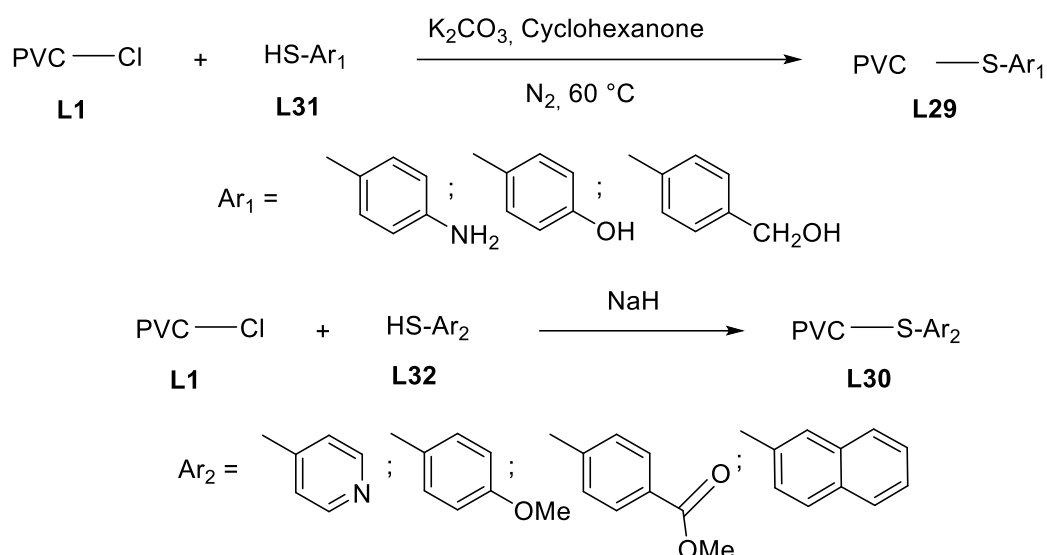


Figure 1.8 – Scheme of functionalized PVC with a mobile hydrogen atom and without it

The study found that hydrophobic bacteria, such as *S. aureus*, have higher adhesion than hydrophilic bacteria, *E. coli*, on unmodified PVC and modified samples. *E. coli* retention decreased from 100 % on unmodified PVC to 50–70 % on modified samples. This could be due to acid-base interaction between *E. coli* and polymer samples, or the hydrophobic nature of the bacteria. The findings could help develop methods for preventing nosocomial infections and increasing sterility in the medical environment.

In the work of Reinecke and his colleagues [19], the substitution profile of PVC **L1** with halogenated thiophenol compounds ( $\text{ZArSNa}$  **L34**, where  $\text{Z} = \text{Hal}$ ) was studied. Modification was carried out using two different types of salts:  $\text{ZArSNa}$  (salt prepared and isolated before the functionalization reaction) and  $\text{ZArSH}/\text{K}_2\text{CO}_3$  (salt obtained *in situ*) (Figure 1.9).

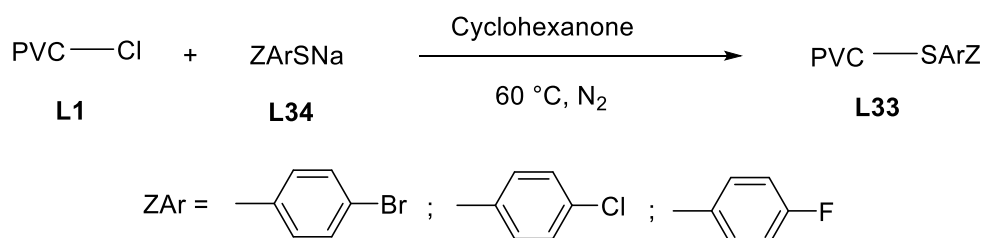


Figure 1.9 – Scheme of substitution of PVC with halogenated thiophenol compounds

It is shown that the results on the degree of functionalization (obtained by  $\text{ZArS-PVC}$  **L33**) depended on the halogen and experimental conditions. The study reveals that

the functionalization of polyvinyl chlorides (PVC) can be significantly influenced by the acidity and nucleophilicity of the modifier. The first salt achieved 68 % functionalization for 4-bromothioyphenol, 48 % for 4-chlorothioyphenol, and 40% for 4-fluorothioyphenol after 25 minutes. The second salt showed 35 %, 38 %, and 80 % functionalization, respectively. The study also examined the thermal stability of functionalized PVC. It found that thiol modifiers with chlorine or bromine atoms did not significantly affect PVC's stability. However, fluorine thiol compounds were more effective, increasing the decomposition temperature. Overall, all halogenated thiol modifiers reduced PVC's glass transition temperature from 51.4 to 85.2 °C.

Previously, the Reinecke group used a substitution pathway with two types of modifiers - thioaromatic and thioaliphatic [20]. The study evaluates the impact of hydrogen bonds on the final properties of functionalized polyvinyl chloride. Results show that functionalization with aliphatic thiols reduces dehydrochloride content by no more than 10 % after 24 hours, while aromatic thiols achieve a degree of modification of 32–68 % without negative effects. Cross-linking occurs after 6 hours when modified with p-thiobenzoic acid. The degree of functionalization of thiols forming hydrogen bonds is twice as high as that of thiols preventing their formation. The glass transition temperature ( $T_g$ ) depends on the type of modifier and its degree of transformation. The degree of rigidity of modified PVC varies depending on the type of modifier and the degree of functionalization. The study also found that fractional free volume (FFV) increases for all modifiers and at various degrees of functionalization.

Tiemblo and co-authors [21, 22] used PVC grafting fragments such as 4-mercaptopyridine, 4-methoxybenzenethiol, 4-mercaptophenol and 2-mercaptanaphthalene as luminescent probes to study the microstructure of the polyvinyl chloride chain. The detection of relaxation in untreated PVC was made possible by the extinction of phosphorescence and fluorescence of modified PVC.

### **1.6 PVC-O bond functionalization**

The functionalized dehydrochlorination of polyvinyl chloride (DPVC) L35 obtained by thermal and chemical methods are functional materials for various applications. Epoxidation of DPVC causes the inclusion of oxirane activity. Szakács and

Iván in their study report the production of PVC epoxy-DPVC **L36** with high yields [23]. They were obtained by reaction of epoxidized PVC with an excess of *m*-chlorobenzoic acid (*m*-CPBA) in an inert atmosphere (Figure 1.10).

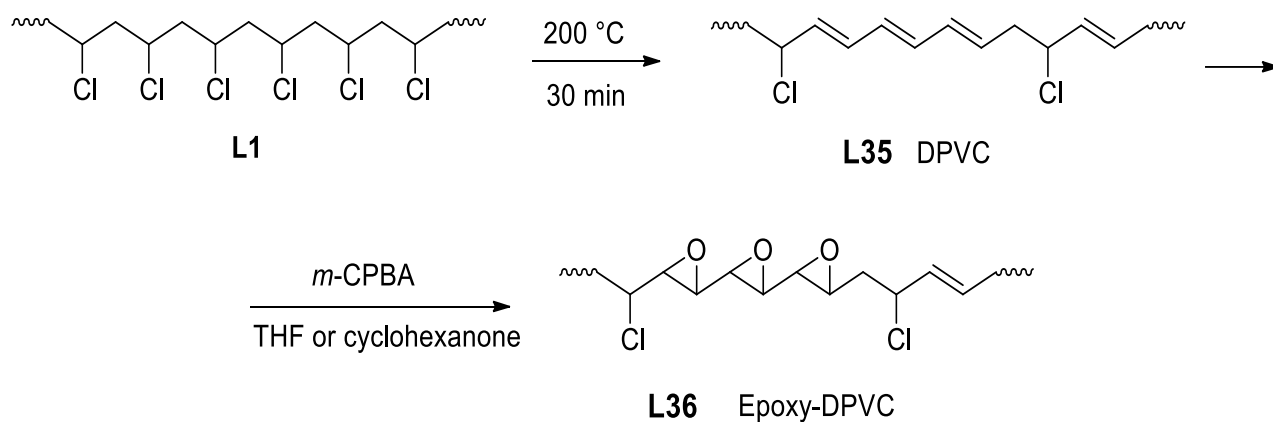


Figure 1.10 – Scheme of production of PVC epoxy-DPVC

Epoxy groups can be used for chemical modifications, but cyclohexanone is ineffective. To increase epoxidation, temperature (25 to 40 °C) and reaction time (2.5 to 21 hours) need to be increased. *m*-CPBA can form orthocarbonates with cyclohexanone, but tetrahydrofuran medium results in higher epoxidation. Epoxidized PVC derivatives can be used in the polymer industry as a light-curing resin.

Bicak and co-authors also received epoxidized PVC [24]. The reaction was carried out by two methods: boiling a mixture of PVC/KOH in isopropyl alcohol for 1 hour followed by heat treatment at 200 °C with and heating the PVC/liquid paraffin mixture at a temperature of 210 °C for a specified time. Epoxidation of DPVC granules was performed with *tert*-butylhydroperoxide (*t*-BuOOH) in the presence of a Mo(Acac)<sub>2</sub> catalyst. The epoxy-PVC granules obtained by the first method yielded light brown substances soluble in THF with an epoxy content of 3.2 mmol/g during the reaction for 24 hours. However, the authors note the greater effectiveness of the second method, since the degree of epoxidation was observed up to 4.1 mol/g after a 16-hour reaction. Of great interest is the production of esterified PVC **L37** by nucleophilic substitution with RO<sup>-</sup> **L38** alkylates, or in an alcohol/alkali metal system. Thus, Mekki and Belbachir [25] received an innovative environmentally friendly catalyst based on montmorillonite called «Maghnite-K» [26] during the esterification of PVC with ethanol, ethylene glycol and phenol (Figure 1.11).

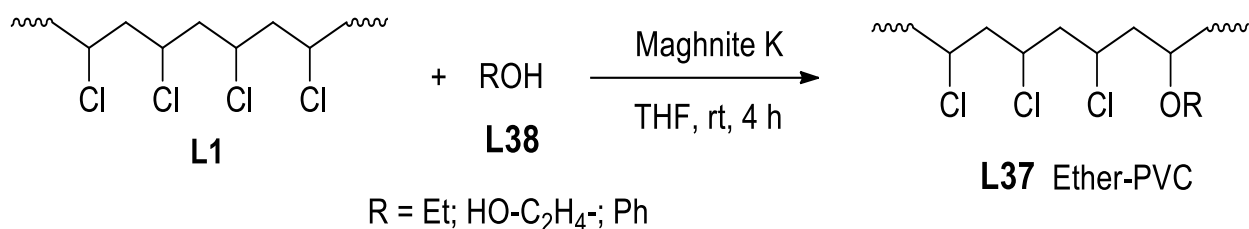


Figure 1.11– Scheme of esterification of PVC with ethanol, ethylene glycol and phenol

The esterification of PVC under optimal conditions occurred with yields from 50 to 83 %. The authors note the high solubility of the obtained PVC esters in organic solvents such as ethyl acetate, DMFA, DMSO and THF. In addition, it is noted that the functionalization of PVC **L1** with alcohols **L38** in the presence of the catalyst "Maghnite-K" occurred bypassing dehydrochlorination.

Yoshioka and colleagues reported the hydroxylation of PVC **L1** NaOH in ethylene glycol at 190 °C (Figure 1.12) [27].

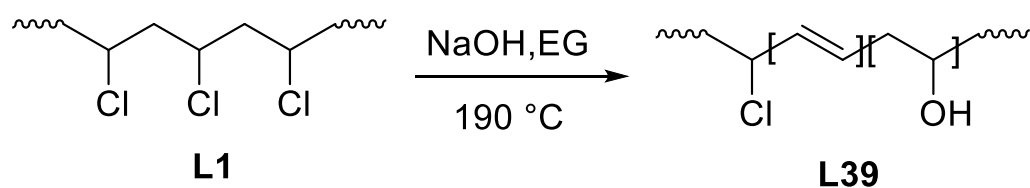


Figure 1.12 – Scheme of hydroxylation of PVC

The degree of hydroxylation increased over time with a maximum yield of OH-PVC **L39** 40 % for 45 minutes. The reaction efficiency was highest at moderate alkali concentrations, with lower rates at higher concentrations due to phase changes on PVC particles, which prevented the penetration of OH<sup>-</sup>. The solvent significantly impacted the dechlorination rate, with dechlorination occurring 150 times faster in 1.0 m NaOH/ethylene glycol (EG) and faster at atmospheric pressure than in high-pressure NaOH/water.

The Bahaffi group proposed a method for modifying PVC **L1** by esterification with sodium ethylene glyxide **L40** to obtain a functional material **L41** that can be used in ion chromatography (Figure 1.13) [28].

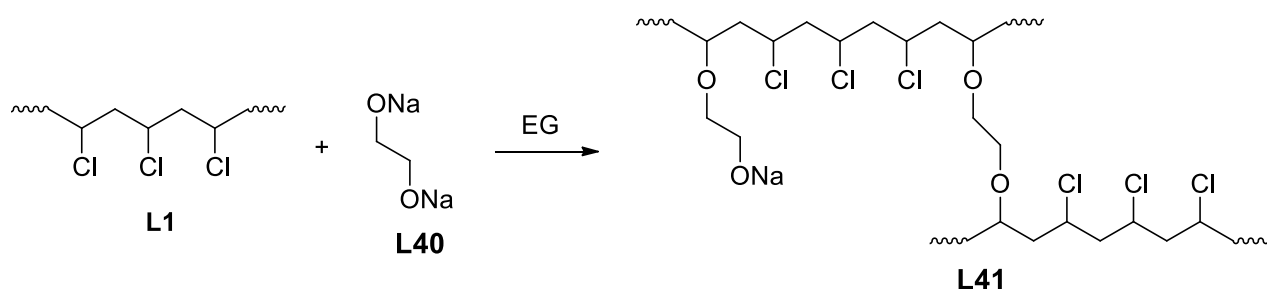


Figure 1.13 – Scheme of modifying PVC by esterification with sodium ethylene glycolate

Such ion-exchange resins were obtained by encapsulating silica gel particles in ethylene glycol-PVC **L41**, followed by immersion in a solution of tetramethylammonium hydroxide to increase ion exchange capacity. The separation ability of the material obtained in this way has been successfully proven for mixtures of cations ( $\text{Li}^+$ ,  $\text{Mg}^{2+}$ ,  $\text{Sr}^{2+}$  and  $\text{Ca}^{2+}$ ) and anions ( $\text{Cl}^-$ ,  $\text{NO}_3^-$  and  $\text{SO}_4^{2-}$ ).

### 1.7 Prospects of mechanochemical approaches to PVC modification

Mechanochemical grinding in a ball mill is a striking example of "green methods" for producing a number of compounds without the use of solvents, catalysts based on transition metals, etc., thereby it is environmentally safe and low-waste. It is worth saying that the influence of mechanical force on the reaction, the degree of hardness and the size/weight of the grinding balls, as well as the intensity of ball grinding are crucial to achieve high monomer conversion. It is necessary to take into account the maximum temperature at which the polymer can be obtained and modified, since local overheating of the reaction system has been reported due to heating of grinding balls during mechanochemical grinding [29]. The structure of the obtained polymers is usually confirmed by  $^1\text{H}$  NMR or IR spectroscopy [30].

In addition to judging mechanosynthesis as a "green method" for producing functional polymers, it is worth noting the use of industrial/household waste [31, 32] or agricultural waste [33] as source connections.

Mechanosynthesis is often used to produce various polymers. Polymerization under conditions of reduced or no solvent content, including the formation of coordination bonds, can serve as an example of such reactions [34] under mechanochemical conditions, namely by the ball-milling method. Therefore, the methods of obtaining polymers under mill grinding conditions, which were previously used to



destroy them, are of interest in the chemical community around the world. It is noted that in recent decades mechanosynthesis has attracted increasing attention due to environmental aspects, including for the production of various types of polymers [35].

Among the mechanochemical methods for the synthesis of polymer molecules, it is also worth noting the mechanosynthesis of polystyrene and poly(2-vinyl naphthalene). Thus, Cho and Bielawski proposed a method for the mechanochemical production of polymers by the mechanism of radical polymerization of 2-vinyl naphthalene in a vibrating ball mill [36]. Also, Yoo and co-authors reported on a mechanochemical method for polymerization of vinyl in a solid state [37].

Among the possibilities of synthetic mechanochemistry, it is interesting to obtain functional polyphenylenes. A series of papers led by Vogt, Grätz and Borchardt on polymerization to obtain polyphenylenes by using mechanosynthesis under Suzuki cross-coupling conditions has been published [38, 39]. Recently, Nirmani *et al.* have developed a mechanochemical Suzuki polymerization method to produce a number of polyfluorene-conjugated polymers [40].

In conclusion, it should be noted that mechanochemical synthesis has become a convenient, and at the same time environmentally safe, resource-saving method for obtaining homo- or copolymers of various types, as well as for fast and effective functionalization of polymers by introducing substituents into terminal bonds and side branches of the chain with a high degree of transformation of the initial polymers without destroying the main skeleton. Thus, mechanosynthesis can also be used as a "green approach" to the production of chemically modified polyvinyl chlorides.

### **1.8 Application of Modified PVC**

Modified PVC materials have various applications. One application is in the synthesis of PVC membranes. Modified PVC membranes have shown potential for application in the treatment of wastewater. Abhari *et al.* [41] used modified PVC to improve the hydrophobicity of PVC membranes, making them suitable for nanofiltration processes and the dye removal from aqueous solutions, dye removal efficiency of 90 %. Various modifications have been explored to enhance the properties of PVC membranes for oil treatment. Al-Ani *et al.* [42] modified PVC by used titanium oxide nanoparticle

to create an ultrafiltration membrane (UF) that effectively treated actual refinery wastewater. The hypothesis of this work was that TiO<sub>2</sub>-NPs would function as a hydrophilic modification of the PVC membrane and excellent self-cleaning material, which in turn would greatly extend the membrane's lifetime. Furthermore, Skórczewska et al [43] modified the plasticized PVC membranes with Camellia oleifera seed-oil-based cyclohexyl ester (COSOCE) which have demonstrated improved hydrophilicity, mechanical properties, and thermal stability, COSOCE can replace dioctyl-phthalate (DOP) as a PVC plasticizer for oil treatment.

Another application is in the production of extrusion-molded PVC waterproof coiled material. Jinying [44] developed a method to *in-situ* modify PVC resin using octamer polyhedral oligomeric silsesquioxane, which improved the ageing resistance, tensile strain performance, and seepage resistance of the waterproof coiled material.

Moreover, PVC **L1** modified for different pharmaceutical applications. One study, Rabie et al. [45], demonstrates the use of polyvinyl chloride modified with glycine methyl ester **L42**. Subsequent hydrolysis of intermediate **L43** led to the production of MPVC **L44**, as a precursor for functionalized conjugates for biomedical applications. The conjugates were prepared by chemically reacting MPVC with chitosan and epichlorohydrin (Figure 1.14), and further modified with Cs and salicylic acid.

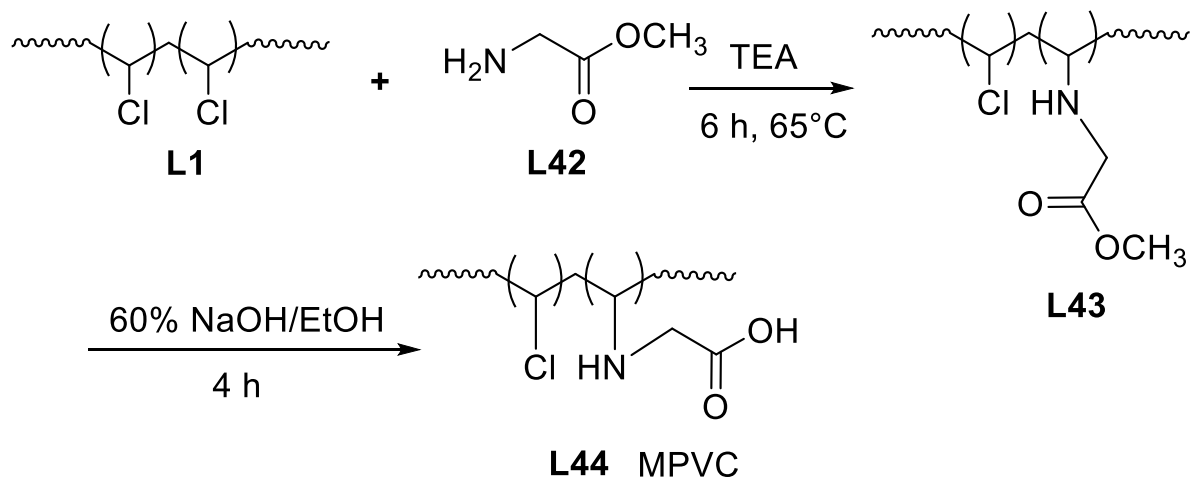


Figure 1.14 – Scheme of modification polyvinyl chloride with glycine methyl ester

The antibacterial activity of the prepared materials was tested against different bacteria, as well as yeast, and their minimum inhibition concentration was determined.

Another study Beveridge et al. [46], described the construction of a PVC membrane selective electrode for the determination of Cyproheptadine in pharmaceutical preparations and human fluids by chemical modification of flexible PVC tubing with azide. These modifications provide convenient handles for click chemistry linkages *via* azide–alkyne cycloaddition.

Also, it has become a popular biomedical material due to its compatibility with biosystems. Shen et al. [47], cross-linked PVC surfaces to O-butyryl chitosan (OBCS) **L45** via amino linkages to create a blood-compatible biomaterial. The OBCS reacted with 4-azidobenzoic acid **L46**, forming Az-OBCS **L47** (Figure 1.15), which then cast on a PVC film surface and irradiated with a mercury lamp (8 W, 254 nm UF-tube light) for 3min, and the cross-linked Az-OBCS-PVC **L48** ensued. It showed excellent antiplatelet adhesion and good antithrombogenicity. The immobilized OBCS also improved antithrombogenicity. The air-in-water contact angle of Az-OBCS-PVC **L48** films decreased significantly compared to blank PVC films, indicating that the grafted films were more hydrophilic than the blank films.

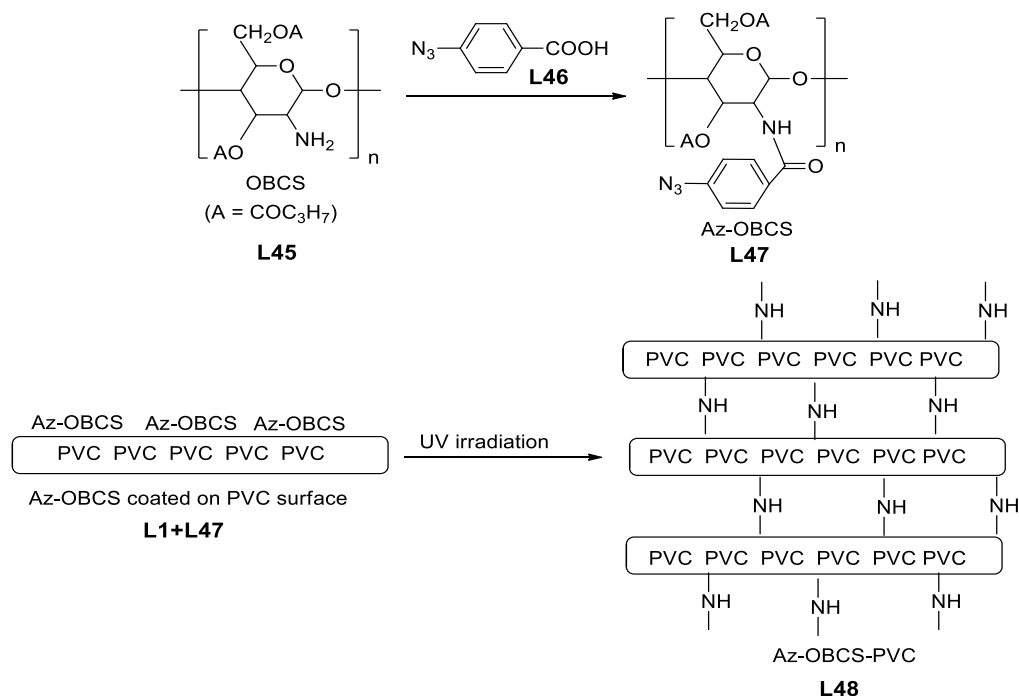


Figure 1.15 – Scheme of cross-linked PVC surfaces to O-butyryl chitosan (OBCS)

For the same goal, Jayakrishnan et al. [48] grafted poly(ethylene glycol) (PEG 600) via an amine linkage to improve blood compatibility. The resulting isocyanate-PVC

(Isocy-PVC) **L49** was obtained by sequential amination with ethylenediamine and hexamethylene diisocyanate (HMDI) through the formation of **L50** (Figure 1.16). Reaction times varied, with insoluble products being obtained over a longer period of time. The air-water contact angle was  $47^\circ$ , and the free energy of the solid/water surface was almost a quarter of the unmodified surface. The PEG modifier reduces the thermal stability of  $T_g$  and  $T_d$ . The platelet adhesion test showed less significant adhesion for PEG-PVC **L51** film, indicating better blood compatibility.

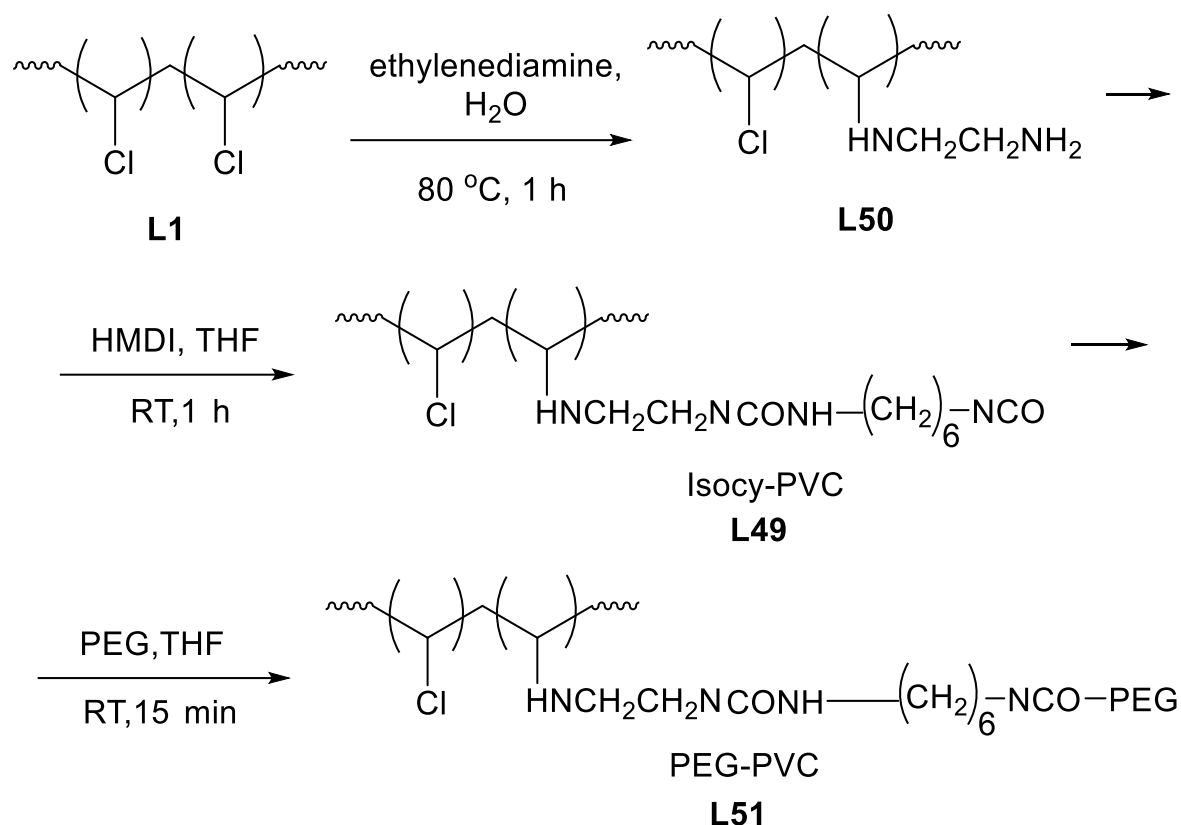


Figure 1.16 – Scheme of poly(ethylene glycol) grafted via an amine linkage

As for applications in chemistry, by using the same strategy shown in Figure 1.14, Ahmed et al. [49], grafted castor oil onto PVC-matrix by using a polyurethane spacer, (PVC–HNCH<sub>2</sub>CH<sub>2</sub>NH–CONH–Ar–CH<sub>2</sub>–Ar–NHCO–Castor oil). The PVC-based material effectively removed heavy and toxic metals for Cr(IV), Cu(II) and Ni(II) ions, with better efficiency towards chromium ions. The removal of metallic ions was improved up to 150 min of contact time; after that, the removal efficiency leveled off at greater values. Another researcher, Li et al. [50] developed a PVC-supported tetraethylenepentamine (TEPA-PVC) catalyst for the Knoevenagel condensation.

Commercial PVC was allowed to react with an excess of TEPA at 80°C. TEPA-PVC was a cross-linked material ready for use. The yields of attempted Knoevenagel reactions were 80-97 %, with its catalytic activity remaining unchanged even after recovery. The reaction was stereoselective when ethyl cyanoacetate was used, producing only the E isomer.

Additionally, PVC modified with mercaptan compounds has applications. The pyridinated PVCs (Pyr-PVC) obtained as shown in (Figure 1.8), were assessed by Tiemblo *et al.* [51] as membranes for gas permeation, including O<sub>2</sub>, N<sub>2</sub>, CO<sub>2</sub>, and CH<sub>4</sub>. Different levels of substitution were used in Pyr-PVCs for gas transport tests. Measurements of the diffusion and permeation coefficients were made at 35 °C as a function of time. The four gases' diffusion coefficients in the pyridinated PVC samples first indicated a sharp decline, but after a week, the trend leveled out. Furthermore, Duvall [52], was modified PVC with 4-mercaptopyridine and achieve a high degree of modification without degradation or side reactions, and also the modified PVC have been further alkylated and form PVC ionomers and polyelectrolytes.

## **1.9 Membrane techniques**

### **1.9.1 Membrane Filtration Types**

Membrane technology is one of the best-advanced separation and treatment systems that have been widely used in different applications. Membrane separation processes may be classified according to the size range of separated materials and the driving force used in separation. there are four popular types; microfiltration (MF), ultrafiltration (UF), nanofiltration (NF) and reverse osmosis (RO) which separate the compounds in liquor according to molecular dimensions under hydrostatic pressure (Table 1.1) [53, 54].

Table 1.1 – The characteristics of membranes used in different membrane filtration processes

Type of process	Pore size, $\mu\text{m}$	Driving force, bar	Application
Microfiltration (MF)	0.1–1.0	0.1–2	Sterile filtration, Clarification.
Ultrafiltration (UF)	0.01–0.1	0.1–5	Separation of macromolecular solutions.
Nanofiltration (NF)	0.001–0.01	3–20	Removal of hardness and desalting.
Reverse Osmosis (RO)	<0.001	<0.5	Separation of salts and micro solutes from solutions.

For this study, the ultrafiltration membrane (UF) is used, and Wenten [55] reported the advantages and disadvantages of this membrane as the following:

Advantages:

- Available in various sizes, making the process suitable for many different separations.
- Separation can be performed at low pressures, conversions can be high, colloids can be effectively removed, and macromolecular species can be concentrated.
- Simple and compact. Operation can be restored relatively easily after shutdown.
- Good and constant quality of treated water in terms of particle removal regardless of raw feed water quality and process compactness
- Particularly suitable to applications involving temperature-sensitive materials.

Disadvantages:

- UF cannot separate dissolved salts or low MW species. It cannot be used to desalt water.
- UF membranes not commonly used to fractionate macromolecular mixtures. Efficient fractionation by UF is only possible if the species differ in MW.

### 1.9.2 Configurations and Operations of Membranes

Membranes can be classified based on their configurations: namely, flat sheet and tubular membrane modules. The module used for each configuration also differs. Flat

sheet membranes are used in plate-and-frame and spiral wound modules while tubular membranes are used in hollow fiber and tubular modules.

Although the merits and drawbacks of the different configurations can be argued, the plate and frame configuration may offer certain advantages over other module configurations. Flat sheet plate and frame membranes offer benefits in simplicity, better flow control on both the permeate and feed side, ease of sheet replacement, less fouling tendency over tubular configurations (excessive fouling and membrane integrity problems) [56, 57], while also being easier to prototype in a laboratory environment.

Membrane operating processes are dependent on membrane modules. There are two flow regimes in which membrane filtration can be operated: dead-end and cross flow, as shown Figure 1.17.

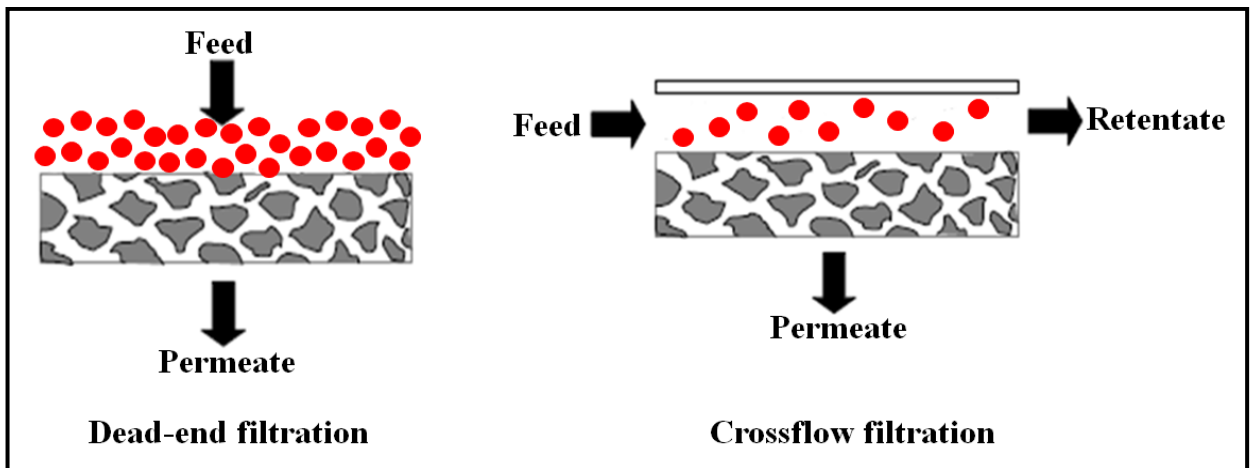


Figure 1.17 – Schematic view of dead-end and cross flow mods for flat sheet membranes

The flow regime through a membrane impacts flux and membrane fouling. Dead-end mode produces one treated water stream, but pollutant compounds block pores, causing decreased flux and fouling. Regular cleaning is necessary for constant flux. Cross flow reduces fouling and allows higher fluxes, reducing fouling compounds on membrane surfaces. In cross flow, the influent stream divides into concentrate which contains retained pollutants, and permeate or treated water [58].

### 1.9.3 Materials and Properties of Membranes

The selection of material is an essential factor in the achievement of desired performance in membrane application. The membranes can be classified to organic

(polymers) and inorganic (ceramic), as well as, composite or mixed matrix membrane (MMMs).

### 1) Polymeric membranes

Polymeric membranes are widely used due to their flexibility, mechanical strength, and ability to design selective barriers. Polymeric materials commonly used in separating membranes, including polyvinyl chloride (PVC), polyvinylidene fluoride (PVDF), polyethersulfone (PES), cellulose acetate (CA), polyacrylonitrile (PAN), and polysulfone (PSf), *etc* (Table 1.2) [59, 60].

Table 1.2 – Polymers used for membrane fabrication and their properties

Polymer	Advantages	Disadvantages
PVC	Excellent mechanical strength, high corrosion resistance, Low cost.	Hydrophobic nature/ Using amphiphilic copolymer.
PVDF	Good hydrophobic property, semi-crystalline polymer, good mechanical strength Stability, good thermal stability.	dramatically decreasing of hydrophobicity in continuous use/ blending method for improving the hydrophobicity (Graphene), hydrophobic property.
PSf	Excellent mechanical strength, Excellent resistance to caustic, good resistance to moderate chlorine, Operating at high temperature and pressure.	Hydrophobic nature/ incorporation of zinc oxide (ZnO).
CA	Good film forming, relatively low cost, high flux, good toughness, biocompatibility.	Poor mechanical property/ using homogeneous braid reinforced.
PAN	Low price, Excellent aging-resistance, high hydrophilicity, good stability, good solvent resistance.	Low mechanical stability

The properties of the membrane preparation material affect its hydrophobicity, surface charge, roughness, porosity, and retention rate, which affects membrane performance and fouling behavior [61, 62].

### 2) Nanocomposite membranes

Water treatment has traditionally used membrane-based technologies, but the shortcomings of standard polymeric membranes have led to the use of composite membranes, UV-initiated grafting, and nanocomposite membranes [63]. Nanocomposite



membranes are attractive due to their unique physicochemical features, such as large specific surface area, high reactivity, and strong sorption [64]. A variety of nanostructures, including graphene oxide/titanium oxide, iron oxide, silicon dioxide, and zinc oxide, have been used for this purpose.

Silicon dioxide ( $\text{SiO}_2$ ) nanoparticles are less hazardous, available, and low-cost, with functional groups on their structure. They improve membrane anti-fouling properties and are environmentally inert. Due to their small particle size, narrow distribution, and high affinity towards water, they enhance membrane surface hydrophilicity, resulting in high permeability and unsaturated residual bonds, making modification simpler [65].

### **1.9.4 Preparation and Synthesis of Membranes**

In recent years, there are several strategies for producing membranes. These include phase inversion, interfacial polymerization, stretching, track etching, and electro-spinning [66].

Among the above methods, the phase inversion method is most significant and common process for preparing polymeric flat-sheet membranes from various monomers [67]. It involves the controlled transformation of a polymer from a liquid to a solid state, often starting with liquid-liquid de-mixing. The morphology and mechanism of the membrane are influenced by factors such as polymer selection, coagulation bath composition, solvent, and film casting conditions. Non-solvent induced phase inversion (NIPS) is a widely used method for producing asymmetric membranes with porous sub-layer structures and dense skin layers. This method is commonly used to create asymmetric membranes with porous sub-layer structures [68].

### **1.9.5 Membrane in carwash wastewater**

UF is one of the most superb techniques in membrane technology for many purification processes. The utilization of UF membrane is the focus of membrane research in the carwash sector. The pore sizes of the UF membranes are usually (10-100 nm) (0.01-0.1  $\mu\text{m}$ ) and the oil droplets sizes are (0.1–10  $\mu\text{m}$ ). Thus, most of oil droplets can be removed efficiently with UF.

### 1) Impact carwash wastewater on the environment

Many countries are still lagging behind in developing their awareness of disposal car wash wastewater, where wastewater is discharged to main drains or lands without any treatment [69]. A large amount of water is used in addition to detergents, kerosene, petrol and diesel during car washing, then the wastewater is released, carrying residues of hydrocarbons, oils, grease, and detergents that pass from the carwash services to the drains or enter to the rainwater drainage system, which leads to a quality deterioration waters and severe damage to many forms of aquatic life, causing serious environmental problems [70].

Zaneti et.al. [71], reported that when detergents (like anionic surfactant) are used in car washes, and disposal to the surface water caused excessive growth of plant and degrades. This also results low levels of dissolved oxygen, change in the animals' populations, and overall water quality degradation. Also, Chukwu et al. [70], found some types of phosphate-containing detergents used can cause excess algae growth in local waterways such as open drains or in other waterways.

According to Nekoo et al. [72], organic matter (e.g., gasoline, diesel, waste engine oils, and surfactants) are the most common sources in car wash wastewater which contribute to the high concentration of chemical oxygen demand (COD) which indicates the presence of pollutants that are stable and not biodegradable easily, resulting in aesthetic losses, toxic effects on ecosystems, and changes in biodiversity.

A study by Rai et al. [73], have stated that the oil and grease in the wastewater of car washes may come from the leakage of petroleum products and lubricants from cars in addition to the oil spills on washing floors. Oil and grease layer in water bodies block sunlight, obstruct photosynthesis, prevent oxygen replenishment, and thus, caused toxic impacts on microorganisms responsible for biological wastewater treatment.

Overall, the removal or minimization of contaminants in car wash wastewater is necessary to reduce the risk of environmental pollution by developing efficient and low-cost treatment or recycling of treated wastewater which is the best option to overcome this problem in car wash wastewater management.

## 2) Legislation standards for carwash wastewater

In order to conserve natural resources and give a high-quality wash, new carwash techniques must be used, including water reusing. Some nations have achieved considerable advancements in the reuse of wastewater by establishing laws and regulations, whereas other nations still lack sufficient planning and restrictions [74]. Environmental legislation and regulations from the worldwide have been published for wastewater and disposal into the public sewage system.

Though many countries have their own legislations of environmental quality, but the carwash sector rarely enforced application of these laws [75]. Greywater standard on carwash wastewater have been created in countries like United States, Australia, and Europe. Some countries in Europe restrict the consumption of water or impose a reclamation (recycling and reuse) percentage approximately 70–80% to meet the specific water quality standard [76].

The effluent discharges of carwash wastewater used Standard based on Sewage and Effluent Discharge. Wastewater composition standards (the standards of permissible discharges of substances into water bodies) have been established in city of Yekaterinburg, Sverdlovsk region by the Regulation № 2329 of 2021. Furthermore, Iraq has established Iraqi National Standards set by the Regulation 25 of 1967 for wastewater drained to the water source or into public sewers. This legislation applied for the carwash wastewater and focused on chemical oxygen demand (COD), biological oxygen demand (BODs), oil and grease and total suspended solids (SS), yet less focused on the surfactant concentration. The legislation standards for the parameter limits of wastewater are shown in Table 1.3.

Table 1.3 – The legislation standards for the parameter limits of wastewater

Parameters	Standard in Yekaterinburg, Sverdlovsk region (Regulation No. 2329 of 2021) WW composition, mg/L			Iraqi National Standards (Regulation No. 25 of 1967) WW composition, mg/L		Malaysia (Industrial Effluents) Regulations 2012 WW composition, mg/L	
	North Canal Basin	South Canal Basin	Sewerage Basin	Water Source	Public Sewers	St. A	St. B
1	2	3	4	5	6	7	8
Suspended solids	300	96.80	31.48	-	-	50	100
BOD <sub>5</sub>	169.40	40.10	30.90	<5	<40	2	40
COD	500.00	176.90	-	-	<100	80	200
Petroleum products	2.21	0.60	1.30	-	10, if water drained/source water is 1:1000; 5, if water drained/source water is 1:500; 3, if water drained/source water is 1:300	1	10
Sulphates	80.10	69.00	90.44	200	<400, if the water drained/source water is 1:1000	0.5	0.5
Chlorides	53.54	72.00	139.0	200	<600, if the water drained/source water is 1:1000	-	-
Ammonium	25.40	3.30	8.54	1	-	-	-
Anionic surfactant	0.80	1.60	2.17	-	-	-	-
Phosphates-P	0.24	0.24	2.45	0.13	0.98	-	-
Phenol	0.008	0.023	-	0.005	0.01-0.05	0,001	1
Chromium (6+)	0.0128	0.01	-	0.05	0.1	0.05	0.05
Chromium (3+)	0.0107	0.01	-	0.05	0.1	0.2	0.1
Iron	0.50	1.032	-	0.3	2	1	5
Zinc	0.05	0.051	-	0.5	2	2	2
Copper	0.0312	0.0221	-	0.05	0.2	-	-
Nickel	0.0099	0.0094	-	0.1	0.2	0.2	1
Aluminium	0.17	0.22	-	0.1	5	10	15
Manganese	0.20	0.10	-	0.1	0.5	0.2	1

### **1.9.6 Review of membrane techniques in carwash sector (Commercial and modified membrane techniques)**

In Table 1.4, a summary of numerous studies on membrane techniques used for the treatment of wastewater from car washes is provided. Different commercial and synthesis membrane experimented with carwash effluents that have a various contaminants like detergents/surfactants, oil/grease and others.

Bruggen et al. [77], investigated seven types of commercial UF membranes with carwash effluents. Because of surfactants have a major role in membrane performance, so in this study, synthetic detergent solutions present in car wash effluents were employed. Three types of surfactants were utilized of detergents of the car washes: sodium dodecyl sulfate (SDS) as anionic surfactant, cetrimide as cationic surfactant, and Triton X-100® as nonionic surfactant. The results showed that the best performing membrane in terms of rejections of anionic, cationic, and nonionic surfactants were C100F and Ultrafilic UF Due to its molecular weight and molecular weight Cut-Off (MWCO) of these membranes.

In another study, Boussu et al. [78], showed that the desirable quality and the intended use (recycling or discharge) of the purified wastewater will determine whether to use UF or NF membranes. Four typical membranes were used; two types of UF membranes and the others are NF membrane; for analyzing COD and anionic, cationic and non-ionic surfactants of carwash wastewater. The authors concluded that with the proper membrane type (least membrane fouling) and process format (a hybrid process combining UF and/or a biological treatment with NF), membrane processes can be effective.

UF membrane would be the best option if use the purified wastewater for recycling and the surfactants presence doesn't cause a problem. In a related study - Boussu et al. [79] investigated the application of NF membrane in the carwash sector using two different NF membranes and revealed that the removal efficiency of NF membrane was 100 % at removing COD and surfactants. The membrane with the shortest (MWCO), NF270, had the highest retentions, which is consistent with the results. Anionic surfactants (Sodium dodecylbenzene sulfonate (SDBS)) are better retained than other

surfactants because the negative charges of the surfactant and the membrane surface are electrostatically attracted to one another.

In general, the rejection of membranes with decreasing pore sizes improves. Istirokhatun et al. [80] studied the applicability of four different commercial UF membranes with various molecular weight cut-off during filtration in a cross flow set up. In this study PES10 had the highest rejection for all pollutants, which is evident in the fact that this membrane has the smallest MWCO. The UF membranes have within 90–95 %, 78–100 %, and 100 % rejection with respect to COD, oil and grease, and turbidity; respectively.

The concentration of COD can indicate contaminants outside of the vehicle such as various composting dust, bird droppings, or fallen fruit. As well as detergents contributing to increased levels of COD in effluents and has been identified as COD in many studies [81, 82]. Lau et al. [81] investigated the treatment of effluents from carwash by using three various types of commercial polymeric membranes UF and NF, during filtration in a lab-scale cross flow unit and clarified that the COD removal depend on the properties of the membrane and the best removal (91.5 %) was gained by the NF270. In a similar study, Uçar [82], filtered carwash wastewater by four UF membranes of varying MWCO and one NF membrane. The COD measurements be made to specify the detergent in this study. Results showed that the COD removal efficiency corresponding to 97 % for NF membrane more than the UF membrane. Furthermore, these studies emphasize the importance of pre-treatment when using membranes for treatment carwash wastewater.

Polymeric modified membranes have been employed for solving issues relating to water treatment or water reuse due to their exceptional efficiency, cost-effectiveness, clean technology, and environmental friendliness by efficiently eliminating oil, grease, detergent, and a highly hazardous surfactant from car wash effluents [60, 83]. There are few studies on the use of modified membrane for the car wash wastewater treatment. Kiran et al. [84] were fabricated two membranes; polyethersulfone (PES) and Cellulose acetate (CA); using hydrophilic polymer sulfonated poly ether ether ketone (SPEEK) and nanoclay as bentonite and compared with commercial polyethersulfone (PES) membrane as a function of the removal of carwash effluent.

Table 1.4 – Car wash wastewater treatment methods based on commercial membranes

Membrane	Characteristics		Influent characteristics	Effluent characteristics	Ref.
	MWCO (kDa)	Material			
UF	100	Cellulose	Synthetic solutions: Nonionic surfactant 100 mg/L; Anionic surfactant 100 mg/L; Cationic surfactant 100 mg/L	Nonionic surfactant 55.9–94.6 mg/L; Anionic surfactant 48.3–90.1 mg/L; Cationic surfactant 5.2–83.3 mg/L	[77]
	150	PES			
	20	PES			
	10	PES			
	100	PVDF			
	250	PVDF			
	100	PAL			
UF	150	PES	COD 208–316 mg/L; Nonionic surfactant 26–39 mg/L; anionic surfactant 0–0.8 mg/L; cationic surfactant 4.3–7.9 mg/L	COD 192 mg/L; Nonionic surfactant 23 mg/L; anionic surfactant 0; cationic surfactant 7.3 mg/L	[78]
	100	PAL		COD ND; Nonionic surfactant 24 mg/L; anionic surfactant 0; cationic surfactant 3.9 mg/L	
NF	1.2	PES		COD 106 mg/L; Nonionic surfactant 21 mg/L; anionic surfactant 0.4 mg/L; cationic surfactant 0.9 mg/L	
	0.17	polyamide		COD 10 mg/L; Nonionic surfactant 1 mg/L; nionic surfactant 0.1 mg/L; cationic surfactant 0.2 mg/L	
NF	0.17	polyamide	SS 60–140 mg/L; COD 208–382 mg/L; nonionic surfactant 32–51 mg/L; Anionic surfactant 0.7–2.5 mg/L; cationic surfactant 1.7–3.7 mg/L	COD 33–100 mg/L	[79]
	1.2	PES			
UF	10	PES	COD 700 mg/L; O&G 36 mg/L; turbidity 186.6 NTU	COD 33.3–40 mg/L; Turbidity 0.22–0.25 NTU; O&G 0–2 mg/L	[80]
	25	PS		COD 40–70 mg/L; turbidity 0.24–0.57 NTU; O&G 2–8 mg/L	
	50	PS			
	100	PS			
UF	1	polyamide	pH 7.3; COD 314 mg /L; EC 729 $\mu$ S/cm; $PO_4^{3-}$ -P 9.05 mg/L	pH 7.34– 7.59, COD 64.5–85.5 mg/L; EC 523– 629 $\mu$ S/cm; $PO_4^{3-}$ - P < 1 mg/L	[82]
	5	PES			
	10	PES			
	50	PAN/Ultrafilic			
NF	0.2–0.4			pH 7.61; COD 8.1 mg/L; EC 391 $\mu$ S/cm; $PO_4^{3-}$ -P < 0.05 mg/L	
UF	100	PVI difluoride	COD 75.0–738.0 mg/L; Turbidity 34.7–86.0 NTU; TDS 89.2–151.8 mg/L; EC 138.8–260.7 $\mu$ S/m	COD 56.11–82.41 mg/L; turbidity 92.37–96.85 NTU; TDS 13.59–16.56 mg/L; EC 16.9–19.6 $\mu$ S/m	[81]
	30	PES		COD 54.85–83.89 mg/L; turbidity 97.27–97.34 NTU; TDS 17.61–31.45 mg/L; EC 23.57–35.44 $\mu$ S/m	
NF	0.3	polyamide		COD 70.9–91.49 mg/L; turbidity 94.42–98.75 NTU; TDS 59.99–61.53 mg/L; EC 61.92–63.62 $\mu$ S/m	

A higher flux for CA/SPEEK/bentonite membrane (52.3 L/m<sup>2</sup>h) was observed more than the commercial PES membrane (41.5 L/m<sup>2</sup>h). Also, the higher rejection 60 % COD and 82 % turbidity was gained for CA/SPEEK/bentonite membrane. FTIR study found that commercial PES (10 kDa) has higher binding affinity with carwash effluent.

Also, Kamelian et al. [85] preparation 10 types of acrylonitrile-butadiene-styrene (ABS) membranes with pore size ranged between (82.4–113.9 μm) and revealed that the removal of turbidity, COD and solids all increased with pore size decreasing, and this achieves the fact that the removal efficiency rises in the membranes with smaller pore size.

### **Conclusion to the chapter 1**

In conclusion, post-polymerization functionalization (post-modification) is a fairly simple and effective way to introduce various functional groups into the backbone of conjugated polymers (including PVC), which usually does not lead to a change in the length of the polymer chain. Therefore, the resulting polymers usually differ from the original ones only in the attached groups or side chains, which affects their properties.

As is it was shown above, PVC is susceptible to functionalization with fragments of *N*-, *O*-, *S*-centered nucleophiles in solutions, which leads to the formation of its corresponding derivatives with varying degrees of substitution of chlorine atoms. This method is also used to dechlorinate PVC-containing waste during recycling. Considering that PVC and its derivatives are widely used to create materials for various applications, including the production of membranes for water treatment, the search for new approaches for the synthesis of polymer materials with improved and new characteristics remains an urgent research task.

The main disadvantages of modifying PVC in solution include: likelihood obtaining PVC derivatives with low solubility and the occurrence of side processes of dehydrochlorination, leading to the formation of ethylene fragments, as well as a long reaction time.



In the course of this work, the possibilities of modifying PVC with certain reagents were investigated both in solutions and under mechanical synthesis conditions, however, chemical modification of PVC under ball-milling conditions has not studied so far, which consists of contacting the reagents under conditions of mixing and grinding in a ball mill (BM), with ~ 35 % of steel balls (10 cm diameter) loaded into a steel milling jar with a capacity of 50 ml, at a rotation speed of 500 rpm.

PVC and other polymer materials have various applications including the the synthesis of membranes for application in the treatment of wastewater. Among these membarenes the ultrafiltration ones have such advantages as simplisity, various sizes availability, high effisiensiy of water separation/purification even at low pressure and otheres.

## **Chapter 2. Experimental Studies of The Synthesis of Functionalized PVC Derivatives**

### **2.1 Features of Post-Modification of Polymers**

Post-functionalization is a fairly simple and efficient way to introduce different functional groups into the base of conjugated polymers, which usually does not result in a change in the length of the polymer chain. Therefore, the resulting polymers usually differ from the original ones only in the attached groups or side chains, which has an impact on their properties. As is known, PVC is subject to functionalization by fragments of *N*-, *O*-, *S*- nucleophiles in solutions, leading to the formation of its corresponding derivatives with different degrees of substitution of chlorine atoms.

This method is also used to dechlorinate PVC-containing waste during its disposal. Among the known disadvantages of PVC modification in solutions are: the possibility of obtaining PVC derivatives with low solubility and the course of dehydrochlorination side processes leading to the formation of ethylene fragments, as well as a long reaction time.

Thus, given that PVC and its derivatives are widely used in the creation of materials for various applications, including the manufacture of membranes for water treatment, the search for new approaches to the synthesis of polymeric materials based on it, suitable for the manufacture of UF membranes, is an urgent research task.

### **2.1 Laboratory support for experimental research**

Experiments on the synthesis of PM PVC derivatives were carried out in a chemical laboratory equipped with special utensils and devices, including the following equipment necessary for research:

- Distiller brand АДЭа-4;
- Drying cabinet brand ШС-3;
- Photocolorimeter brand КФК-2;
- Ionometric pH meter-converter И-500, made by Akvilon;
- Hot plate stirrer;
- Planetary Ball mill (Retsch PM100) using a 50 ml stainless steel reactor with 4 stainless steel grinding balls of size 10 mm loaded into it.

$^1\text{H}$  NMR spectra were recorded at room temperature using a Bruker Avance-400 (or Bruker Avance-500) spectrometer, 298 K, resolution  $\pm 0.01$  ppm, internal TMS standard. GPC measurements were carried out on an Agilent 1200 chromatograph with an erosol light scattering detector (ELSD) (Agilent technologies, USA) and an Agilent Resipore column,  $300 \times 7.5 \text{ mm}^{-2}$  pcs. in a series. Infrared spectroscopy (IR) was executed through FTIR instrument (model: ALPHA IR Fourier Spectrometer, Bruker), taken using a  $500\text{--}4000 \text{ cm}^{-1}$  spectrum.

All materials, reagents and solvents used were purchased from commercial suppliers and used without further purification, which presented in Table 2.1.

Table 2.1 – Data on commercial PVC, reagents and solvents

Name	Chemical formula, characteristics
Polyvinylchloride (PVC)	$(\text{C}_2\text{H}_3\text{Cl})_n$ . MM. = 65 kg/mol; white granules; $\rho=1380 \text{ kg/m}^3$
Dimethylformamide (DMF)	$(\text{CH}_3)_2\text{N}-\text{C}(=\text{O})\text{H}$ , colorless liquid, solvent, $\rho=945 \text{ kg/m}^3$ ; boiling point $153 \text{ }^\circ\text{C}$
Calcium carbonate (potash)	$\text{K}_2\text{CO}_3$ , white powder alkaline reagent
Cyclohexanone	$(\text{CH}_2)_5\text{CO}$ , colorless oily liquid, solvent, $\rho=948 \text{ kg/m}^3$ , boiling point $153 \text{ }^\circ\text{C}$
Ethanolamine <b>2</b>	<i>N</i> -nucleophile, $\text{C}_2\text{H}_7\text{NO}$ , amino alcohol, oily liquid, miscible with water, alkaline properties, $\rho=1012 \text{ kg/m}^3$ , boiling point $170 \text{ }^\circ\text{C}$
Ethylenediamine <b>3</b>	<i>N</i> -nucleophile, $\text{C}_2\text{H}_8\text{N}_2$ , liquid $\rho=899 \text{ kg/m}^3$ . boiling point $119 \text{ }^\circ\text{C}$ .
Na-salts of azoloazines <b>7, 8</b>	<i>N</i> -nucleophiles, heterocyclic compounds consisting of two nitrogen-carbon rings: a five-membered azole and a six-membered azine, Na-salt
Potassium phthalimide <b>11</b>	<i>N</i> -Nucleophile, $\text{C}_8\text{H}_4\text{KNO}_2$ , loose crystals of weak basicity
<i>p</i> -Substituted phenols <b>13, 14</b>	<i>O</i> -Nucleophiles, 4- <i>n</i> -octylphenol <b>13</b> , 4- <i>n</i> -heptylphenol <b>14</b>
Thiophenols <b>17, 18, 19</b>	<i>S</i> -Nucleophiles, thiophenol <b>17</b> , <i>tert</i> -butylthiolphenol <b>18</b> , <i>tert</i> -octylthiolphenol <b>19</b>

The reagent numbers in Table 2.1 correspond to their numbering in the synthesis schemes of modified PVC derivatives shown below.

## 2.2 Description of Methods and Characteristics for Synthesis of PVC Derivatives Modified by *N*- and *S*- Nucleophiles

The study of the possibility of obtaining new PVC derivatives was carried out using two different approaches to synthesis, namely: a) in a solvent environment and b) mechanosynthesis, that is, under ball grinding conditions with micro-addition of solvent.

### A) Method for the synthesis of PVC derivatives in solution:

About 50 ml of one of the solvents (DMF or cyclohexanone) was placed in a glass flask equipped with gas inlet and outlet tubes, stirring was turned on, and in small portions as dissolution progressed the following was loaded: 0.5 g of PVC, a 2-fold stoichiometric excess of the test modifying nucleophilic reagent (relative to 100% chlorine content in PVC) and 1.6 g  $K_2CO_3$ . The flask was placed in an oil-bath, the argon supply was turned on, and the mixture of components was heated to 60–80 °C with stirring. Next, the mixture was kept at this temperature and in an argon atmosphere for 12–24 hours. The resulting reaction mixture was cooled and poured into a glass beaker containing 150 ml of a cold mixture of methanol and distilled water in a ratio of 2:1. The resulting precipitate of the reaction product was filtered and washed on the filter three times with 10 ml of a mixture of methanol and distilled water in a ratio of 2:1. The resulting paste-like mass was purified several times by dissolving it in THF or DMF and reprecipitation from methanol, the precipitate formed was filtered, washed with methanol and air-dried for 24 hours.

### B) Method for the synthesis of PVC derivatives by mechanosynthesis:

The following was loaded into a 50 ml stainless still ball mill drum, containing four 10 mm stainless still milling balls: 0.5 g of PVC, a 20-fold stoichiometric excess of the corresponding nucleophilic reagent (relative to the 100% chlorine content in PVC), 0.8 g of  $K_2CO_3$ . After that few drops of DMF or cyclohexanone were added and the resulting mixture was ball-milled at 500 rpm for 4-hours.

After every hour of the reaction, the mill was stopped and a visual inspection of the reaction mass in the drum was carried out. After the external change in the reaction mixture ceased, the mill was stopped, the polymer was unloaded from the drum and purified from accompanying impurities: excess  $K_2CO_3$ , KCl salt formed as a result of

dehydrochlorination of PVC, as well as excess PVC modifier reagent. To do this, the resulting mixture was washed several times with small portions (10–15 ml each) of a mixture of methanol and distilled water in a ratio of 2:1 until the pH of the washing mixture was ~7. To completely wash the polymer from impurities, it was pre-mixed with methanol diluted with water, and then filtered from the washing solution after each washing. The resulting solid was purified several times by dissolving it in THF or DMF and reprecipitation from methanol, the precipitate formed was filtered, washed with methanol and air-dried for 24 hours.

## **2.4 Investigation of the possibility of modification of PVC with fragments of *N*- and *S*-nucleophiles**

### **2.4.1 The effect of ball grinding on the PVC structure**

The possibility of modifying PVC was investigated both by carrying out the reaction in a solvent environment and by the method of mechanochemistry, which consists of contacting PVC and reagents under conditions of mixing and grinding in a drum ball mill, with ~ 35 % steel loaded into the drum balls with a diameter of 10 mm, when rotating a 50 ml drum at a speed of 500 rpm.

As a first step stage, in order to study the effect of ball milling on the properties, commercial PVC (MW = 65 kg/mol) was processed in a ball mill at 500 rpm for 4–12 hours. Using gel permeation chromatography (GPC) (Figure 2.1) and <sup>1</sup>H NMR spectroscopy (Figure 2.2), it was found that ball milling does not lead to the destruction of the main chain or dehydrochlorination of PVC, since no change in its molecular weight and changes in the spectra were observed <sup>1</sup>H NMR.

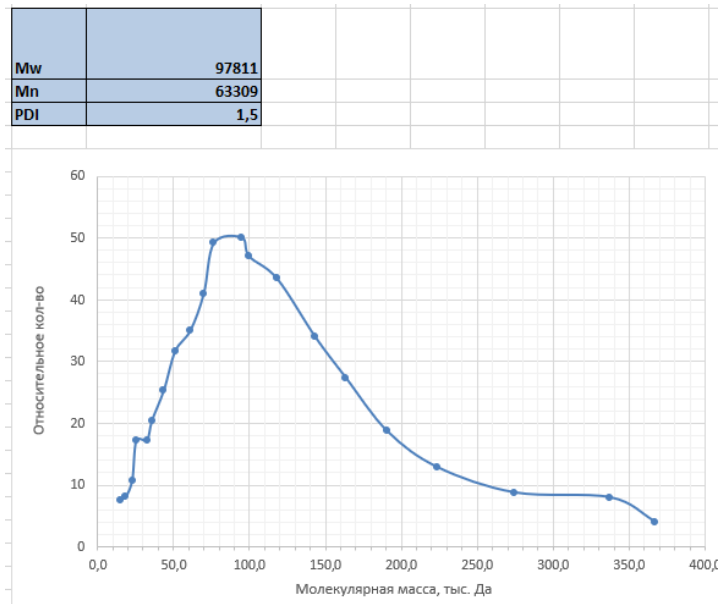


Figure 2.1 – GPC Data of polymer **2.1** after ball-milling

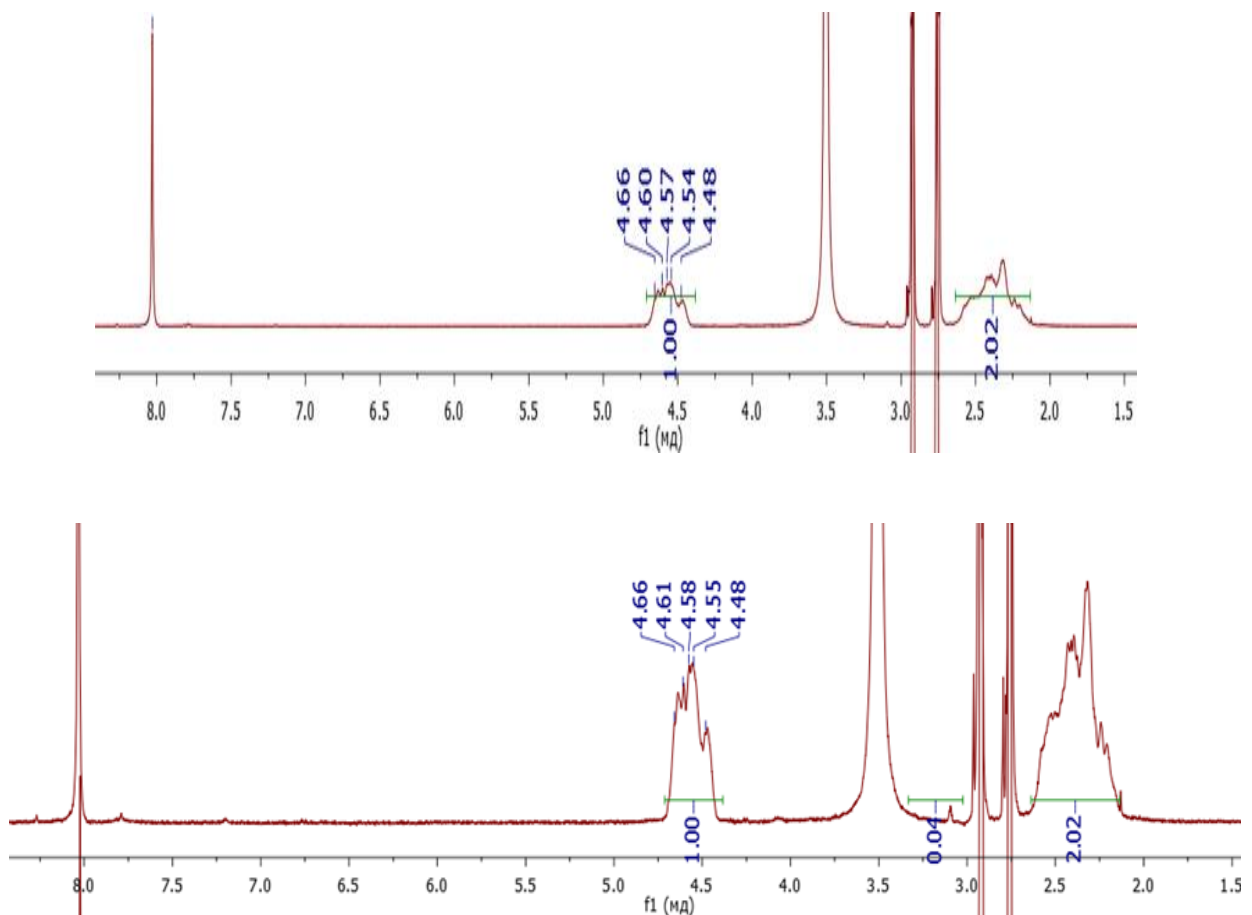


Figure 2.2 – Comparison of <sup>1</sup>H NMR (DMF-d<sub>7</sub>) of PVC **2.1** before (top) and after (bottom) ball-milling at 500 rpm for 4 h

As a next step, the interaction of PVC with *N*-, *O*-, *S*-nucleophiles in solutions and under mechanical synthesis conditions was studied.

### 2.4.2 Study of PVC functionalization with *N*-nucleophile fragments

Several *N*-nucleophiles were selected to study the functionalization of PVC. Thus, it was found that the interaction of PVC with ethanolamine or ethylenediamine in a DMF solution in the presence of  $K_2CO_3$  upon heating at 80 °C for 12 hours does not lead to substitution products, leading only to partial dehydrochlorination product **2.6** (Figure 2.3).

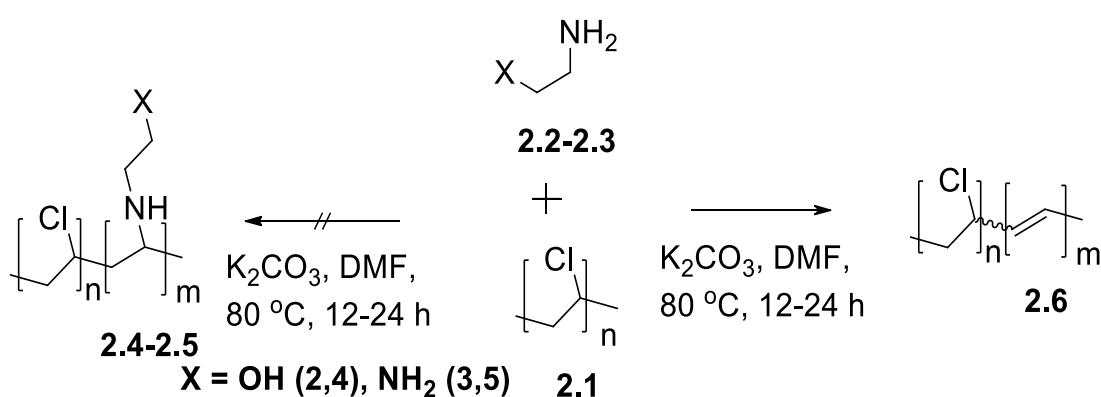


Figure 2.3 – Scheme of functionalization of PVC with *N*-nucleophiles

The formation of dichlorination product suggested based on  $^1\text{H}$  NMR data, such as presence of signals of protons at the  $sp^2$ -hybridized carbon atoms as multiplets around 5.10–5.25 ppm (Figure 2.3) along with the signals of the remaining protons of PVC moiety as multiplets around 4.50–4.75 ppm (Figure 2.4).

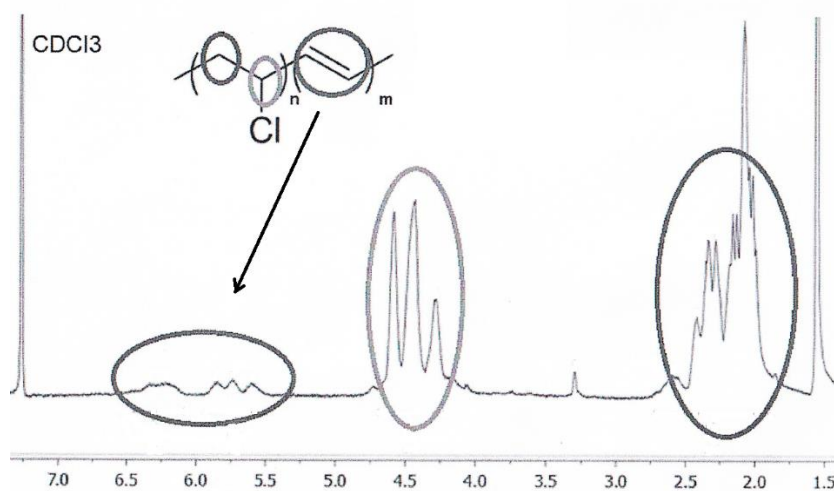


Figure 2.4 –  $^1\text{H}$  NMR (in  $\text{CDCl}_3$ ) of polymer **2.6**

Based on the literature [86] potassium or sodium azolium salts are common *N*-nucleophiles for the PVC modification.

So far, no examples of modification of PVC with azine-based *N*-nucleophiles were reported. Therefore, as a next step the functionalization of PVC with preliminary prepared Na-salts of azoloazines **2.7**, **2.8** in a DMF solution were studied (Figure 2.5). However, no substitution of chlorine atoms was observed and only unchanged PVC was isolated.

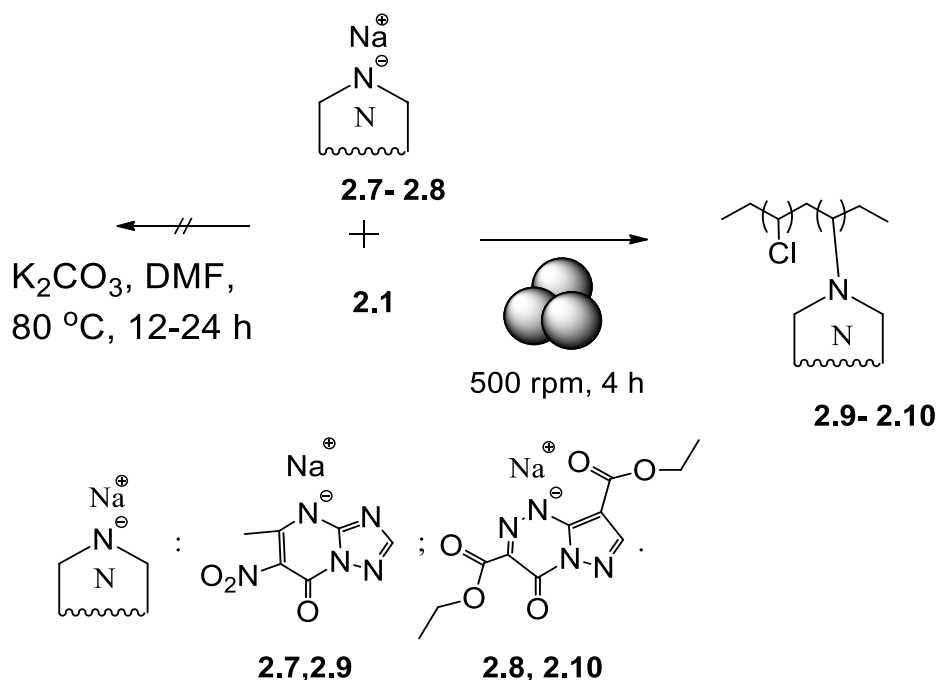


Figure 2.5 – Scheme of modification PVC with sodium salts of azoloazines **2.7-2.8**

From another hand the use of mechanosynthesis turned out to be effective for the post-modification of various polymers. At the very beginning the optimization of the reaction conditions was carried out. Thus, no reaction was observed under ball-milling at 100-400 rpm even at 8 hours, and only unreacted PVC was isolated. While at 500 rpm in 4 hours azoloazine-modified PVCs **2.9** and **2.10** were obtained in the form of light yellow and brown solids, respectively (Figure 2.5). In the  $^1\text{H}$  NMR spectra of these polymers (Figure 2.6), one can note the presence of signals from the protons of azoloazine fragments in the form of single-proton singlets in the region of 8 ppm (CH-azole), as well as signals from substituents of azine fragments. In addition, characteristic signals of protons of PVC fragments were observed in the form of multiplets at 4.42–4.75 ppm.



(CH<sub>2</sub>CHXCH<sub>2</sub> (X = Cl, Het) (Figure 2.6). According to <sup>1</sup>H NMR the modification degree was 15% for (**2.9**) and 20% for (**2.10**). The degree of modification was estimated from the ratio of integral intensities of unsubstituted CHX groups (X = Cl or azaheterocycle) of main chain of PVC versus integral intensity of peaks of protons of CH group of azoleazine substituents. In addition, to confirm the loading of azoloazine moieties into PVC core in polymers **2.9** and **2.10** their GPC analysis was carried out. Based on the GPC data the M<sub>n</sub> of polymer **2.9** was 104.7 kDa (PDI = 1.4) and for polymer **2.10** M<sub>n</sub> = 80.4 kDa (PDI = 1.4), which is higher than M<sub>n</sub> starting PVC (M<sub>n</sub> ~ 65 kDa). Finally, based on the data of elemental analysis, a reducing of Cl content compare to starting PVC along with an increasing the content of nitrogen in polymer samples takes place, and the data of elemental analysis in 3 parallels were very close (ca 0.3%) to each other, which confirms the similarity of polymer composition in the whole polymer volume. It worth to mention that the alkylation reaction of azoloazines in many cases affords a mixture of *N*-alkylated derivatives with the alkyl fragments introduced into azole- and/or azine moiety. And in case of above-mentioned polymers **2.9**, **2.10** one may also assume the formation of a mixture of *N*-alkylated products.

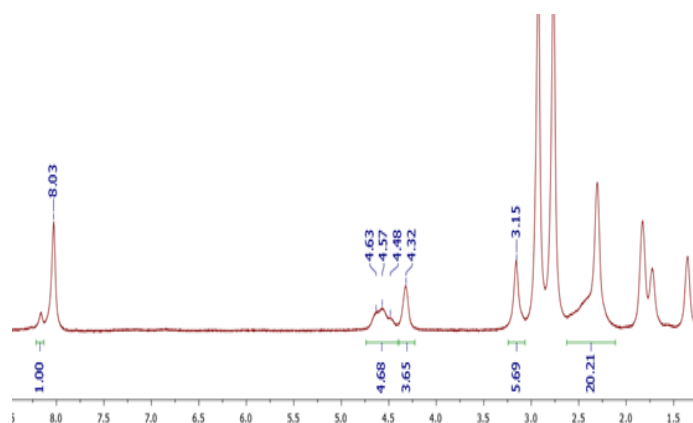


Figure 2.6 – <sup>1</sup>H NMR (DMF-d<sub>7</sub>) of polymer **2.10**

Based on the fact that both azaheterocycles have proven biological activity, namely antiviral **2.7** [87] or antidiabetic **2.8** [88] activity, the resulting polymers **2.9** – **2.10** can be considered as examples of so called polymer drugs. However, some additional biological studies will be needed.

Potassium phthalimide **2.11** is another typical *N*-nucleophile, and it has been used for the PVC modification in solution [4], and as a final step the reaction between PVC and **2.11** under mechanical conditions was studied. Thus, under ball-milling for 4 hours at 500 rpm polymer **2.12** was obtained (Figure 2.7). The structure of polymer was confirmed by means of  $^1\text{H}$  NMR (Figure 2.8) and GPC.

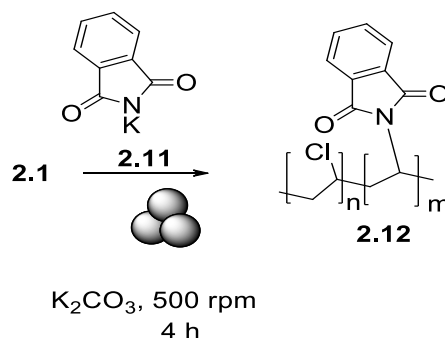


Figure 2.7 – Scheme of modification PVC with potassium phthalimide

Thus, in  $^1\text{H}$  NMR (Figure 2.8) the signals of protons of phenylene moiety were observed as multiplet in the area of 7.1–7.65 ppm was observed along with signals of protons of PVC moiety, such as characteristic multiplets of  $(\text{CH}_2\text{CHXCH}_2)$  moiety as multiplets around 4.50–4.75 ppm. According to GPC data, modification of PVC the number-average molecular weight for polymer **2.12**  $M_n = 97$  kDa (PDI = 1.54).

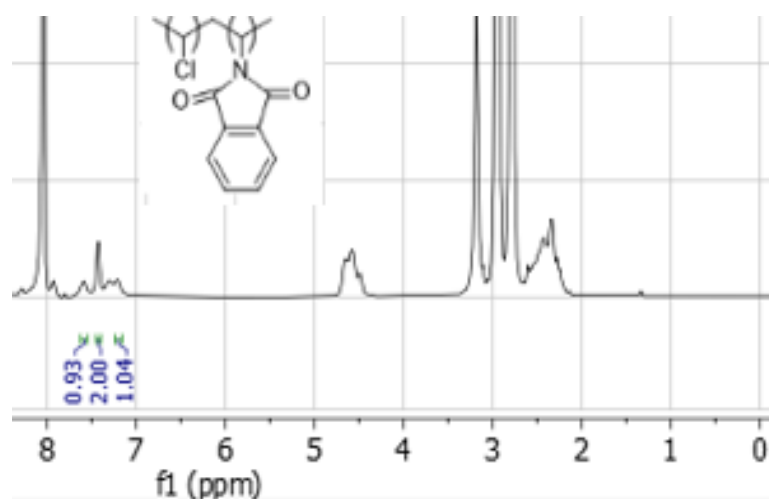


Figure 2.8 –  $^1\text{H}$  NMR (DMF- $d_7$ ) of polymer **2.12**

In conclusion, it was demonstrated that the use of mechanochemistry makes it possible to effectively carry out post-modification of PVC with fragments of such atypical

*N*-nucleophiles as phthalimide or cyclic azines. In the latter case, representatives of the so-called polymer drugs were obtained.

### 2.4.3 Study of the interaction of PVC with some *O*-nucleophiles

In the course of continuing research, the possibility of functionalizing PVC with fragments of some *O*-nucleophiles, namely para-substituted phenols, was studied under mechanosynthesis conditions. Thus, the reaction of PVC with phenols **2.13–2.14** in the presence of  $K_2CO_3$  under ball-milling conditions at 500 rpm for 4 hours was carried out. As a result of the experiment, colorless precipitates were obtained, which apparently represent inclusion compounds with a phenol content of up to 10% (according to  $^1H$  NMR data), since according to GPC data there was no increase in the molecular weight of the expected reaction products, namely polymers **2.15–2.16**. Thus, under mechanical synthesis conditions no formation of *O*-modified PVC products was observed (Figure 2.9).

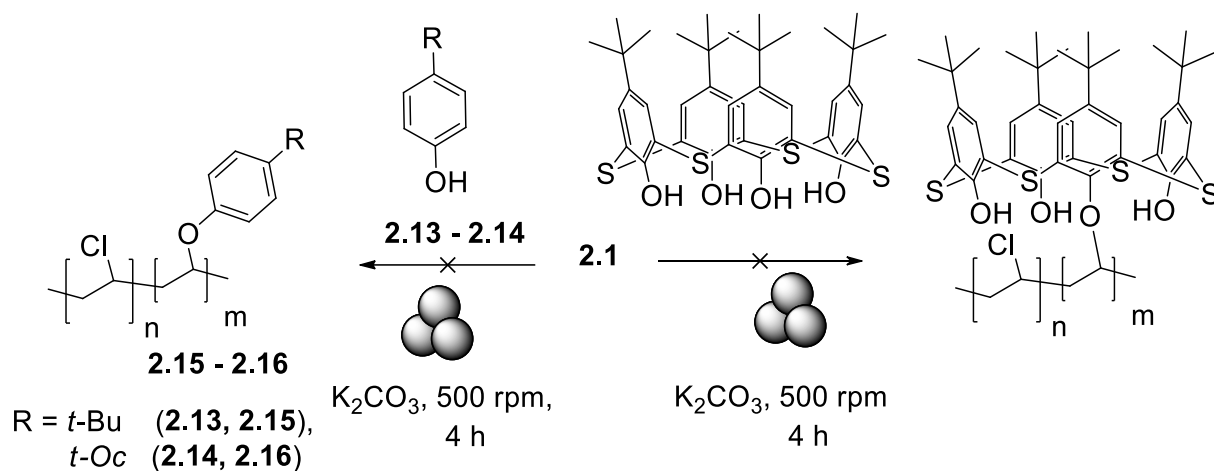


Figure 2.9 – Attempts of the modification of PVC with fragments of *O*-nucleophiles

The applicability of mechanosynthesis was also studied in the reaction of PVC with thiocalix[4]arene – in the presence of  $K_2CO_3$  under mechanical grinding conditions at 500 rpm for 4 hours no PVC modification product was observed.

### 2.4.4 Study of PVC functionalization with *S*-nucleophile fragments

Perhaps the most common synthons used to modify PVC in solutions are *S*-nucleophiles, in particular thiophenols. As part of the work, the possibilities of modifying

PVC with fragments of thiophenols **2.17**– **2.22** were investigated under mechanical synthesis conditions under ball-milling at 500 rpm in the presence of  $K_2CO_3$  for 4 hours (Figure 2.10). Additionally, polymeric Schiff bases **2.31**, **2.32** were synthesized by reacting PVC with preliminary prepared Schiff bases **2.29**, **2.30** under ball-milling at 500 rpm in the presence of  $K_2CO_3$  for 4 hours (Figure 2.10). All polymers had the form of dark yellow sediments.

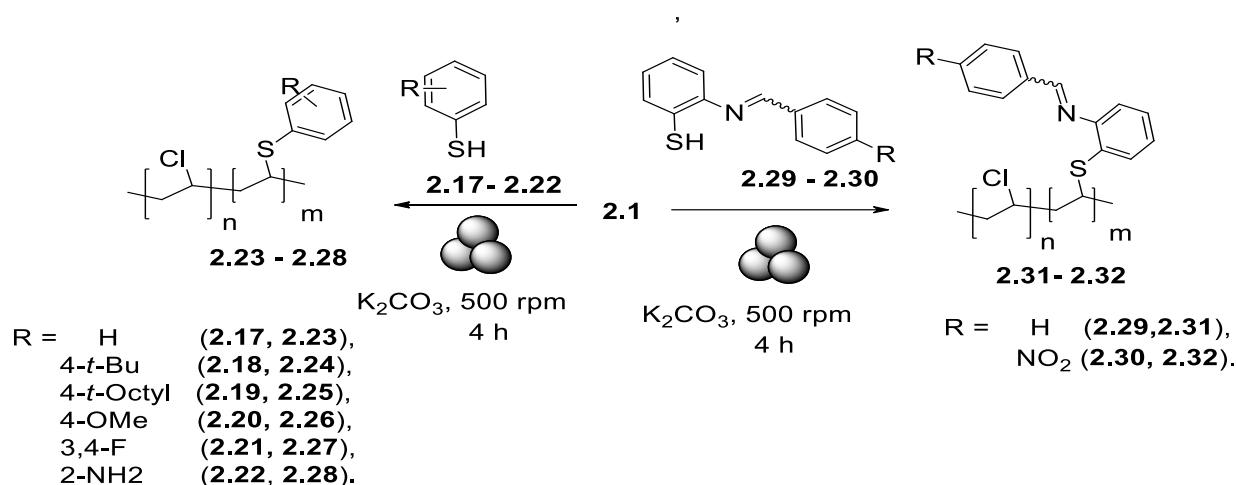


Figure 2.10 – Scheme of modification PVC with S-Nucleophiles

In the  $^1H$  NMR spectra of polymers **2.23**–**2.28**, along with the resonance signals of the CHX protons (X = Cl or S-aryl) of PVC fragments, observed in the form of multiplets at 4.45–4.75 ppm, there are resonance signals of the protons of aromatic fragments in the form of multiplets in the region 7.20–7.65 ppm. According to GPC data, modification of PVC leads to an increase in the number-average molecular weight for polymer **2.23** to  $M_n = 100.96$  kDa (PDI = 1.37), polymer **2.24** to  $M_n = 105$  kDa (PDI = 1.42), polymer **2.26** to  $M_n = 135.42$  kDa (PDI = 1.26), and for polymer **2.27** to  $M_n = 125$  kDa (PDI = 1.36).

In the  $^1H$  NMR spectra of polymer Schiff bases **2.31**, **2.32**, in addition to the resonance signals of the protons of the CHX fragments (X = Cl or S-aryl) and the S-aryl substituent, there are characteristic resonance signals of the N=CH protons of the azomethine fragment in the form of a singlet around 9.00 ppm, as well as resonance signals of protons of aromatic substituents of the azomethine fragment. According to GPC data, the  $M_n$  of the resulting polymer was 120 kDa (PDI = 1.4) for **2.31**, 122 kDa (PDI = 1.3) for **2.32**.

The possibility of modifying PVC with fragments of  $\alpha$ -aminomethylphosphonates was also investigated. To do this, a four-component reaction was carried out between PVC, *o*-aminothiophenol **2.22**, diethylphosphonate **2.33** and benzaldehyde **2.34** in the presence of  $K_2CO_3$  under ball milling conditions at 500 rpm for 4 hours (Figure 2.11).

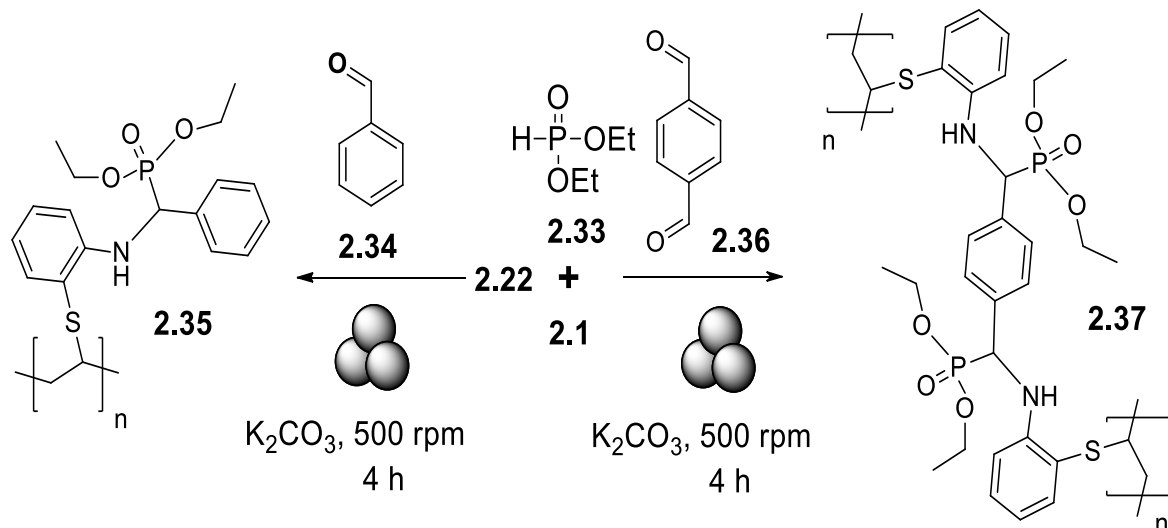


Figure 2.11 – Scheme of Kabachnik–Fields reaction

The resulting polymeric  $\alpha$ -aminomethylphosphonate **2.35** was isolated as a dark brown precipitate and characterized by  $^1H$  NMR and IR spectroscopy (Figures 2.12–2.13).

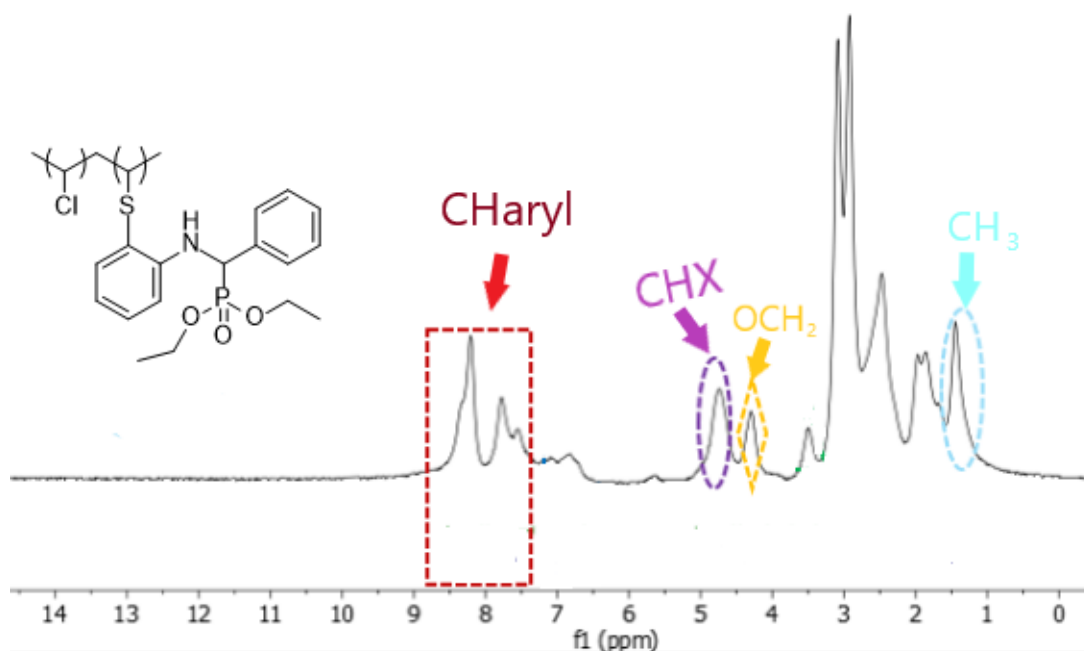


Figure 2.12 –  $^1H$  NMR ( $DMF-d_7$ ) of polymer **2.35**

Thus, the  $^1\text{H}$  NMR spectrum contains signals of aromatic fragments in the form of a multiplet at 7.25–7.55 ppm, a proton resonance signal at the  $sp^3$ -hybridized carbon atom of the aminomethylphosphonate fragment in the form of a broadened singlet at 3.75 ppm, and resonance signals of the protons of the  $\text{OCH}_2\text{CH}_3$  group in the form of a multiplet at 4.14 ppm and a multiplet at 1.20 ppm.

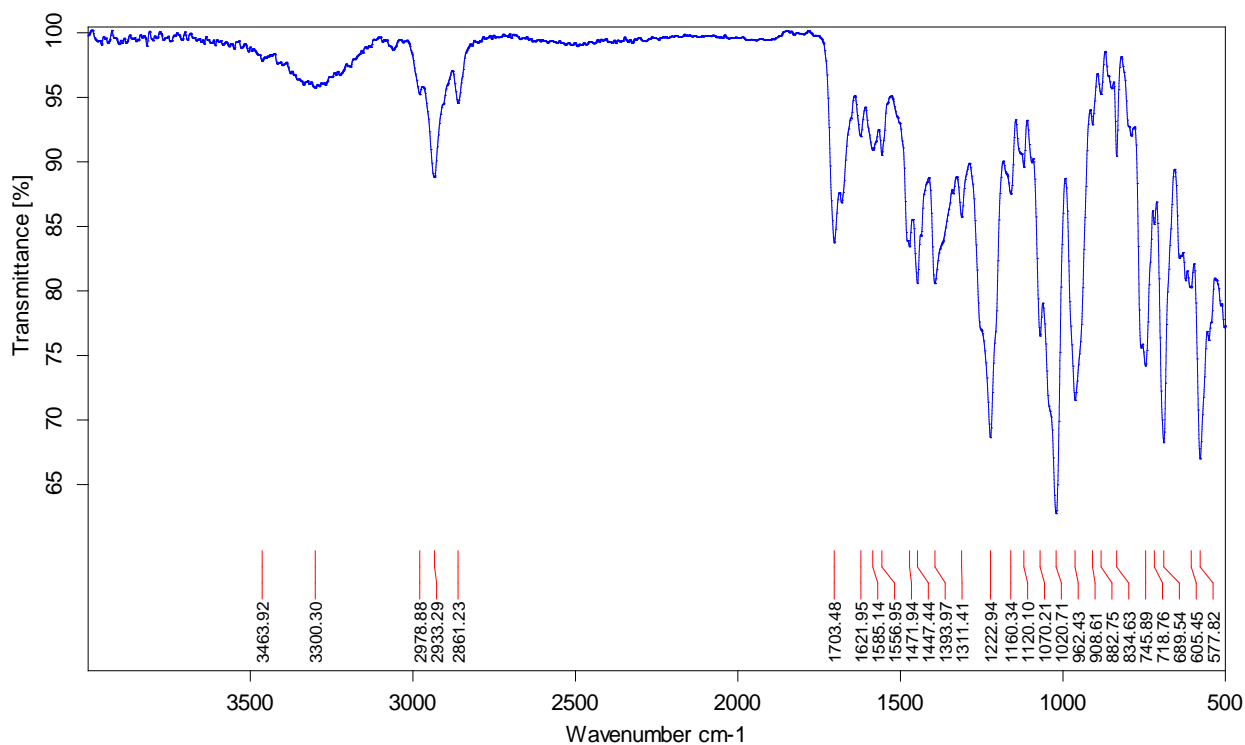


Figure 2.13 – IR spectra of polymer **2.35**

In the IR spectra, absorption bands of the  $\text{P}=\text{O}$  group were observed at  $1165\text{ cm}^{-1}$ , as well as absorption bands of  $\text{P}-\text{C}-\text{O}$  fragments at  $1055\text{ cm}^{-1}$ ,  $\text{OCH}_3$  at  $2960\text{ cm}^{-1}$  and  $\text{NH}$  of the amide fragment at  $3460\text{ cm}^{-1}$ . According to GPC data, the  $M_n$  of the resulting polymer **2.35** was 93 kDa (PDI = 1.42).

Also, as part of the work, an attempt was made to obtain a cross-linked polymer  $\alpha$ -aminomethylphosphonate, namely polymer **2.37**, by a four-component reaction between PVC, *o*-aminothiophenol **2.22**, diethylphosphonate **2.33** and terephthalaldehyde **2.36** under ball-milling at 500 rpm for 4 hours (Figure 2.11). As a result, a colorless precipitate was obtained, insoluble in organic solvents.

Next, the possibility of introducing a fragment of a component of a number of biologically active substances benzo[d]thiazol-2-thiol **2.38** [89], into PVC was

investigated. As a result, azole-modified PVC **2.39** was obtained in the form of a yellow precipitate (Figures 2.14, and 2.15).

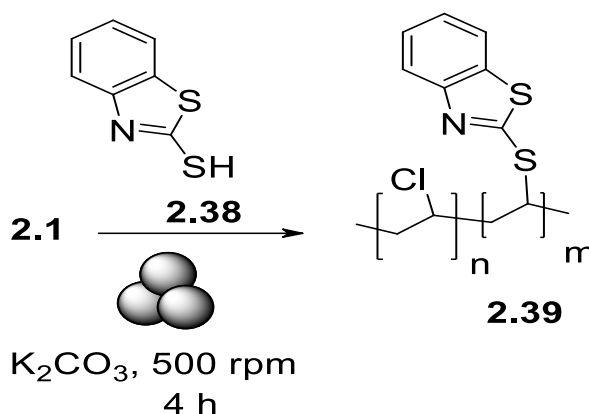


Figure 2.14 – Scheme of interaction PVC with benzo[d]thiazol-2-thiol

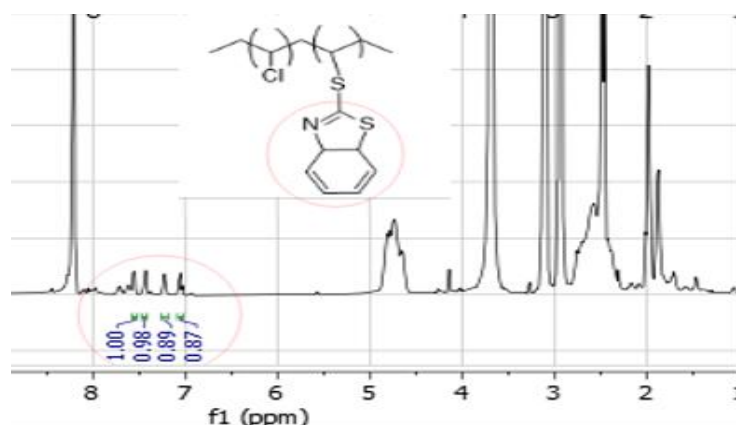


Figure 2.15 –  $^1\text{H}$  NMR (DMF- $d_7$ ) of polymer **2.39**

Polymers based on iptycenes are of interest for porous materials for separation and adsorption technologies [90]. As part of the work, the possibility of introducing fragments of triazatriptycene, 1,2,4-triazine-3-thione **2.40**, into PVC was investigated. To do this, interaction between PVC and **2.40** was carried out under ball-milling conditions at 500 rpm for 4 hours in the presence of  $\text{K}_2\text{CO}_3$  (Figure 2.16). As a result, tryptycene-substituted PVC **2.41** was obtained.

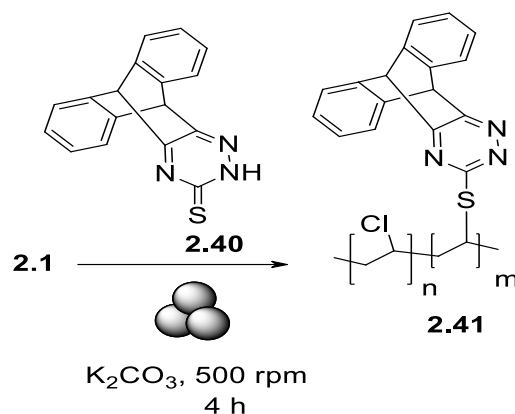


Figure 2.16 – Scheme of interaction PVC with triazatriptcene

The resulting polymer was isolated as a green-yellow precipitate and characterized by  $^1\text{H}$  NMR (Figure 2.17).

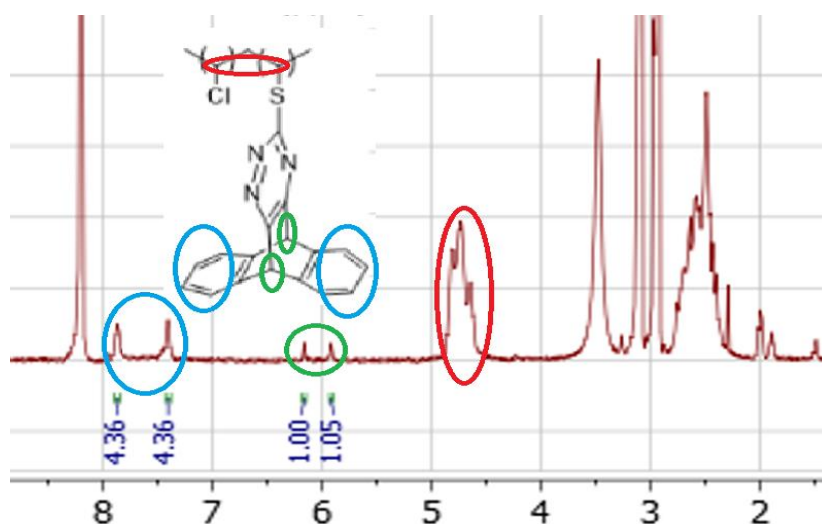


Figure 2.17 –  $^1\text{H}$  NMR (DMF- $d_7$ ) of polymer **2.41**

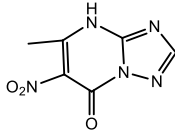
Thus, in the NMR spectrum of polymer **2.41** there are characteristic signals of protons of PVC fragments in the form of multiplets at 4.42–4.75 ppm ( $\text{CH}_2\text{CHXCH}$  ( $\text{X} = \text{Cl}$ ,  $-\text{SAr}$ )), as well as signals of the triptycene fragment in the form of two multiplets, namely signals of the protons of the iptycene fragment in the form of two singlets in the region of 5.23 ppm and 5.56 ppm and two multiplets in the region of 7.10–7.12 ppm and 7.52–7.754 ppm. According to GPC data, the molecular weight of the polymer **2.41** was  $M_n = 107$  kDa (PDI = 1.38).



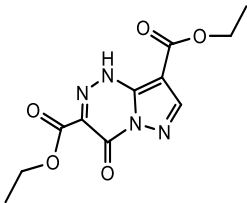
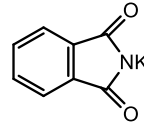
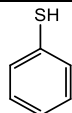
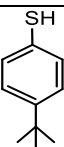
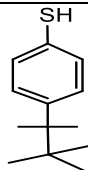
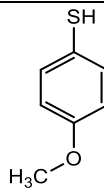
## 2.4.5 Results of analysis of post-modification PVC derivatives

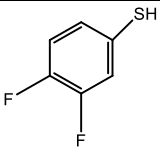
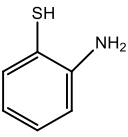
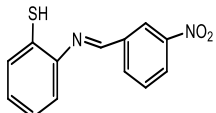
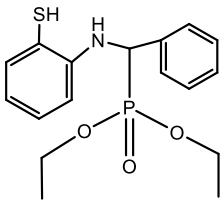
In Table 2.2, illustrate the characteristics of obtained post modified PVC derivatives by mechanosynthesis.

Table 2.2 – Characteristics of post-modification of PVC derivatives by nucleophilic reagents under mechanosynthesis conditions

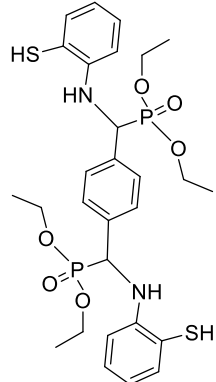
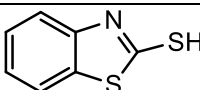
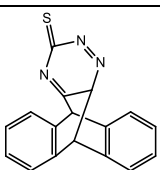
Polymers' Numbers	Name of the nucleophile	Compounds' Structure	Method for confirm polymer structure
1	2	3	4
Polymer <b>2-9</b>	5-methyl-6-nitro-[1,2,4]triazolo[1,5-a]pyrimidin-7(4H)-one		<sup>1</sup> H NMR, GPC, IR

Continuation of the table 2.2

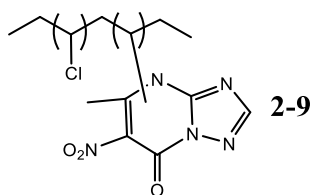
1	2	3	4
Polymer <b>2-10</b>	diethyl 4-oxo-1,4-dihydropyrazolo[5,1-c][1,2,4]triazine-3,8-dicarboxylate		<sup>1</sup> H NMR, GPC, IR
Polymer <b>2-12</b>	potassium 1,3-dioxoisindolin-2-ide		<sup>1</sup> H NMR, GPC, IR
Polymer <b>2-23</b>	3-mercaptobenzene-1-ylum		<sup>1</sup> H NMR, GPC, IR
Polymer <b>2-24</b>	4-(tert-butyl)benzenethiol		<sup>1</sup> H NMR, GPC, IR
Polymer <b>2-25</b>	4-(tert-octyl)benzenethiol		<sup>1</sup> H NMR, GPC, IR
Polymer <b>2-26</b>	4-methoxybenzenethiol		<sup>1</sup> H NMR, GPC, IR

Polymer 2-27	3,4-difluorobenzenethiol		<sup>1</sup> H NMR, GPC, IR
Polymer 2-28	2-aminobenzenethiol		<sup>1</sup> H NMR, GPC, IR
Polymer 2-32	2-((3-nitrobenzylidene)amino)benzenethiol		<sup>1</sup> H NMR, GPC, IR
Polymer 2-35	diethyl (((2-mercaptophenyl)amino)(phenyl)methyl)phosphonate		<sup>1</sup> H NMR, GPC, IR

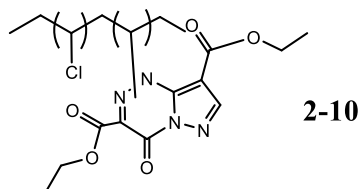
Continuation of the table 2.2

1	2	3	4
Polymer 2-37	tetraethyl (1,4-phenylenebis(((2-mercaptophenyl)amino)methylene))bis(phosphonate)		<sup>1</sup> H NMR, GPC, IR
Polymer 2-39	benzo[d]thiazole-2-thiol		<sup>1</sup> H NMR, GPC, IR
Polymer 2-41	(9s,10s)-10,11-dihydro-9,10-[5,6]epitriazinoanthracene-14(9H)-thione		<sup>1</sup> H NMR, GPC, IR

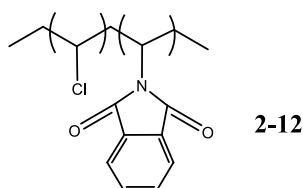
**Polymer 2-9:** light yellow solid; <sup>1</sup>H NMR (400MHz, DMF-*d*7): δ (ppm) 2.19–2.62 (m, 23H, -CH<sub>2</sub>-CHCl-, -CH<sub>2</sub>-CH(HetAr), CH<sub>3</sub> (HetAr)), 4.42–4.71 (m, 10H, -CH<sub>2</sub>-CHCl-, -CH<sub>2</sub>-CH(HetAr)), 7.95 (s, 1H, H-3 (HetAr)). Found: C 30.66, H 3.62, N 6.07, Cl 23.58. GPC: M<sub>n</sub> = 104.7 kDa (PDI = 1.4), IR (KBr), ν, cm<sup>-1</sup>: 1650 (C=O, (amide carbonyl 1640-1690)), 1551(C=N), 1212 (C-N), 1310 (NO<sub>2</sub>), 571(C-Cl).



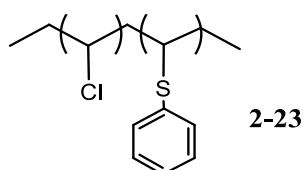
**Polymer 2-10:** brown solid;  $^1\text{H}$  NMR (400MHz, DMF-*d*7):  $\delta$  (ppm) 2.19–2.60 (m, 4H,  $-\text{CH}_2-\text{CHCl}$ ,  $-\text{CH}_2-\text{CH}(\text{HetAr})$ ), 3.15 (s, 6H,  $\text{CH}_3-\text{CH}_2-\text{O}-$ ), 4.32 (s, 4H,  $\text{CH}_3-\text{CH}_2-\text{O}-$ ), 4.39-4.73 (m, 5H,  $-\text{CH}_2-\text{CHCl}-$ ,  $-\text{CH}_2-\text{CH}(\text{HetAr})$ ), 7.95 (s, 1H, H-7 (HetAr)). Found: C 32.77, H 3.50, N 5.14, Cl 15.29. GPC:  $M_n = 80.4$  kDa (PDI = 1.4), IR (KBr),  $\nu$ ,  $\text{cm}^{-1}$ : 1715 (C=O), 2851-2923 (C-H), 1551 (C=C), 1641-1693 (C=N), 1107 (C-N), 1189 (C-O), 557 (C-Cl).



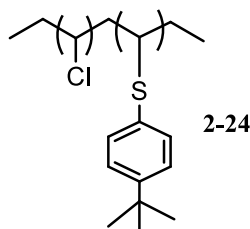
**Polymer 2-12:** brown solid;  $^1\text{H}$  NMR (400MHz, DMF-*d*7):  $\delta$  (ppm) 2.15–2.64 (m, 16H,  $-\text{CH}_2-\text{CHCl}$ ,  $-\text{CH}_2-\text{CH}(\text{HetAr})$ ), 4.37–4.73 (m, 8H,  $-\text{CH}_2-\text{CHCl}$ ,  $-\text{CH}_2-\text{CH}(\text{HetAr})$ ), 7.12–7.35 (m, 2H, HetAr), 7.58 (s, 1H, HetAr), 7.92 (s, 1H, HetAr). GPC:  $M_n = 97$  kDa (PDI = 1.54).



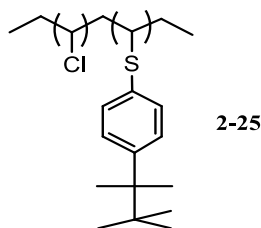
**Polymer 2-23:** white solid;  $^1\text{H}$  NMR (400MHz, DMF-*d*7):  $\delta$  (ppm) 2.15–2.64 (m, 16H,  $-\text{CH}_2-\text{CHCl}$ ,  $-\text{CH}_2-\text{CH}(\text{HetAr})$ ), 4.37–4.73 (m, 8H,  $-\text{CH}_2-\text{CHCl}$ ,  $-\text{CH}_2-\text{CH}(\text{HetAr})$ ), 7.12–7.35 (m, 2H, HetAr), 7.58 (s, 1H, HetAr), 7.92 (s, 1H, HetAr). GPC:  $M_n = 100.96$  kDa (PDI = 1.37).



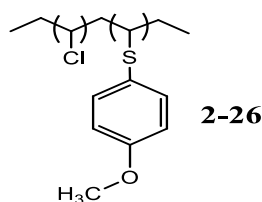
**Polymer 2-24:** orange solid;  $^1\text{H}$  NMR (400MHz, DMF-*d*7):  $\delta$  (ppm) 1.28 (s, 9H, tBu), 2.16-2.61 (m, 52H,  $-\text{CH}_2-\text{CHCl}-$ ,  $-\text{CH}_2-\text{CH}(\text{OC}_6\text{H}_4)$ ), 4.40–4.72 (m, 26H,  $-\text{CH}_2-\text{CHCl}-$ ,  $-\text{CH}_2-\text{CH}(\text{OC}_6\text{H}_4)$ ), 6.80 (d,  $J = 8.0$  Hz,  $\text{C}_6\text{H}_4$ ), 7.22 (d, 2H,  $J = 8.0$  Hz,  $\text{C}_6\text{H}_4$ ). GPC:  $M_n = 105$  kDa (PDI = 1.42), IR (KBr),  $\nu$ ,  $\text{cm}^{-1}$ : 1336 ( $\text{sp}^3$  bend C-H), 2923-2864 ( $\text{sp}^3$  stretch C-H), 561 (C-Cl).



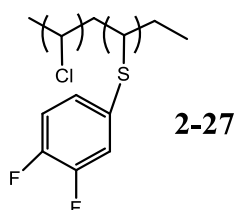
**Polymer 2-25:** white solid;  $^1\text{H}$  NMR (400MHz, DMF-*d*7):  $\delta$  7.25–7.21 (m, 2H), 6.82 – 6.77 (m, 2H), 4.70–4.45 (m, 1H), 1.37–1.34 (s, 6H), 0.79–0.75 (s, 9H), IR (KBr),  $\nu$ ,  $\text{cm}^{-1}$ : 1336 ( $\text{sp}^3$  bend C-H), 2923-2864 ( $\text{sp}^3$  stretch C-H), 561(C-Cl).



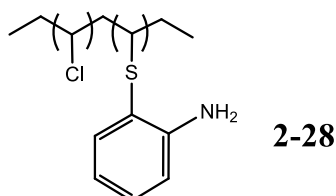
**Polymer 2-26:** yellow solid;  $^1\text{H}$  NMR (400MHz, DMF-*d*7):  $\delta$  7.82–7.38 (d,  $J = 8.8$  Hz, 2H), 7.36–6.94 (d, 2H), 4.22–3.90 (d,  $J = 7.1$  Hz, 3H), 2.62–2.23 (t,  $J = 6.6$  Hz, 1H), 2.11–1.74 (m, 2H). Degree of substitution 80 %. GPC:  $M_n = 135.42$  kDa (PDI = 1.26).



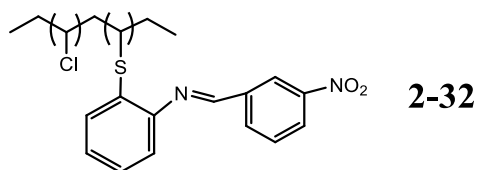
**Polymer 2-27:** beige solid;  $^1\text{H}$  NMR (400MHz, DMF-*d*7):  $\delta$  7.89–7.61 (s, 1H), 7.45–7.14 (d, 2H), 5.18–4.52 (d, 1H). Degree of substitution 61 %. GPC:  $M_n = 125$  kDa (PDI = 1.36) IR (KBr),  $\nu$ ,  $\text{cm}^{-1}$ : 1481 (C=C aromatic), 2928 (C-H), 908 (C-F), 1368 (C-S).



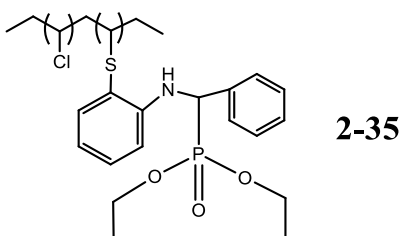
**Polymer 2-28:** light purple solid;  $^1\text{H NMR}$  (400MHz, DMF-*d*7):  $\delta$  7.44 –7.25 (m, 1H), 7.20–7.07 (d,  $J = 6.8$  Hz, 1H), 6.95 – 6.83 (t,  $J = 7.1$  Hz, 1H), 6.71–6.56 (d,  $J = 8.7$  Hz, 1H), 5.38–5.18 (s, 2H), 4.71–4.43 (t, 1H), 2.35–1.97 (s, 2H), IR (KBr),  $\nu$ ,  $\text{cm}^{-1}$ : 2834–2933 (C-H), 3061 (N-H), 1706 (C=C), 1589 (N-H bend), 1338 (C-S), 824(C-Cl), degree of substitution 67 %.



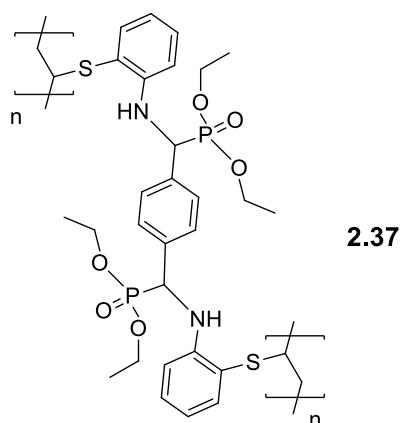
**Polymer 2-32:** yellow solid;  $^1\text{H NMR}$  (400 MHz, DMSO):  $\delta$  8.43–8.37 (d,  $J = 7.5$  Hz, 1H), 8.26–8.21 (d,  $J = 7.9$  Hz, 2H), 8.21–8.13 (d,  $J = 7.9$  Hz, 2H), 7.68–7.60 (t,  $J = 7.7$  Hz, 2H), 7.59–7.52 (d,  $J = 8.0$  Hz, 2H), 4.65–4.26 (t, 1H). GPC:  $M_n = 122$  kDa (PDI = 1.3), IR (KBr),  $\nu$ ,  $\text{cm}^{-1}$ : 1596 (C=N), 1622 (C=C), 2851 (C-H), 1311 ( $\text{NO}_2$ ), 556 (C-Cl).



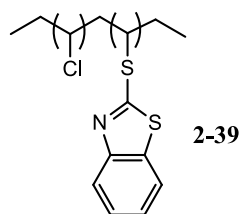
**Polymer 2-35:** dark-brown solid;  $^1\text{H NMR}$  (400MHz, DMF-*d*7): )  $\delta$  8.36–8.12 (d, 5H), 7.85 – 7.45 (d, 4H), 7.17–6.62 (d, 1H), 4.83 – 4.59 (s, 4H), 4.39 – 4.16 (s, 2H), 1.60 – 1.26 (s, 3H). Degree of substitution 68 %. GPC:  $M_n = 93$  kDa (PDI = 1.42), IR (KBr),  $\nu$ ,  $\text{cm}^{-1}$ : 1222 (P=O), 1020 (P-C-O), 3300 (NH), 2978- 2861 ( $\text{OCH}_3$ ), 556 (C- Cl).



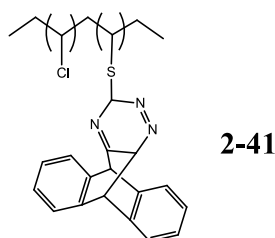
**Polymer 2.37:** beige solid; IR (KBr)  $1165$   $\text{cm}^{-1}$  (P=O),  $1055$   $\text{cm}^{-1}$  (P-C-O), at  $2960$   $\text{cm}^{-1}$  ( $\text{OCH}_3$ ),  $3460$   $\text{cm}^{-1}$  (NH amide).



**Polymer 2-39:** yellow solid;  $^1\text{H}$  NMR (400MHz, DMF-*d*7):  $\delta$  7.58–7.53 (d,  $J = 7.7$  Hz, 1H), 7.46–7.42 (d,  $J = 8.0$  Hz, 1H), 7.25–7.20 (t,  $J = 7.5$  Hz, 1H), 7.08–7.02 (t,  $J = 7.5$  Hz, 1H), 4.89–4.57 (t, 1H), 2.01–1.96 (t,  $J = 6.3$  Hz, 2H), 1.91–1.84 (d,  $J = 4.8$  Hz, 1H). Degree of substitution 10 %. GPC:  $M_n = 115$  kDa (PDI = 1.4), IR (KBr),  $\nu$ ,  $\text{cm}^{-1}$ : 1629 (C=N), 2856-2934 (C-H), 862 (C-S), 557(C-Cl).



**Polymer 2-41:** Green-yellow solid; Yield: 10 %;  $^1\text{H}$  NMR (400MHz, DMF-*d*7):  $\delta$  7.90–7.82 (s, 4H), 7.47–7.36 (s, 4H), 6.15(s, 1H) , 5.91 (s, 1H), 4.85–4.61 (t, 1H), 2.84–2.33 (m, 2H). Degree of substitution 3 %. GPC:  $M_n = 107$  kDa (PDI = 1.38), IR (KBr),  $\nu$ ,  $\text{cm}^{-1}$ : 2936 (C-H), 1667 (C=C alkene), 1567 (C=N), 1335(C-S).



Thus, within the framework of this section, the possibility of post-modification of PVC with fragments of *S*-nucleophiles, namely thiophenols and their derivatives, benzo[*d*]thiazole and 3-mercapto-1,2,4-triazine containing a tryptycene fragment, was shown under conditions mechanosynthesis. In the latter case, tryptycene-containing PVC was obtained.

Before selecting polymers for the manufacture of UF membranes, a preliminary test of their solubility in a mixture of tetrahydrofuran and N-methyl-2-pyrrolidone (NMP) was carried out. Of the synthesized polymers, only PVC derivatives modified with thiophenols showed solubility acceptable for the preparation of membrane casting solutions.

The next stage of the work was devoted to the synthesis of new types of UF membranes using the phase inversion method based on commercial PVC, PVC derivatives obtained by mechanosynthesis and based on PVC modified with silicon dioxide nanoparticles.

### **Conclusion to the chapter 2**

Based on the purpose of this work, the following three mechanosynthetic PVC derivatives were selected for the production of UF membranes: PVC modified with thiophenol **23** (PVC-TF); PVC modified with 4-*tert*-butylthiophenol **24** (PVC-BTP); PVC modified with 4-*tert*-octylthiophenol **25** (PVC-OTP). Taking into account the *oleophilicity* of the modifying units introduced into the structure of these polymers, *due to the presence of alkyl and aromatic fragments* inherent in the components of petroleum products, it was assumed that the use of polymers **23-25** to modify the structure of UF membranes could improve their retention of petroleum products.

## Chapter 3. Investigation of the possibility of manufacturing UF membranes based on PVC and its modified structures

### 3.1 Laboratory support for experimental research

All chemical materials used in this study were used without any purification. The chemical materials used in this work lists in Table 3.1.

Table 3.1 – Reagents and Materials for the Synthesis of UF Membranes

Name	Chemical Formula, Characteristic
Silicon dioxide nanoparticles	SiO <sub>2</sub> . Specific surface area ~ 640 m <sup>2</sup> /g, ρ=937 kg/m <sup>3</sup> , particle size 15–20 nm
Sodium Dodecyl Sulfate (SDS)	Surfactant. C <sub>12</sub> H <sub>25</sub> NaSO <sub>4</sub> , M.M. 288.372 g/mol
N,N-dimethylacetamide (DMAc)	CH <sub>3</sub> CON(CH <sub>3</sub> ) <sub>2</sub> . ρ = 940 kg/m <sup>3</sup> (25°C). Weaver = 164–166 °C, solvent
Post-modified PVC	PVC-OTF, PVC-BTF; PVC-TF
Tetrahydrofuran (THF)	(CH <sub>2</sub> ) <sub>4</sub> O. ρ=899 kg/m <sup>3</sup> (25°C). T <sub>lamp</sub> = 65–67 °C, solvent
N-methyl-2-pyrrolidone (NMP)	C <sub>5</sub> H <sub>9</sub> NO. ρ=1028 kg/m <sup>3</sup> (25°C). T <sub>kip.</sub> =202°C, solvent

Experiments on the preparation of PVC and PM PVC derivatives UF membranes were carried out in a chemical laboratory equipped with special glassware and instruments, including, in addition to those listed in section 2.1, the following additional equipment necessary for research:

– WW filtration plant equipped with a membrane module and a device for casting membranes onto a glass plate. Figures (3.1) and (3.2) show a photographic picture and a schematic diagram of UF experimental system, respectively.

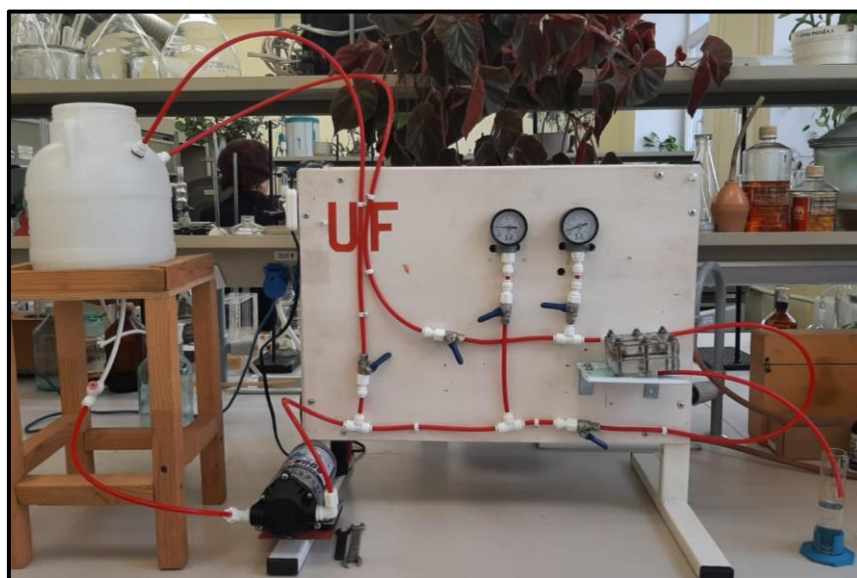


Figure 3.1 – Photographic picture of UF experimental system and Flat sheet membrane module



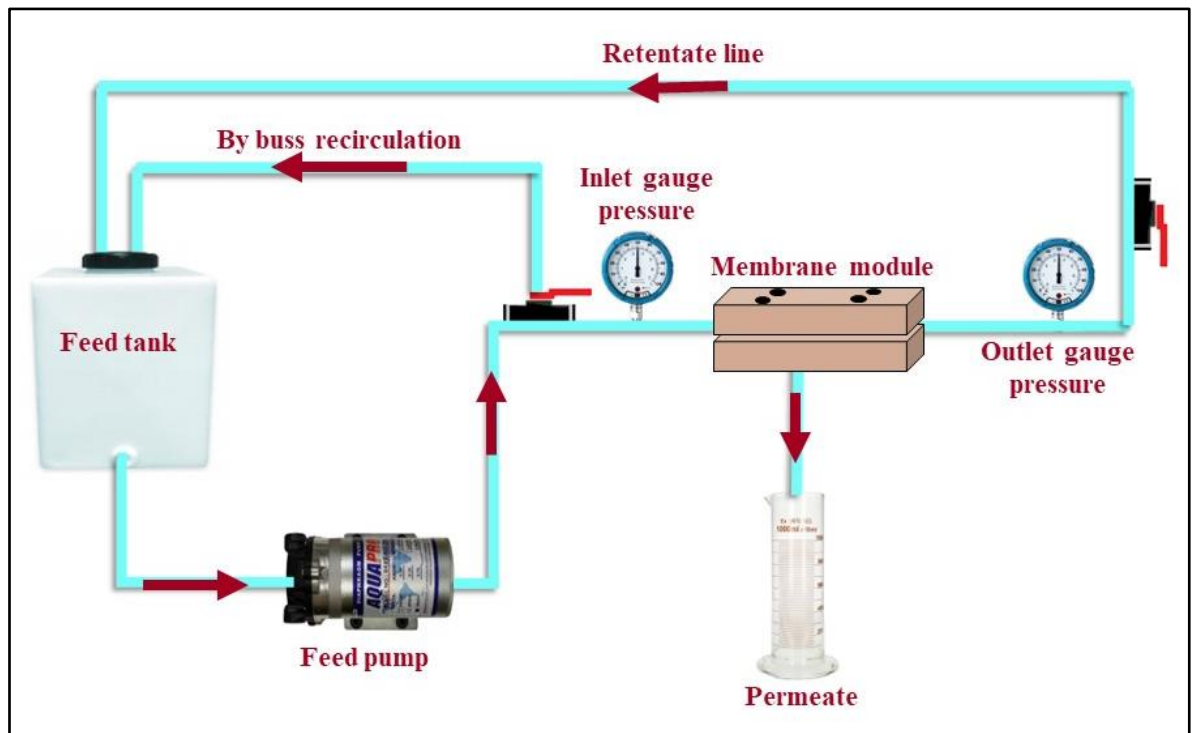


Figure 3.2 – Schematic diagram of the setup used to measure filtration performances

The effluent collected from the carwash unit was placed in the feed tank and circulated through the membrane module by a pump. The valves in the membrane module were adjusted to obtain the desired operating transmembrane pressure and cross flow velocity. The retentate was recycled to the feed tank while the permeate was collected in a beaker. The equipment and apparatus consist of the following parts:

1. Feeding tank.
2. Pump with maximum flow rate of 2 L/min operated by DC current at 24 V.
3. Valve used to regulate the inlet pressure.
4. By buss recirculation.
5. Inlet pressure gauge.

6. Flat sheet membrane module was designed and fabricated by computer numeric control machine (CNC) and CAD-CAM program, it was manufactured from Teflon material (Italy), it consists of input, output and permeate vents, as shown in Figure 3.3. The outer area of the module is about (54.76 cm<sup>2</sup>), and the effective area is about (13.75 cm<sup>2</sup>). The feed and the permeate solution flow in counter-current direction inside the membrane module.

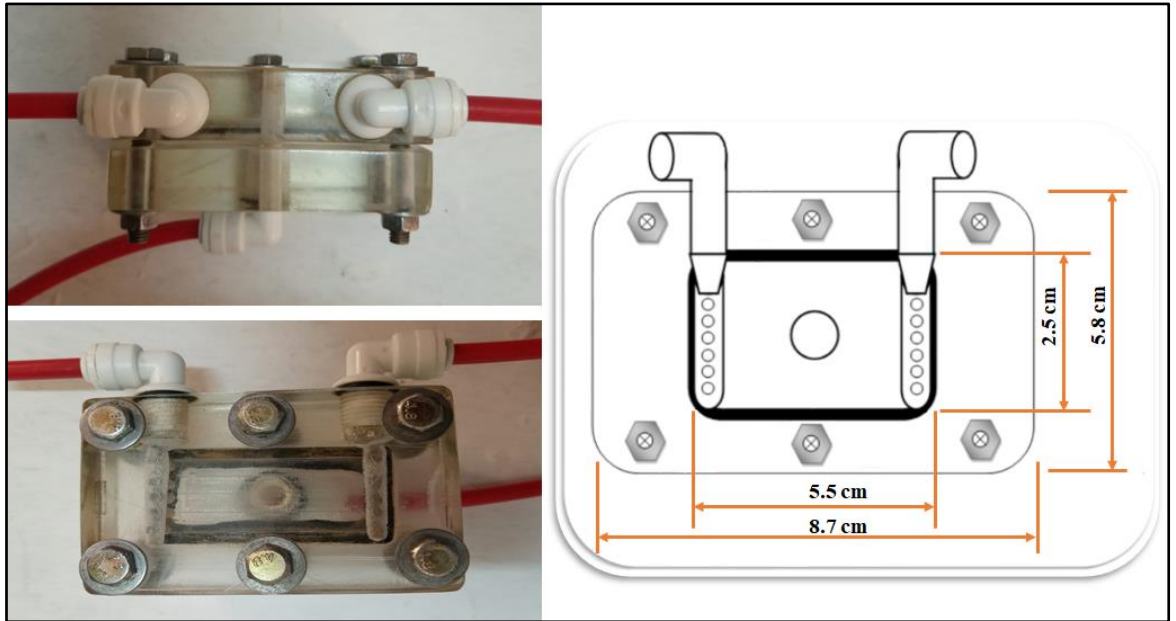


Figure 3.3 – Flat sheet membrane module

7. Outlet pressure gauge.
8. Retentate line.
9. The permeate.

During the experiments, changes in the composition of the studied carwash wastewater which passed through manufactured UF membranes were monitored. For this purpose, as well as to determine the operational efficiency of the created membranes, all parameters were analyzed using HDPE F (ПНД Ф) methods included in the register of the Russian Federation.

Car wash WW were analyzed for:

- chemical oxygen demands (COD) – by the action of a strong oxidizing agent (potassium dichromate in sulfuric acid) on organic impurities contained in the WW sample under conditions of two-hour boiling, using silver sulphate as a catalyst and titrating the excess oxidizer with a solution of Mohr's salt (ПНД Ф 14.1:2.100-97);
- oil content – by gravimetric method, including extraction of petroleum products with petroleum ether (PE) in an acidic environment, evaporation of PE and weighing of the residue (ПНД Ф 14.1:2:4.128-98);

– total suspended solids (TSS) – by filtering a certain volume of the WW sample through a paper filter "blue tape" and drying to a constant mass of the residue on the filter (ПНД Ф 14.1:2.110-97);

– the content of anionic surfactants – the MBAS method (5540 C); recommended by APHA [91]; MBAS method comprises three successive extractions from acid aqueous medium containing excess methylene blue into chloroform ( $\text{CHCl}_3$ ), followed by an aqueous backwash and measurement of the blue color in the  $\text{CHCl}_3$  by spectrophotometry at 652 nm.

In order to investigate and compared the performance of the membranes, the carwash wastewater was tested, which obtained from one of the semi-automatic carwash stations in Yekaterinburg (Sverdlovsk region) from the sedimentation tank which is designed for the collection and preliminary treatment (settling) of wastewater. The Moreover, a simple pretreatment was carried out before starting the work through sedimentation (24 hours) and filtration (1-micron polypropylene filter) of the sample to meet the feeding requirements of the UF membrane.

The characteristics of the main pollutants of the initial composition of the carwash wastewater (CWW) used to evaluate effectiveness of the obtained UF membranes are presented in Table 3.2.

Table 3.2 – Initial quality of the examined CWW samples in station in Yekaterinburg

Pollutants	Units	Values of pollutants
Anionic Surfactants	mg/L	2.6-10.61
Petroleum Products	mg/L	35–172.8
Chemical Oxygen Demand (COD)	mgO <sub>2</sub> /L	220–310
Total suspended solids (TSS)	mg/L	28–649

### **3.2 Description of laboratory techniques for the manufacture of UF membranes based on PVC and its modified structures**

#### **A) Method for preparation PVC- based UF membranes**

PVC flat-sheet membranes were fabricated employing the classical phase inversion technique. Three concentrations (14, 15 and 16 wt.%) of PVC were weighed, pre-dried in the oven at 70 °C for 4 hours to remove moisture and poured them to the DMAc solvent of (86, 85, and 84 wt.%), respectively. For the PVC/DMAc solution, further increase in PVC concentration is not feasible due to the strong increase of dope viscosity. The resulting suspension was stirred with a magnetic stirrer for ~12 hours at 40 °C until a homogeneous transparent yellowish solution suitable for membrane casting was obtained. After that, a certain portion of the resulting PVC dope solution was placed on a glass plate and the membrane was cast using a motorized film applicator with a gap of 200 μm (AFA-IV, China). The process of preparation UF membrane is schematically shown in Figure 3.4.

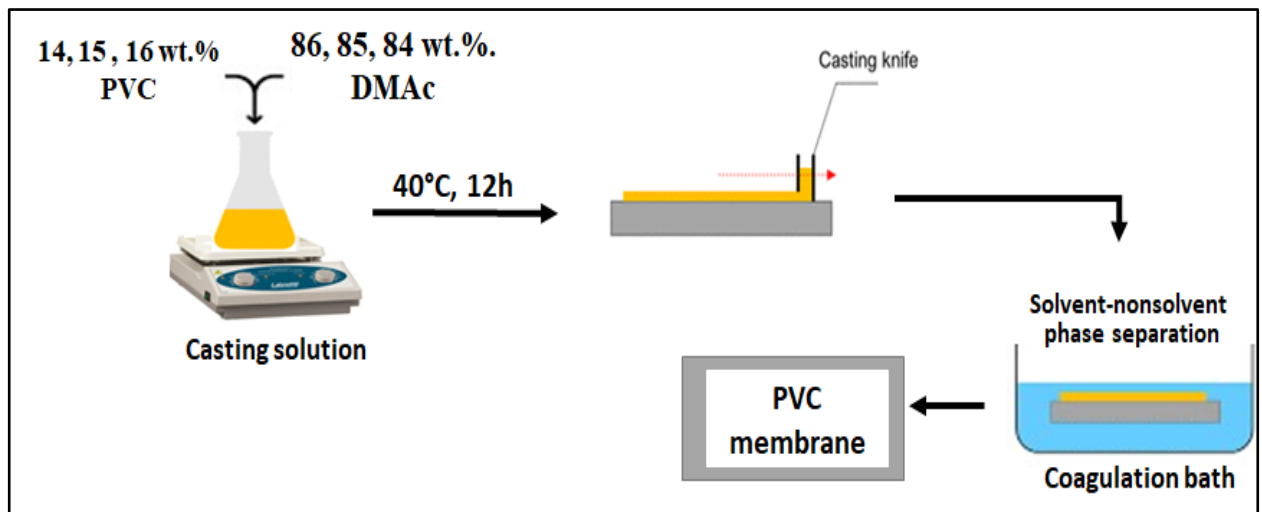


Figure 3.4 – Scheme of preparation of PVC-based UF membrane

Then by using a deionized water bath at room temperature, through a minute, the membrane detached from the glass substrate, indication phase inversion completion. The casting membranes were washed with deionized water to remove residues of the DMAc solvent.

It is worth mentioning that the PVC concentrations (14-16 wt.%) were selected to get UF membrane. Altering polymer concentration is an effective way to tune the membrane pore size. If the concentration is too low, polymer membrane cannot be achieved. And if the concentration is too high, the polymer solution becomes very viscous and observed to slow the exchange of solvent and non-solvent during the phase-inversion process, resulting in smaller surface pores [92, 93], resulting, the membrane will be NF

instead of UF membrane. So, an appropriate polymer concentration is very important to the membrane preparation.

#### B) Method for preparation post-modified PVC derivatives UF membranes

It should be noted that one of the important tasks before the preparation of modified membranes was the selection of the optimal amount of additive of each polymer from those selected for research: **23, 24 and 25**. It was experimentally established that the consistency of the casting solution suitable for the manufacture of membranes is obtained by adding concentration (4 wt.%) [94] of selected polymers to a mixture of two solvents: tetrahydrofuran (THF) and N-methyl-2-pyrrolidone (NMP) with ratio (85:15) [95] and mixed magnetically stirred for 1 h at 25 °C pre condensing condition, then added dried optimal PVC concentration (14 wt.%) gradually to suspension solution and stirring for ~12 hours at 40 °C. The composition of casting solutions and the designation of membranes are given in Table 3.3.

Table 3.3 – Characteristics of casting solutions and designation of membranes

Type of PM PVC	PVC (wt.%)	Polymer concentration (wt.%)	Quantity (wt.%)		Membrane designation
			NMP	THF	
<b>25</b> PVC-OTF	14	4	70	12	PP1
<b>24</b> PVC-BTF					PP2
<b>23</b> PVC-TF					PP3

After that, transferred to ultrasonic for 30 min at 20 °C for removing dissolved air in solutions. The obtained homogeneous transparent yellowish solutions were casted on to glass plates with constant thickness of 100 µm. After that, prepared casting solutions were dipped in to deionized water as non-solvent (after 60 seconds as evaporation time in air). In this step exchanging of solvent and non-solvent leads to membranes formation. After completing phase separation step and finishing membranes formation, the membranes were kept at new container with fresh deionized water for one day to remove reminded solvent in membranes structure and then preserved in DI water.

#### C) Method for preparation PVC-Membranes modified by Silicon dioxide

To obtain nanocomposite membranes, a concentration 14 wt.% of PVC in DMAc solvent was used with the preliminary introduction of various doses of silicon dioxide

nanoparticles modified with sodium dodecyl sulfonate (SDS) into the casting solution. The synthesis diagram of modified silicon dioxide nanoparticles with SDS ( $\text{SiO}_2\text{-SDS}$ ) is shown in Figure 3.5.

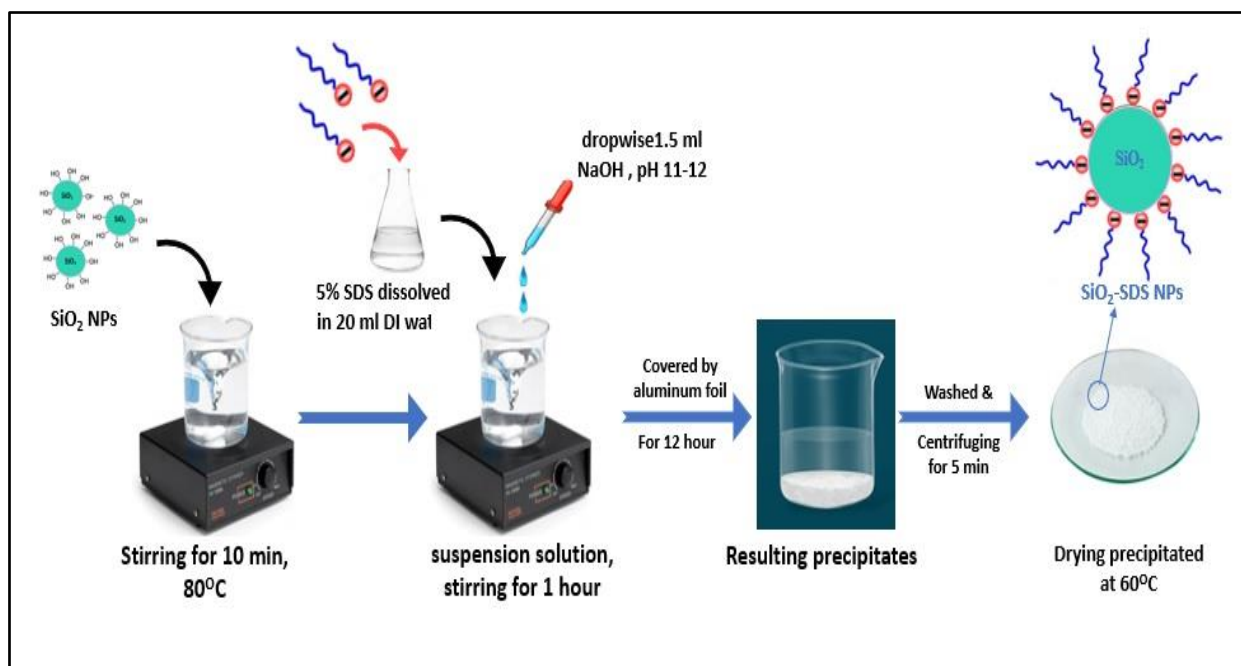


Figure 3.5 – Modifying of  $\text{SiO}_2$  NPs with SDS

To produce modified Silicon dioxide NPs with Sodium dodecyl sulfate (SDS) will carried out by wet chemical synthesis [96]. The silicon dioxide nanoparticles were added to the 500 ml of de-ionized water and mixed well under continuous stirrer with magnetic stirrer for about 10 minutes and then heated up to 80 °C. To the above suspension solution, 5 % SDS (prepared by dissolving in 20 ml of deionized water) was added and stirred for about 1 hour. The NaOH solution (1.5 ml) added drop wisely to the mixture solution for precipitation and the pH was maintained between 11–12. After that, the solution was covered by aluminum foil and left over-night. The resulting precipitates were washed several times with de-ionized water to remove the impurities and then centrifuged for 5 min to remove excess of surfactant and content water. The final product was dried at 60 °C in electrical oven under air atmosphere. After heat treatment, the coated silicon dioxide nanoparticles ( $\text{SiO}_2\text{-SDS}$ ) were formed.

The second step of the technique involved the preparation of a composite membrane. Table 3.4, shows the composition of the PVC/DMAc/SiO<sub>2</sub>-SDS casting solution and the designations of the resulting membranes.

Table 3.4 – Composition of the prepared nanocomposite membranes.

Dose of SiO <sub>2</sub> -SDS wt.%	Membrane designation	Dose of SiO <sub>2</sub> -SDS wt.%	Membrane designation
0	PSS-0	0.15	PSS-0.15
0.05	PSS-0.05	0.20	PSS-0.20
0.10	PSS-0.10	0.25	PSS-0.25

The casting solution prepared by adding dried optimal PVC concentration (14 wt.%) to 86 wt.% DMAc solvent and mixed magnetically stirred overnight. When a clear yellowish casting solution was obtained, SiO<sub>2</sub>-SDS NPs were added with various concentrations (0, 0.05, 0.1, 0.15, 0.2 and 0.25 wt.%), and kept for 15 minutes in a coagulation bath (deionized water) to avoid nanoparticles from aggregating, then preserved in DI water [97, 98]. Three sheets of same membranes were selected to characterize it and observe the mean value of its performance. The process of preparation nanocomposit membrane is schematically shown in Figure 3.6.

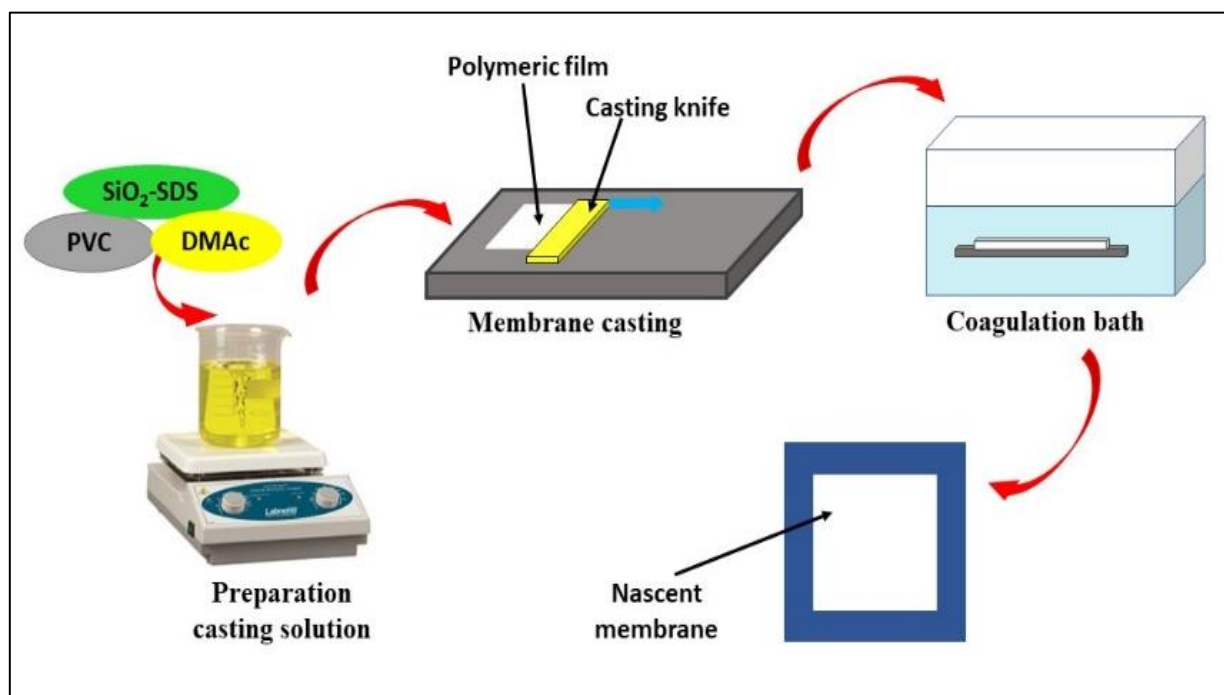


Figure 3.6 – Schematic Diagram of Nanocomposite Membrane Casting

In a similar way 5 samples of flat UF membranes were obtained, which were further examined for generally accepted typical characteristics necessary to evaluate their properties and choose an application.

### 3.3 Studying the Membrane Characterizations Measurements

Fourier-Transform Infrared spectroscopy (FTIR) was utilized for fabricated nascent and MMMs, through an FTIR instrument (model: ALPHA IR Fourier Spectrometer, Bruker). Measurements were taken using a 500–4000  $\text{cm}^{-1}$  spectrum. The surface topography (2D and 3D image), and roughness of MMMs were characterized using atomic force microscopy (AFM) instrument with Scanning Probe Microscope, Nova SPB, (Ntegra Prima), Russia. The membrane surfaces were scanned with image size  $\geq$  (10000 nm, 10000 nm) and topography pixels (512).

The morphology of the synthesized membrane was obtained utilizing SEM Tescan Vega (4 LMS instrument, Czech Republic). Scanning Electron Microscopy (SEM) (model: TESCAN Vega (4 LMS instrument, Czech Republic) was employed to observe the membranes surface and cross-sectional morphologies. For membranes cross-section imaging, the samples were prepared by cutting the membranes in liquid nitrogen. To determine the thickness of the membranes, a thickness gauge (NOVOTEST TP-1) was used. With its help, measurements were taken at various points of the membrane and then the average value of the measurements was taken.

The membrane's porosity ( $\varepsilon\%$ ) is calculated as the pore's volume divided by the membrane's overall volume. The porosity was determined by cutting the dry samples to a specific shape and weight. The membrane was then soaked in DI water overnight and the surface was wiped with a filter paper to get rid of any excess water drops and weighted again. Using Eq. 3.1, it was possible to determine the membranes' porosity [99, 100].

$$\varepsilon = 1 - \frac{\rho_m}{\rho_p}, \quad (3.1)$$

where,

- $\varepsilon$  % is the porosity;
- $\rho_p$  is the polymer density (1.38  $\text{g}/\text{cm}^3$ );
- $\rho_m$  is density of membrane ( $\text{g}/\text{cm}^3$ ) which found by Eq. 3.2:



$$\rho_m = \frac{M}{L \times W \times I}, \quad (3.2)$$

where,

- M is the mass of synthesized membrane (g);
- L, W, I, are length, width, and thickness of the synthesized membrane, respectively, (cm<sup>3</sup>).

The mean pore radius ( $r_m$ ) was determined using the Guerout- Elford-Ferry equation based on the results of the pure water flux and porosity calculations, which states that  $r_m$  can be calculated by Eq. 3.3 [101]:

$$r_m = \sqrt{\frac{(2.9-1.75\varepsilon)8 \eta I Q}{\varepsilon A \Delta P}}, \quad (3.3)$$

where,

- $r_m$  is mean pore radius of membrane (m);
- $\eta$  is water viscosity ( $8.9 \times 10^{-4}$  Pa.s);
- I, is membrane's thickness (m);
- Q is volume of the permeate water per unit time (m<sup>3</sup>/s);
- $\Delta P$  is the operating pressure (Pa).

### 3.4 Studying the Permeability and Rejection of CWW by Obtained UF Membranes

The UF membranes experiments of permeability and wastewater rejection were carried out using a laboratory-scale cross-flow filtration mode by an effective membrane area 13.75 cm<sup>2</sup> at a transmembrane pressure of 1 bar and a temperature of 25 °C. It should be noted that the use of a flat-sheet membrane module is advisable in the laboratory, since it is easy to disassemble it to clean and replace the membrane used. To minimize the error, experiments were conducted three times using fresh membranes when repeating, then average values were calculated.

The permeation flux (J) was Calculated by measuring the permeate volume under operation pressure of 1 bar and 25 °C for pure water and carwash wastewater sample for 90 min. The permeation flux (J) was calculated by Eq. 3.4 [102, 103]:

$$J = \frac{V}{A \times t}, \quad (3.4)$$

where,

- J is permeation flux (L/m<sup>2</sup>.h);

V is the permeate volume (L);

A is the effective surface area of the membrane (m<sup>2</sup>); and

t is time (h).

Analysis of the pollutant concentrations before and after filtration of carwash wastewater through each type of membrane. The membrane rejection (R%) was determined of each pollutant by Eq. 3.5 [104, 105] :

$$R \% = \left[ 1 - \frac{C_p}{C_f} \right] \times 100 , \quad (3.5)$$

where,

C<sub>f</sub> and C<sub>p</sub> are concentrations of pollutants at the permeation and feed wastewater solution, respectively.

Antifouling and permeation experiments were carried out under constant pressure of 1 bar for pure water and carwash wastewater. Firstly, the pure water flux was measured as J<sub>w1</sub> for 30 min, then it was replaced by carwash wastewater sample for 30 min. After that, the fouled membranes were backwashed by DI water for 15 min, and the recovered flux of cleaned membrane was calculated again as J<sub>w2</sub> for 30 min. The flux recovery ratio (FRR), the total fouling ratio (DR<sub>t</sub>), reversible fouling ratio (DR<sub>r</sub>), and irreversible fouling ratio (DR<sub>ir</sub>) were calculated through Equations 3.6–3.9 [106]:

$$FRR = \frac{J_{w2}}{J_{w1}} \times 100 \% . \quad (3.6)$$

$$DR_t = 1 - \frac{J_c}{J_{w1}} \times 100 \% . \quad (3.7)$$

$$DR_r = \frac{J_{w2} - J_c}{J_{w1}} \times 100 \% . \quad (3.8)$$

$$DR_{ir} = \frac{J_{w1} - J_{w2}}{J_{w1}} \times 100 \% . \quad (3.9)$$

### **3.5 Results of the study of permeability and rejection of car wash WW by obtained membranes**

#### **3.5.1 Membranes prepared from non-modified PVC**

The tasks solved in the preparation of PVC-based UF membranes included: studying the influence of the concentration of PVC on the performance characteristics of UF membranes and selection the optimal PVC concentration in the casting solution for modification new types of UF membranes. For the experiments, the concentrations of an

excellent PVC solution were chosen, wt.%: 13, 14, 15 and 16, the resulting membranes were designated, respectively: PVC-13, PVC-14, PVC-15 and PVC-16.

Tables 3.5 and 3.6 show the average results of a study of PVC-UV membranes for permeability and cleaning efficiency of Car wash wastewater (CWW) in Yekaterinburg.

Table 3.5 – Results of a study of the permeability of PVC-based membranes

Type of water	Unit, L/m <sup>2</sup> .h			
	PVC-13	PVC-14	PVC-15	PVC-16
pure water	133.81	154.34	83.07	65.29
CWW	94.55	108.36	67.15	33.70

According to the purpose of this work, the membrane cast from a PVC concentration in a DMAc solution of 13 wt.% was excluded from further research, since its permeability turned out to be significantly lower (by ~30 %) than that of a membrane with a higher PVC concentration in the casting solution – 14 wt.%. That is, the pattern characteristic of membranes obtained by the phase inversion method was not observed. It is known that the polymer concentration used during casting is one of the main factors affecting the porosity and pore size of the membrane, and consequently its permeability. That is, with a decrease in the polymer content in the casting solution, the permeability should decrease due to an increase in the pore size and porosity of the membrane.

In this case, there is a limit of concentrations up and down when a UF membrane cannot be obtained. For example, when this limit is exceeded, usually accompanied by an increase in the viscosity of the polymer solution, the exchange of solvent and nonsolvent during phase inversion slows down. This leads to a decrease in the size of the surface pores [92, 93] and instead of a UF membrane, a nanofiltration membrane is obtained, and vice versa; by decreasing this limit, a membrane with a larger pore size can be obtained than a UF membrane or a membrane with a different structure.

Table 3.6 – Results of the study of the rejection (R %) of pollutants by PVC membranes

Pollutants	Units	Values of pollutants in WW			
		Before cleaning	After cleaning		
		CWW	PVC-14	PVC-15	PVC-16
Anionic surfactant	mg/L	2.610	0.284	0.348	0.861
Oil products	mg/L	41.000	18.300	16.300	10.200
TSS	mg/L	28.000	10.000	15.000	16.000
COD	mgO <sub>2</sub> /L	220.000	80.000	110.000	120.000

From the data obtained, presented in Tables 3.4 and 3.5, it is clear:

1) a natural decrease in the permeability of UF membranes with an increase in the concentration of PVC in the casting solution of the membranes from 14 to 16 %, as when filtering pure water (from 154.34 to 65.29 L/m<sup>2</sup>.h), and for CWW (from 108.36 to 33.70 L/m<sup>2</sup>.h);

2) increasing the degree of purification of wastewater for petroleum products with increasing concentration of PVC in the casting solution. To explain these and other results, data from studies of the structural and morphological characteristics of membranes are required. Taking into account the satisfactory results of cleaning CWW from the studied pollutants and the much greater permeability of the 14 wt.% of PVC membrane compared to the 15 and 16 wt.% of PVC, 14 wt.% was accepted as the optimal concentration for obtaining new types of UF membranes.

### 3.5.2 Membranes prepared from Post modified-PVC derivatives

In accordance with the purpose of this work, three postmodified (PM) PVC derivatives obtained by mechanosynthesis were selected for the production of UF membranes: PVC modified with thiophenol **23** (PVC-TF); PVC modified with 4-tert-butylthiophenol **24** (PVC-BTP); PVC modified with 4-tert-octylthiophenol **25** (PVC-OTP). Taking into account the oleophilicity of the modifying agents introduced into the structure of these polymers, due to the presence of alkyl and aromatic fragments inherent in the components of petroleum products, their use to modify the structure of UF membranes can presumably improve the retention of petroleum products by the obtained UF membranes.

Tables 3.7 and 3.8 show the average results of the study of permeability, as well as the efficiency of CWW purification for the post modified PVC derivatives membranes obtained by mechanosynthesis.

Table 3.7 – Results of a study of the permeability of modified membranes

Type of water	Unit, L/m <sup>2</sup> .h		
	PP1	PP2	PP3
pure water	40.24	45.58	61.82
CWW	28.36	31.03	41.21

Table 3.8 – Results of the study of the rejection (R%) of pollutants by modified membranes

Pollutants	Units	Values of pollutants in WW			
		Before cleaning	After cleaning		
		CWW	PP1	PP2	PP3
Anionic surfactant	mg/L	8.769	1.84	1.98	2.26
Oil products	mg/L	172.8	30.4	32.8	39.2
TSS	mg/L	526	7.0	12.6	15.7

From the data obtained, it can be seen that in comparison with PVC membranes, membranes obtained with the addition of modified polymers showed a higher effect of CB purification with a significant decrease in permeability.

### 3.5.3 Membranes prepared from PVC Modified with Silicon Dioxide NPs-SDS

Tables 3.9 and 3.10 show the average results of the study of permeability, as well as the efficiency of CWW purification by UF membranes obtained on the basis of PVC modified with silicon dioxide nanoparticles.

Table 3.9 – Results of a study of the permeability of modified membranes

Type of water	Unit, L/m <sup>2</sup> .h					
	PSS-0	PSS-0.05	PSS-0.1	PSS-0.15	PSS-0.2	PSS-0.25
Pure water	65.20	104.97	105.46	127.75	101.09	102.305
CWW	25.7	43.39	41.155	55.995	39.755	40.965

Table 3.10 – Results of the study of the rejection (R%) of pollutants by modified membranes

Pollutants	Units	Values of pollutants in WW			
		Before cleaning	After cleaning		
		CWW	PSS-0	PSS-0.05	PSS-0.1
Anionic surfactant	mg/L	10.61	1.900	1.160	0.700
Oil products	mg/L	35.20	13.16	7.95	7.31
TSS	mg/L	649	98	38.9	25.9
COD	mgO <sub>2</sub> /L	310	108	62	58
		CWW	PSS-0.15	PSS-0.2	PSS-0.25
Anionic surfactant	mg/L	10.61	0.540	0.910	1.260
Oil products	mg/L	35.20	3.58	8.54	7.65
TSS	mg/L	649	44	69	70
COD	mgO <sub>2</sub> /L	310	68	80	86

From the data obtained, it can be seen, that in comparison with PVC membranes, membranes obtained with the addition of modified polymers showed a higher effect of CB purification with a significant decrease in permeability.

### **Conclusions to chapter 3**

This chapter was focused on the method of preparation PVC-based UF membranes and their experiments of permeability and car wash wastewater rejection, and the results showing the optimal concentration for non-modified PVC-based UF membranes was 14 wt.% of PVC due to its much greater permeability compared to 15 and 16 wt.% of PVC, which used next to prepare another new type of membranes by using mechanosynthesis and new modified nanoparticles.

Moreover, the rejection of pollutants in car wash wastewater clarified through UF membrane filtration, emphasizing the importance of monitoring pollutant concentrations before and after filtration. Monitoring changes in car wash wastewater composition during filtration was a key aspect of the experimental setup, evaluating the effectiveness of the prepared membranes.

## Chapter 4. Discussion of the Results

### 4.1 Non-Modified PVC Membranes

#### 4.1.1 The Morphology, Topology and other characteristics

One of the most crucial variables in the phase inversion method of membrane fabrication is the polymer concentration in the dope solution since it has an impact on the final membrane structure and, consequently, its performance. Figure 4.1 shows the cross-sectional SEM images of the flat-sheet membranes prepared from different PVC concentration in dope solution.

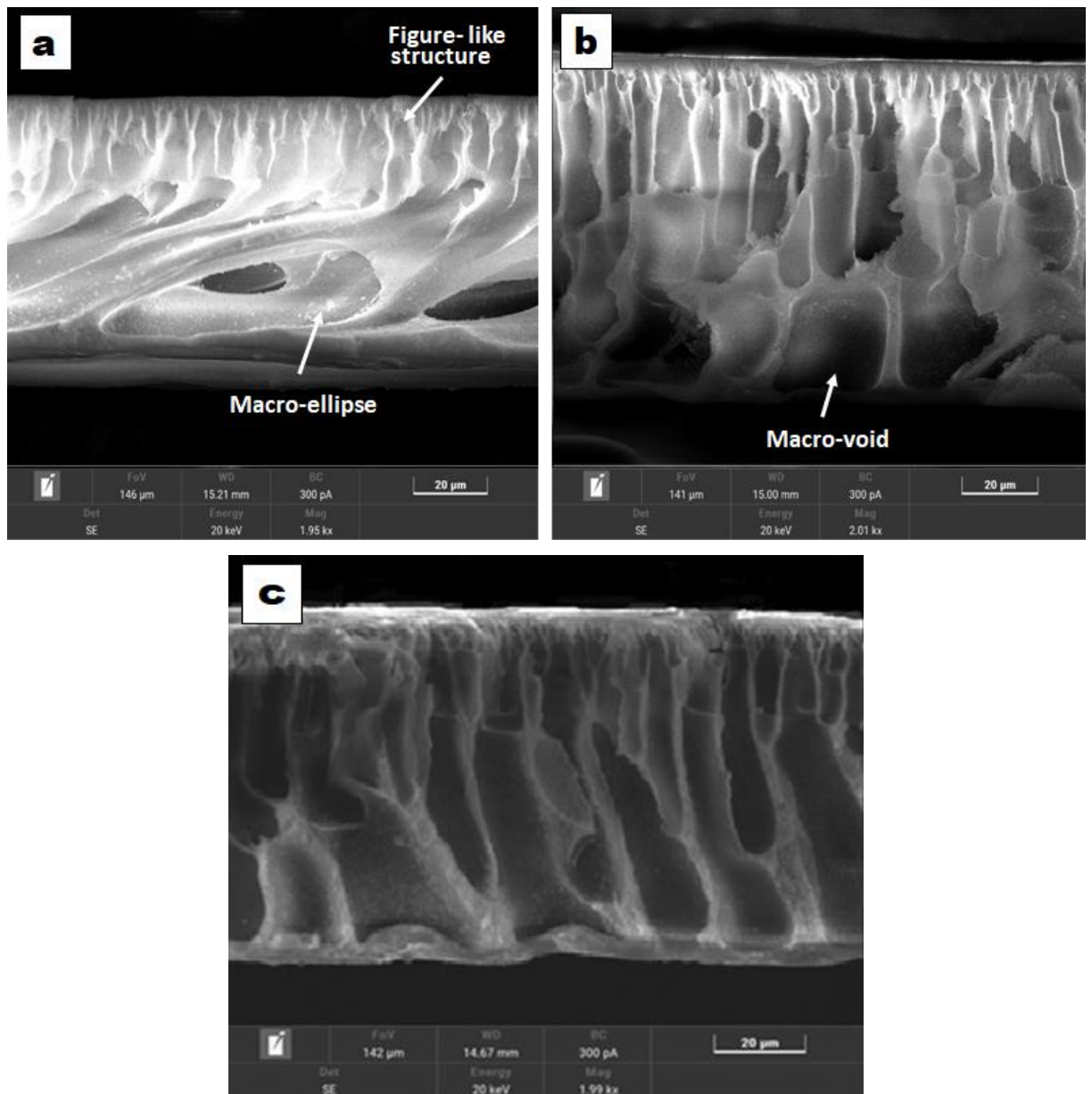


Figure 4.1 – SEM images of cross-sectional morphology of PVC flat sheet membrane: (a) 14 wt.%, (b) 15 wt.%, and (c) 16 wt.%.

The cross-sectional structure for the membrane prepared from 14 wt.% PVC concentration, a small finger-like structure layer is located at the edge of flat-sheet membrane as shown in Figure 4.1a. By increasing the PVC concentration to 15 wt.%, a finger-like structure layer be longer and a second layer is formed like a macrovoids in the shape of spheres, as shown in Figure 4.1b. While the two layers merged together and changed to a thin and long finger-like structure and the macro-voids disappeared with an increase of PVC concentration in dope solution to 16 wt.%, as shown in Figure 4.1c.

The findings of this study corroborate previous reports in the literature. By considering the following factor, the morphology of the manufactured PVC flat-sheet can be explained: with the increase of the polymer concentration the viscosity of the dope solution, accordingly, will become higher, which will lead to slowing the exchange of solvent and non-solvent and thus delay in the demixing of solvent and polymer. Indeed, rapid diffusion flow of non-solvent across the polymer solution causes the creation of macrovoids. The increasing in PVC concentration in the dope solution, will impede the non-solvent ability to diffuse, resulting in a reduction in macro-voids size [107, 108].

The roughness parameters are presented in Table 4.1, as well as the 2D and 3D AFM topological of the membrane prepared with various concentrations of PVC in dope solution are shown in Figures 4.2, 4.3, respectively.

Table 4.1 – Roughness parameters for the AFM images of membranes

PVC membranes	Average roughness Ra, nm	Root mean square Rq, nm	Area peak-to-valley height Rz, nm
PVC-14	7.877	10.363	101.838
PVC-15	6.297	7.986	80.819
PVC-16	4.887	6.155	59.678



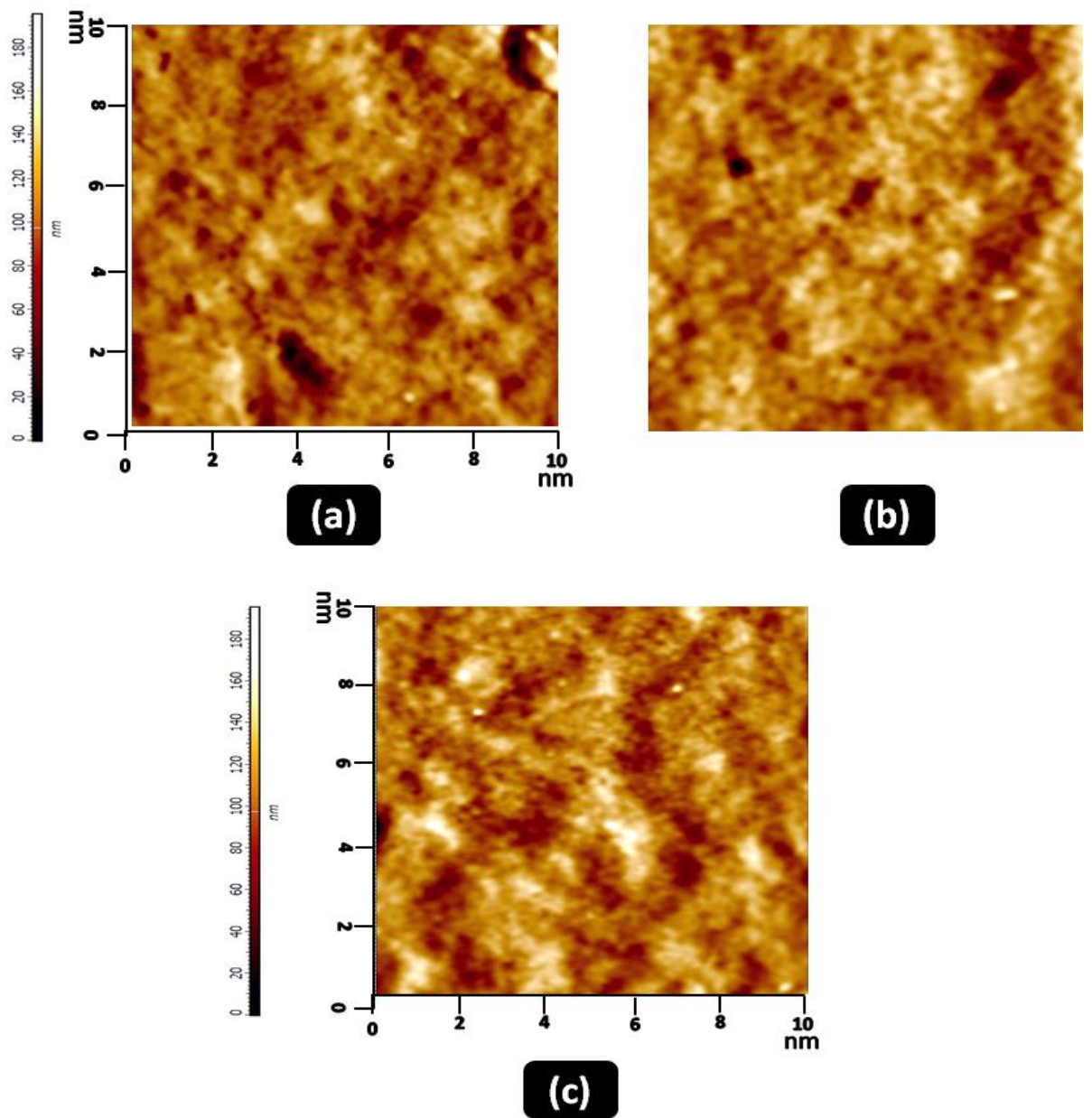


Figure 4.2 – 2D AFM surface topology for the flat-sheet PVC membranes (a) 14 wt.%, (b) 15 wt.%, and (c) 16 wt.%.

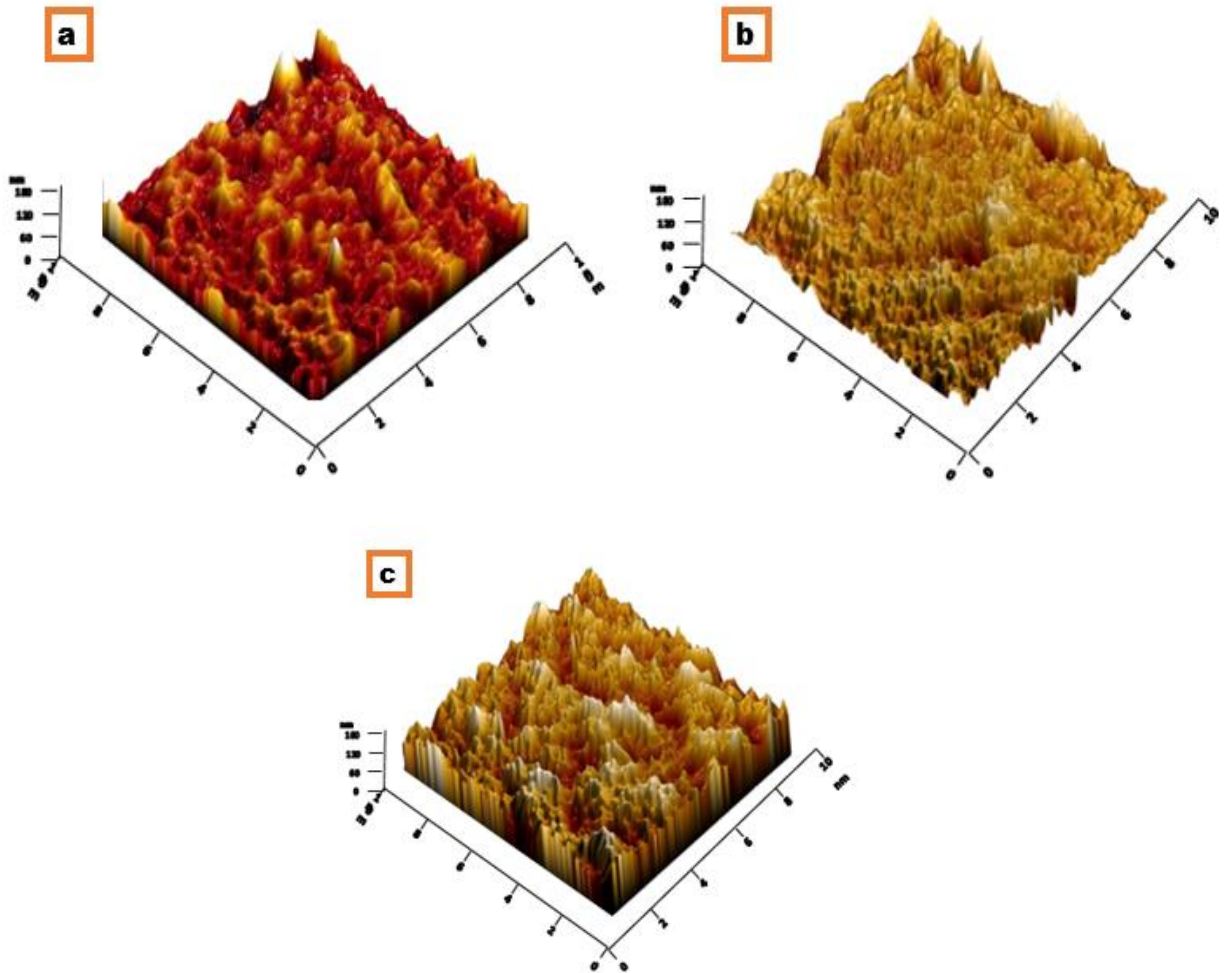


Figure 4.3 – 3D AFM surface topology and roughness for the flat-sheet PVC membranes (a) 14 wt.%, (b) 15 wt.%, and (c) 16 wt.%.

In the AFM image, the dark regions are valleys (i.e., pores) and the bright regions are high points or nodules. Surface roughness is considered the most important factor for improving the antifouling ability of membranes [42, 109]. From AFM images and the roughness parameters ( $R_a$ ) of the synthesized membranes with a PVC concentration from 14 to 16 wt.%, it was observed that the maximum value of  $R_a$  7.877 was recorded for a membrane with 14 wt.% PVC, and the minimum is 4.887 for a membrane with a concentration 16 wt.% PVC. A membrane with a rougher surface has a greater tendency to deposit particles on its surface, where the pollutant particles accumulate in the valleys of a membrane and thus fouling will be more serious. The average pore size of a membrane can affect its roughness, and various studies have shown that membranes with larger pore sizes tend to have higher roughness values compared to membranes with

smaller pore sizes. This concluded that the rougher membrane with concentration 14 wt.% of PVC of the three membranes studied which have a greater pore size and antifouling properties.

Increasing the polymer concentration in the dope solution to 16 wt.% decreased the average roughness by about 38 %, and from Figure 4.5, it can be seen that the pore size decreases at the same concentration (16 wt.%), which indicates that increasing the polymer concentration has an effect on the membrane performance, and Rajesh et al.'s study [110], indicated that the relationship between changes in pore size and the average surface roughness of the membrane was confirmed.

Figure 4.4, shows the effect of PVC concentration during casting on the thickness and porosity of the flat UF membranes.

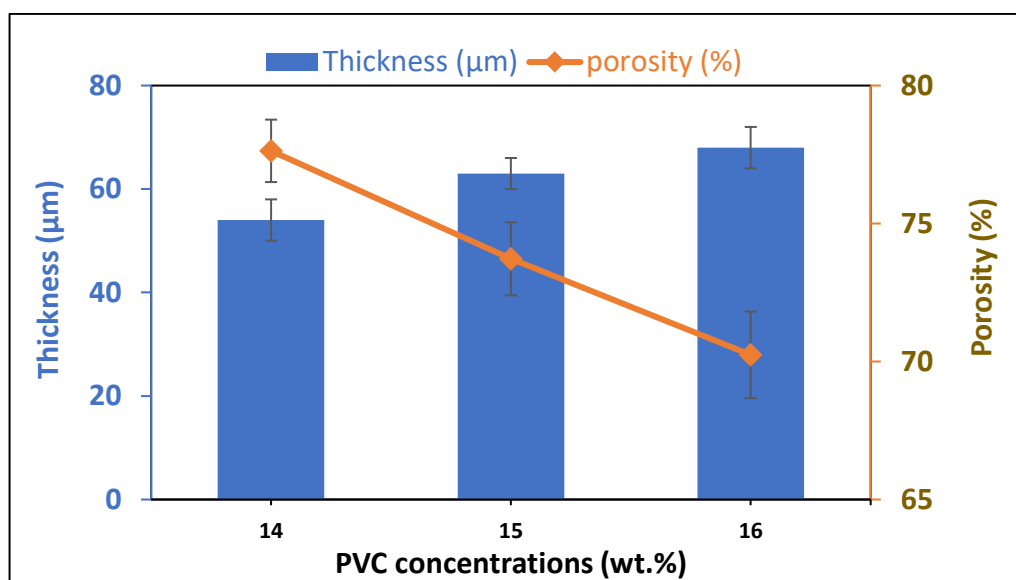


Figure 4.4 – Effect of PVC concentration in dope solution on thickness and porosity.

As can be seen from the figure, the porosity of PVC membranes decreases from 77.63 to 70.24 % as the concentration of PVC increases from 14 to 16 wt.%. This is consistent with the data of Bakeri et al. [111], who reported a decrease in the effective surface porosity of PVC membranes with an increase in the polymer concentration which used in their casting. This behavior concerned to the polymeric dope viscosity and its effect on the definitive membrane structure. An increase in the concentration of PVC in the dope solution resulting a higher viscosity of the dope solution, which might act as a handicap and cause a delayed in solvent/non-solvent exchange during phase inversion,

and, thus, in a major tendency to reduction macrovoids, which decrease the overall void fraction of the membrane. Also, this is related to the morphological structure of the PVC flat sheet membrane, which changed from large macrovoids to a thin and long finger-like structure of the cross-section. That evident the large macrovoid structure contributes to membranes' overall porosity [112]. While, raising the concentration of PVC in the dope solution from 14 to 16 wt.% leads to an increase in the thickness of the membrane. This can be explained by an increase in the viscosity of the dope solution at higher concentrations of PVC [113].

Furthermore, the effect of PVC concentrations on the pore size of membranes were investigated using the Guerout- Elford-Ferry formula and the graph for mean pore diameter (nm) is shown in Figure 4.5. from the figure clearly demonstrates that increasing the PVC from 14 to 16 wt.% has given a smaller pore size. The concentration 14 wt.% PVC revealed the biggest mean pore diameter ( $34.96 \pm 0.48$  nm) compared to the other membranes, and mean pore diameter gradually decreased to  $27.93 \pm 0.54$  nm, with increase in PVC concentrations, this is consistent with the literature [114].

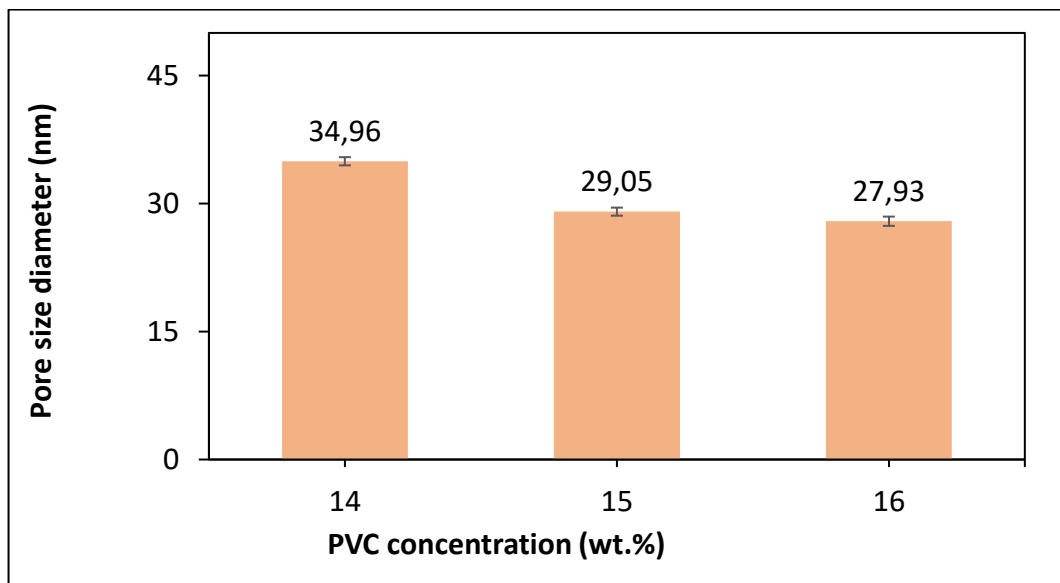


Figure 4.5 – Effect of PVC concentration in dope solution on pore size of membranes

#### 4.1.2 PVC membranes performance evaluation for carwash treatment

The obtained permeation flux (J) for pure water (PW) and carwash wastewater (CWW) for different PVC membranes are presented in Figure 4.6.

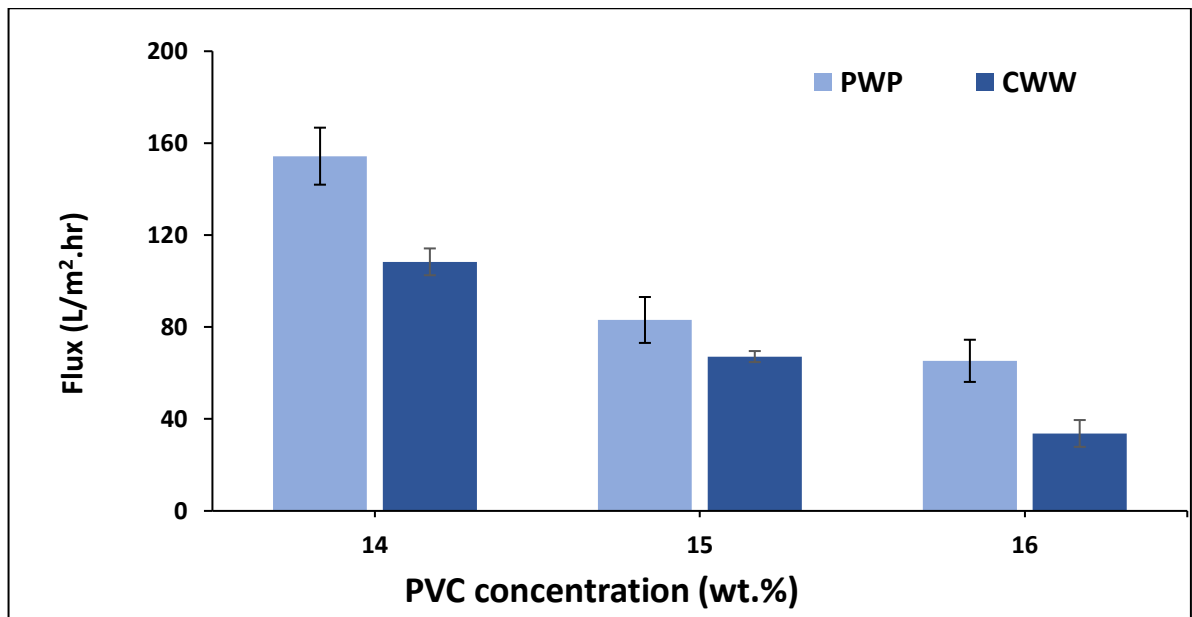


Figure 4.6 – Effect of PVC concentrations on permeation flux for Pure water (PW) and CWW

The permeation flux for PW and CWW of the PVC flat-sheet membranes decreases from (154.34 to 65.29) and (108.36 to 33.70) L/m<sup>2</sup>.hr, respectively, with increase of PVC concentration in dope solution from 14 to 16 wt.%. This is 13.3–57.7% and 12.7–68.9 % higher in terms of permeation flux for PW and CWW, respectively. This result can be attributed mostly to the decrease of the average membrane pore size also to the lower membrane porosity, which is observed when PVC percentage in the dope solution increases. Alsahy et al. [115], noticed decline in the water flux with increase of PVC concentration in dope solution, this related to the narrower of the pore size and pore density, and also decreases in the porosity of the synthesized membranes with the increased of the polymer concentration in dope solution.

The results of the rejection of PVC membranes for wastewater treatment of car washes from the main pollutants (Table 3.5) are presented in Figure 4.7.

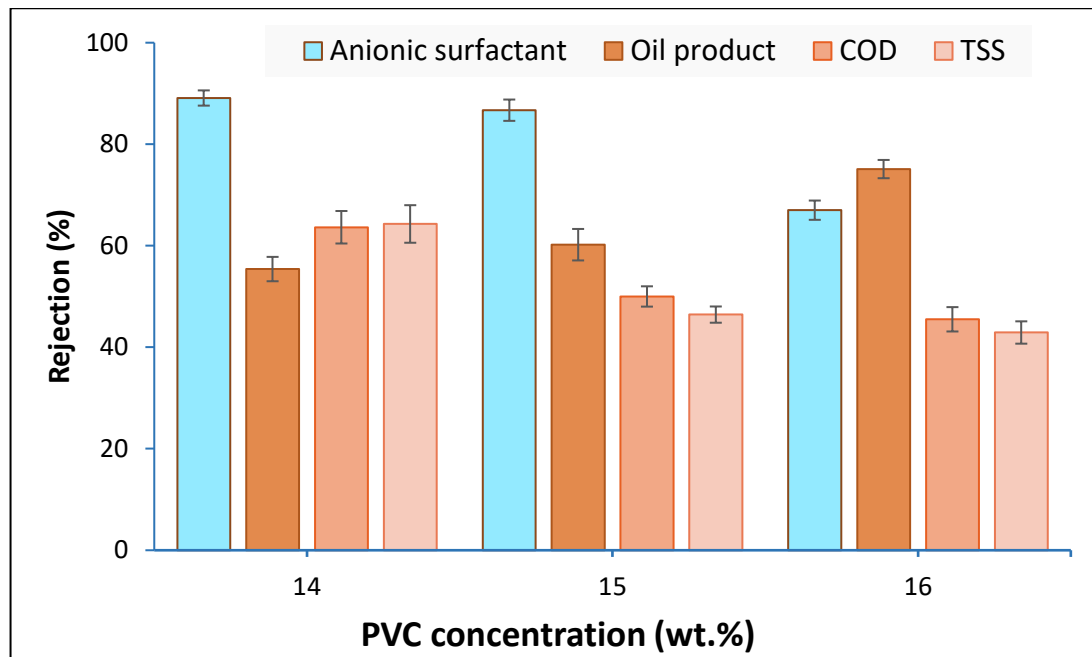


Figure 4.7 – Effect of PVC concentration in PVC membranes on the rejection for carwash wastewater treatment

Oil products are formed from various petroleum compounds used in car washes and can seep from a vehicle's surface, tires, engine parts, and braking system [71]. It has been established that the rejection of oil and grease for carwash wastewater increases from 45.4 to 75.1 % with increase of PVC concentration in dope solution from 14 to 16 wt.%. This indicates that the rejection raises to the maximum at 16 wt.% of PVC concentration and when the permeation flux of CWW about 33 L/m<sup>2</sup>.h. That effect is consistent with the concept of trade-off, which states that lower water permeability invariably results in increased selectivity [116]. Therefore, the observed permeation flux and PVC efficiency trends, observed with the increase of PVC concentration, are produced by interplay of different factors, such as membrane morphology with reduced macrovoids and lower overall porosity, together with smaller membrane pore size.

As can be seen from Figure 4.7, PVC membranes with a concentration of 14 and 15 wt.%, provide a sufficiently high and close in rejection degree of anionic surfactants as (MBAS) in the range from 89.1 to 86.7 %. In contrast, there is a marked decrease in the effectiveness of the membrane with a PVC concentration of 16 wt.% (67 %) due to the membrane's surface having a percentage of large pores. The rejection of COD was 63.6 %, as well as total suspended solids was 64.3 %, which obtained for a membrane with 14 wt.% of PVC concentration for carwash wastewater treatment. Also, it can be

seen similar patterns about the effect of the PVC concentrations (14–16 wt.%) membranes on the rejection of carwash wastewater from both organic substances that cause COD and suspended solids.

Total suspended solids (TSS) in the wastewater of car washes can be in the form of a coarse suspension (particle size less than 100  $\mu\text{m}$ ), a thin suspension or emulsion (particle size 100–0.1  $\mu\text{m}$ ) and colloidal substances (particle size 0.1–0.001  $\mu\text{m}$ ) [117]. Ultrafiltration membranes are characterized by a high degree for removal solid and emulsified suspended substances, which are larger than the pores of the membrane. At the same time, organic substances that cause COD and contained in wastewater in dissolved or colloidal form can stick to the surface of suspended solid substances, and removing them from the water with them [118]. This helps to explain the significant reduction in COD by UF membranes and the patterns of wastewater treatment similar to suspended substances. Another explanation is the partial clogging of pores with suspended substances, which contributes to the retention of large molecules of organic impurities that cause COD.

Variations of permeation fluxes of PVC membranes for CWW are shown in Figure 4.8.

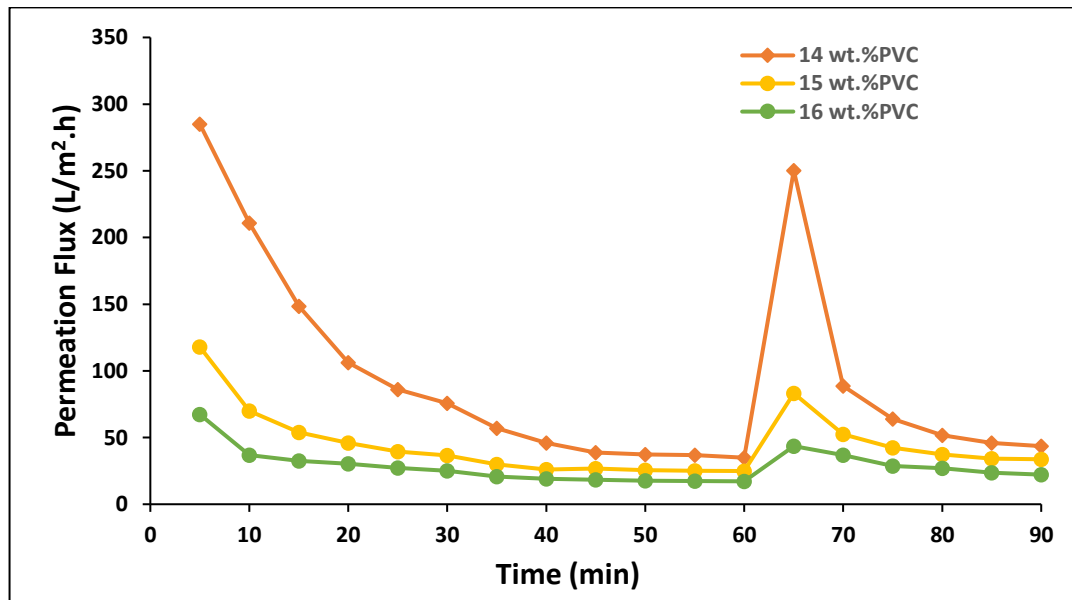


Figure 4.8 – Time-dependent permeation flux of PVC membranes of CWW

It can be noticed that the permeation flux declines instantly as compared to the water flux at the beginning. After back-flushing, the membranes are unable to recover

their water flux as a result of the irreversible fouling. Distinctly, the recovered flux of 14 wt.% PVC membrane is much higher than others. Whereas 15, and 16 wt.% of PVC membranes have lower recovered flux because these membranes suffer earnest irreversible fouling.

The flux recovery ratio (FRR) is a parameter used to examine the membranes' ability to antifouling [119, 120]. Higher FRR indicates that a significant part of fouling is reversible and that a large portion of weak foulant deposits can be eliminated using hydraulic cleaning or back-flushing after the filtration process. The FRR of 14 wt.% of PVC membrane is about 86.21%, while the 15, and 16 wt.% of PVC membranes display much lower values are 63.64% and 54.43%, respectively, as shown in Figure 4.9. The  $R_r$  of 14 wt.% of PVC membrane increases from 13.79 to 45.57 %. Indicating, the foulants deposited on the membrane surface can't be easily removed by back-flushing. As a result, the corresponding  $R_r$  is decreased.

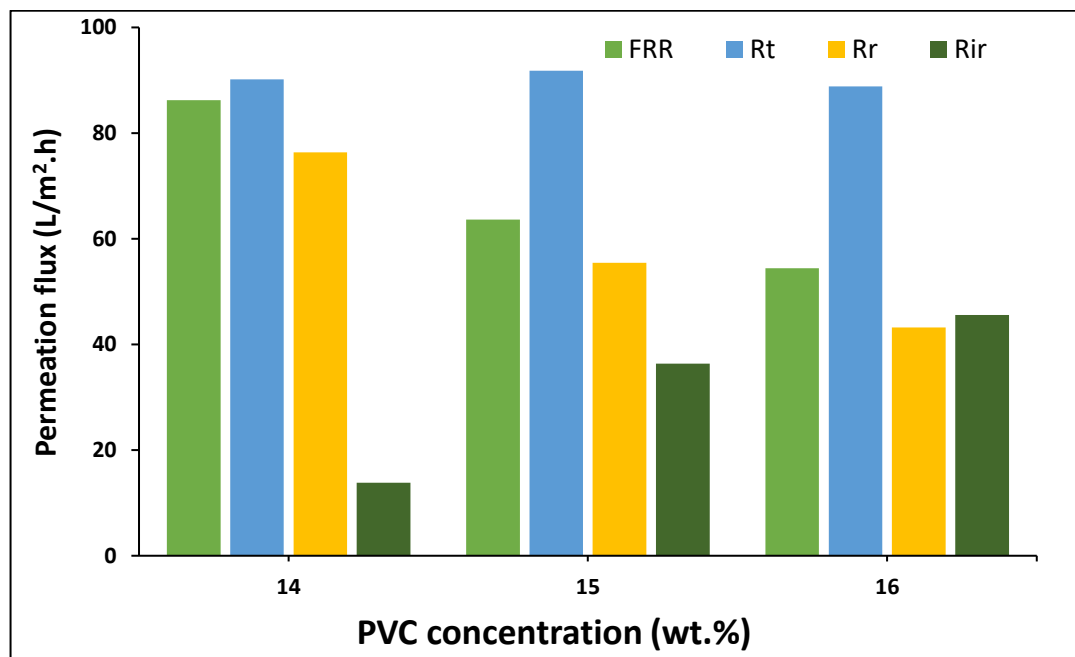


Figure 4.9 – FRR,  $R_t$ ,  $R_r$  and  $R_{ir}$  during the filtration of CWW

The PVC-UF membranes were used for 3-cycle carwash wastewater treatment to evaluate the effect of polymer concentration on membrane in long term. The permeation fluxes cannot completely recover to their initial values due to the irreversible fouling, as seen in Figure 4.10.



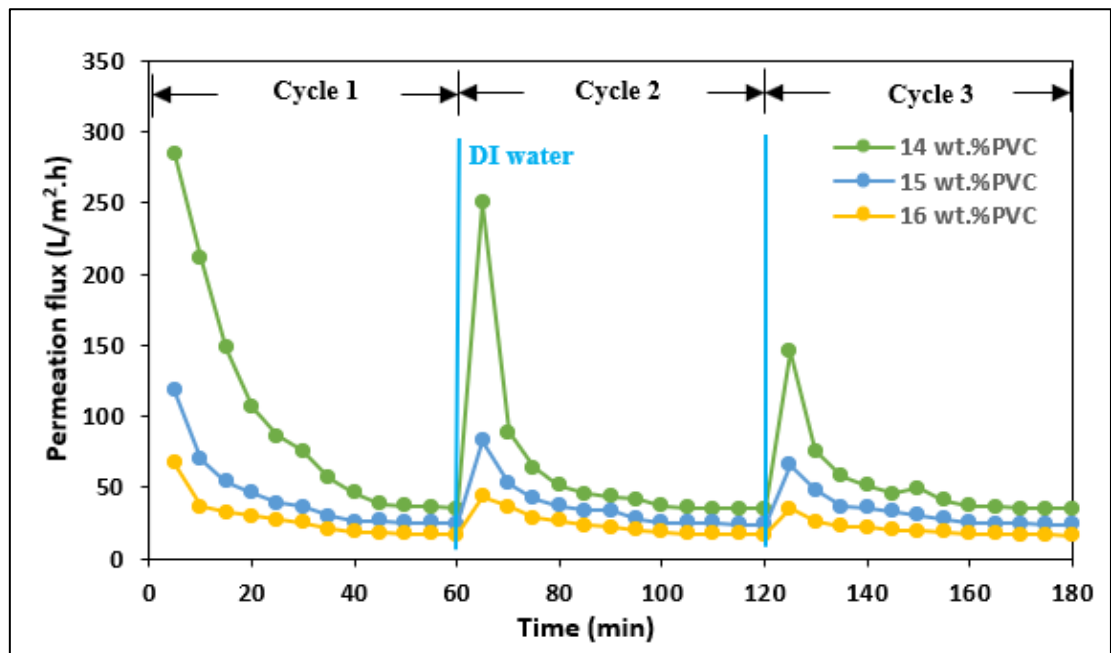


Figure 4.10 – Variations of permeation flux of the PVC-UF membranes for 3-cycle CWW treatment

Every cycle lasted one hour. After each cycle, the fouled membranes underwent a 15-minute back-flushing with DI water. After 3-cycle treatment, the permeation flux of the 14 wt.% PVC membrane is 42.18 L/m<sup>2</sup>h, whereas the permeation flux of the 15 and 16 wt.% PVC are 29.09 and 21.82 L/m<sup>2</sup>h, respectively. The variation in permeation flux corresponds to with the FRR trend. For 14 wt.% PVC membrane, FRR is approximately 55.45 % as 3 cycles ended, which is greater than 15, and 16 wt.% of PVC membranes. This shows that the 14 wt.% PVC membrane significantly has anti-fouling resistance in long-term operation more than other membranes.

## 4.2 Post- Modified PVC Derivatives Membranes

### 4.2.1 Characterizations and Performance Evaluation of PM PVC Membranes

One of the basic methods for characterizing membranes is scanning electron microscopy (SEM), which provides information on the manufactured membranes' topography and morphology [121]. A cross-section sample is created by freezing the sample in liquid nitrogen (-195 °C) and then cracking it, then, an image of the fractured surface is captured with an exact magnifications using a scanning electron microscope

(SEM) [122]. Cross-sectional SEM images of the modified membranes are shown in Figure 4.11.

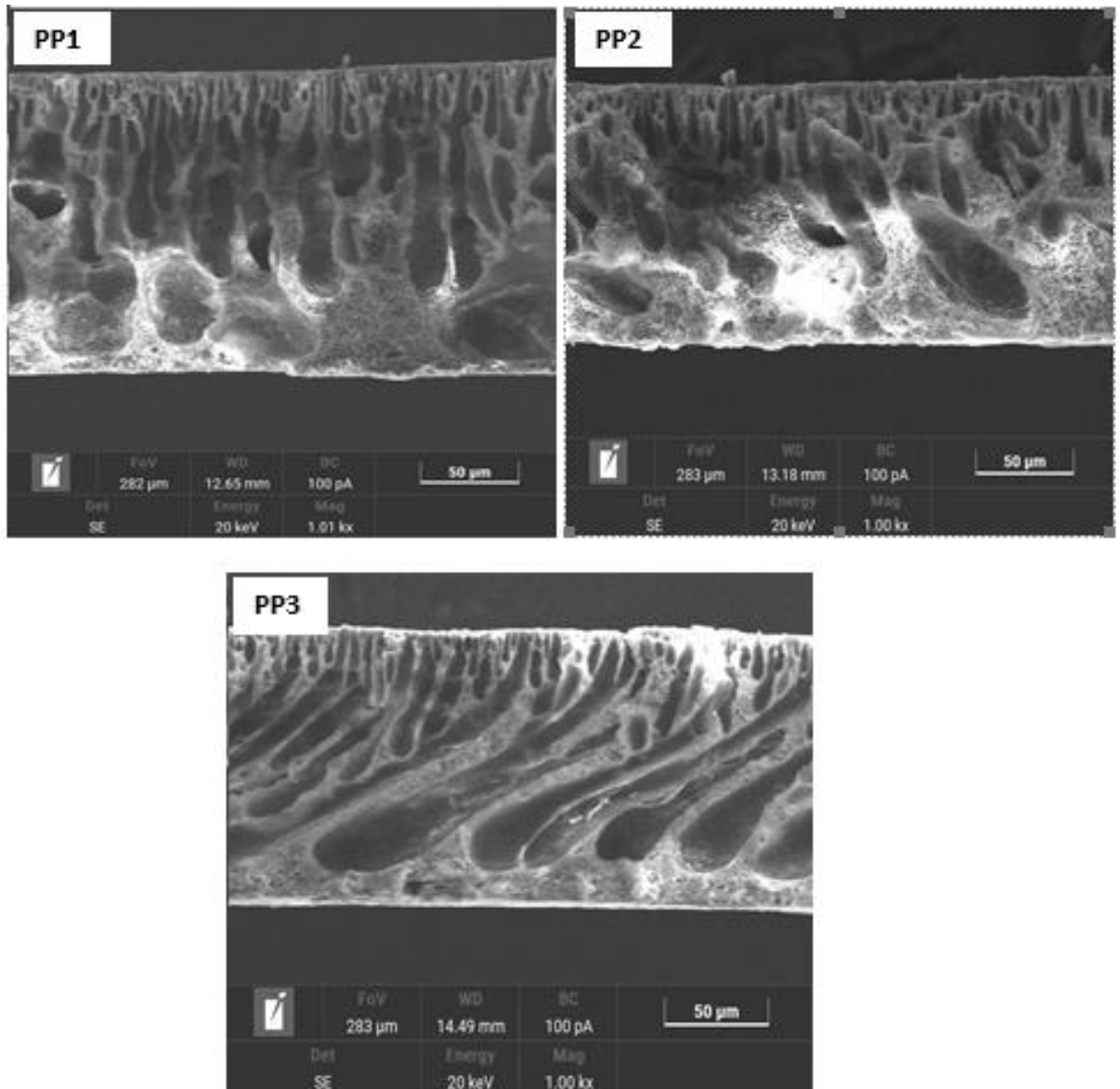


Figure 4.11 – SEM images of cross-sectional morphology of PVC

It can be seen that a few sponge-like structure with more finger-like layer is formed in the cross section of the prepared membranes from post modified PVC. From figure, the structure of the cross section of the membranes PP1 and PP2 appeared a thin finger-like structure layer and a macrovoid structure with a abundance sponge-like structure near the bottom surface, which results a high porosity for these types of membranes, while the cross section SEM for the membrane PP3 revealed a longer finger-like structure layer with a few sponge-like structure formed. These results were appeared also in the results of other researchers [123].

The porosity, and thickness of membranes are important properties required to evaluate the nature of the membrane. Figure 4.12 displays the porosity, and thickness of these different membranes.

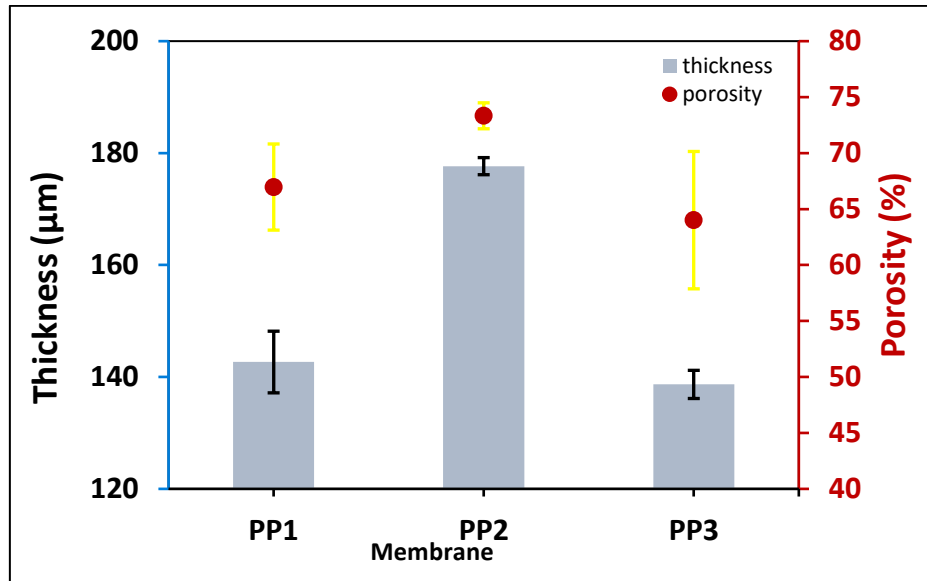


Figure 4.12 – The porosity, and thickness of PM PVC membranes.

It can be noted that the porosity and thickness of the PP2 membrane are higher than the other membranes, which are  $(73.33 \pm 1.16 \%)$  and  $(177.67 \pm 1.53 \mu\text{m})$ , respectively, and the lowest porosity and thickness of the PP3 membrane. This behavior is related to the viscosity of the polymeric dope and its effect on the final membrane structure, as the increased viscosity of the doped solution, which may act as a hindrance and cause a delay in the solvent/non-solvent exchange during phase inversion, leads to a significant tendency to reduce macrovoids, which decrease the overall void fraction of the membrane. Thus, the total void space of the membrane becomes denser and as a direct result of this, the porosity decreases.

Furthermore, the pore size of membranes was investigated using the Guerout-Elford-Ferry formula and the graph for mean pore diameter (nm) is shown in Figure 4.13.

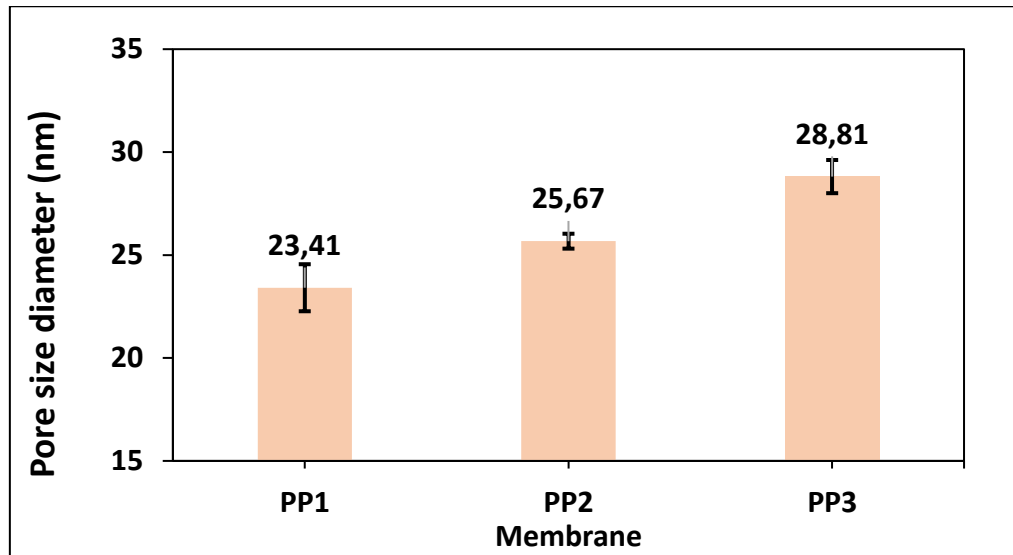


Figure 4.13 – The pore size diameter of PM PVC membranes.

The membrane PP3 revealed the biggest mean pore diameter ( $28.81 \pm 0.8$  nm) compared to the other membranes, these results can be attributed to the nature of the added polymers, which affected the shape and internal microstructure of the final membranes. The obtained permeation flux (J) for pure water (PW) at 25 °C and 2 bar for different types of membranes are presented in Figure 4.14.

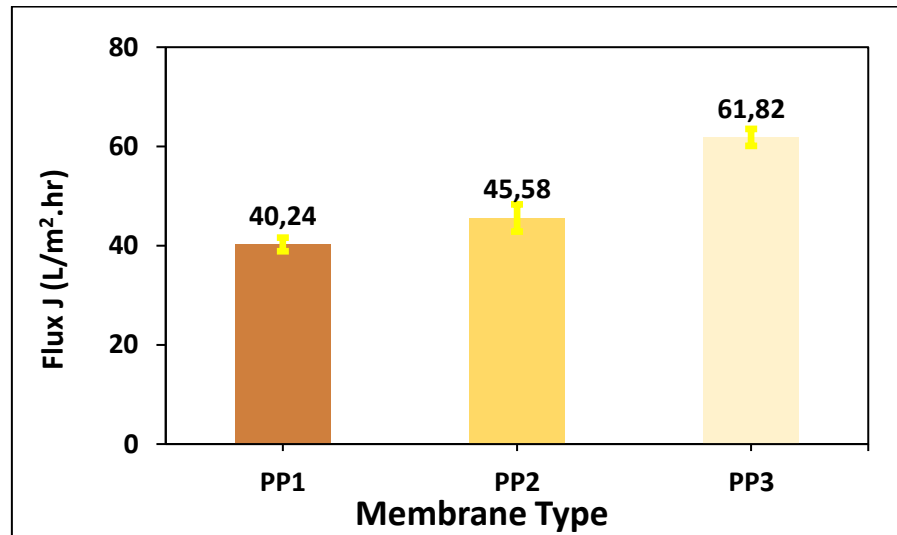


Figure 4.14 – Permeation flux of PM PVC membranes

The highest permeation flux for the three types of flat UF membranes was  $61.82 \pm 1.7$  L/m<sup>2</sup>.h for PP3, while the permeation flux for the other membranes is almost similar,  $40.24 \pm 1.3$  L/m<sup>2</sup>.h and  $45.58 \pm 2.7$  L/m<sup>2</sup>.h for PP1 and PP2 membranes, respectively. This difference in PWF values between the membranes was due to the different viscosity of the casting solution used to prepare the membranes. The higher

viscosity of the casting solution reduces the diffusion exchange rate during the phase reversal between solvent and non-solvent, whereby a denser skin layer with lower porosity will be formed, due to the delayed demixing process. Furthermore, this result can be attributed to the high pore size diameter for the PP3 membrane. These results will ultimately lead to lower permeability of the membranes and higher removal of contaminants.

Figure 4.15 illustrate the rejection of carwash wastewater by PM PVC membranes with specification 172.8 mg/L for oil product, 8.769 mg/L for anionic surfactant and 526 mg/L for TSS.

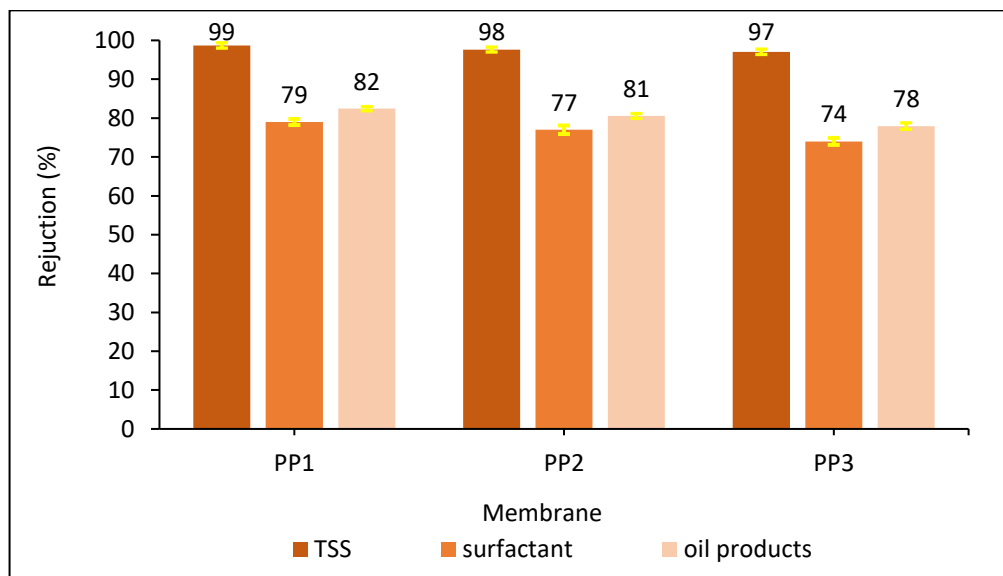


Figure 4.15 – Rejection of TSS, oil products and anionic surfactant of PM PVC membranes

From figure 4.15, the rejection of oil products for carwash wastewater were 82.4 %, 81 %, and 77.3 % , also the rejection of suspended solids was 99 %, 98 %, and 97 % , as well as 79 %, 77 % and 74 % for rejection of anionic surfactant for the membranes PP1, PP2, and PP3, respectively. This indicates that the rejection raises to the maximum when the permeation flux of CWW about 40 L/m<sup>2</sup>.h. That effect is consistent with the concept of trade-off, which states that lower water permeability invariably results in increased selectivity. Therefore, the observed permeation flux and membranes efficiency are produced by interplay of different factors, such as membrane morphology with reduced macrovoids and lower overall porosity, together with smaller membrane pore size.

### 4.3 Nanocomposite PVC Membranes

#### 4.3.1 Characterizations of Nanocomposite Membranes

FTIR analysis of pristine and modified membranes with SiO<sub>2</sub>-SDS NPs are presented in Figure 4.16.

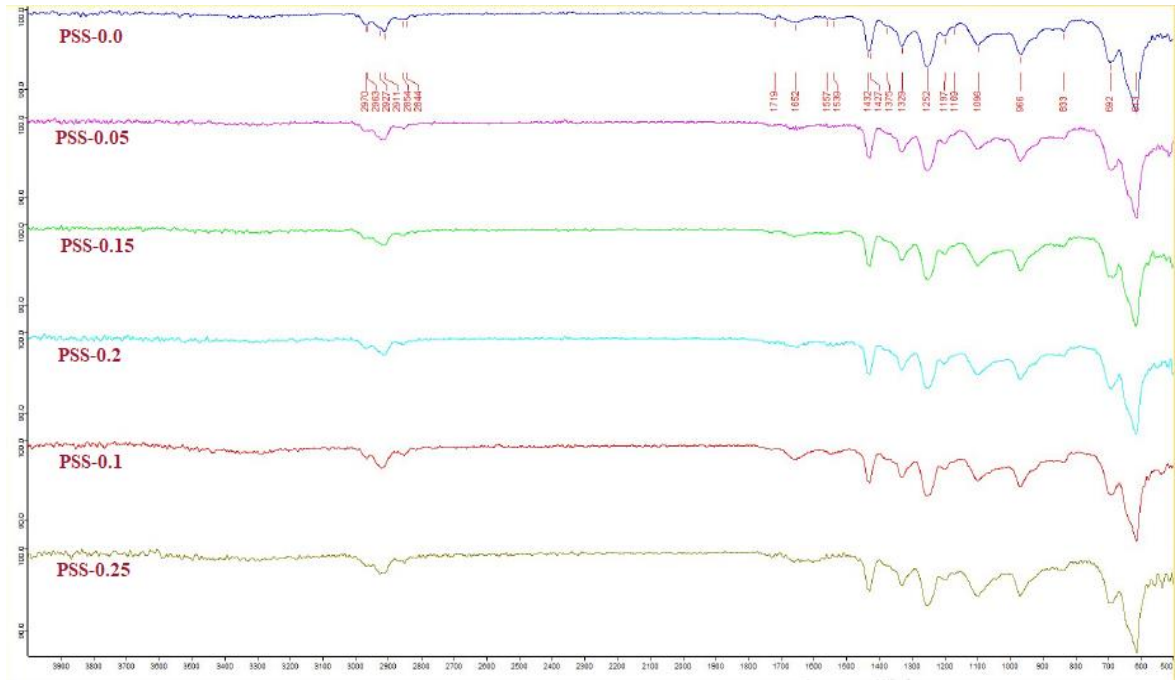


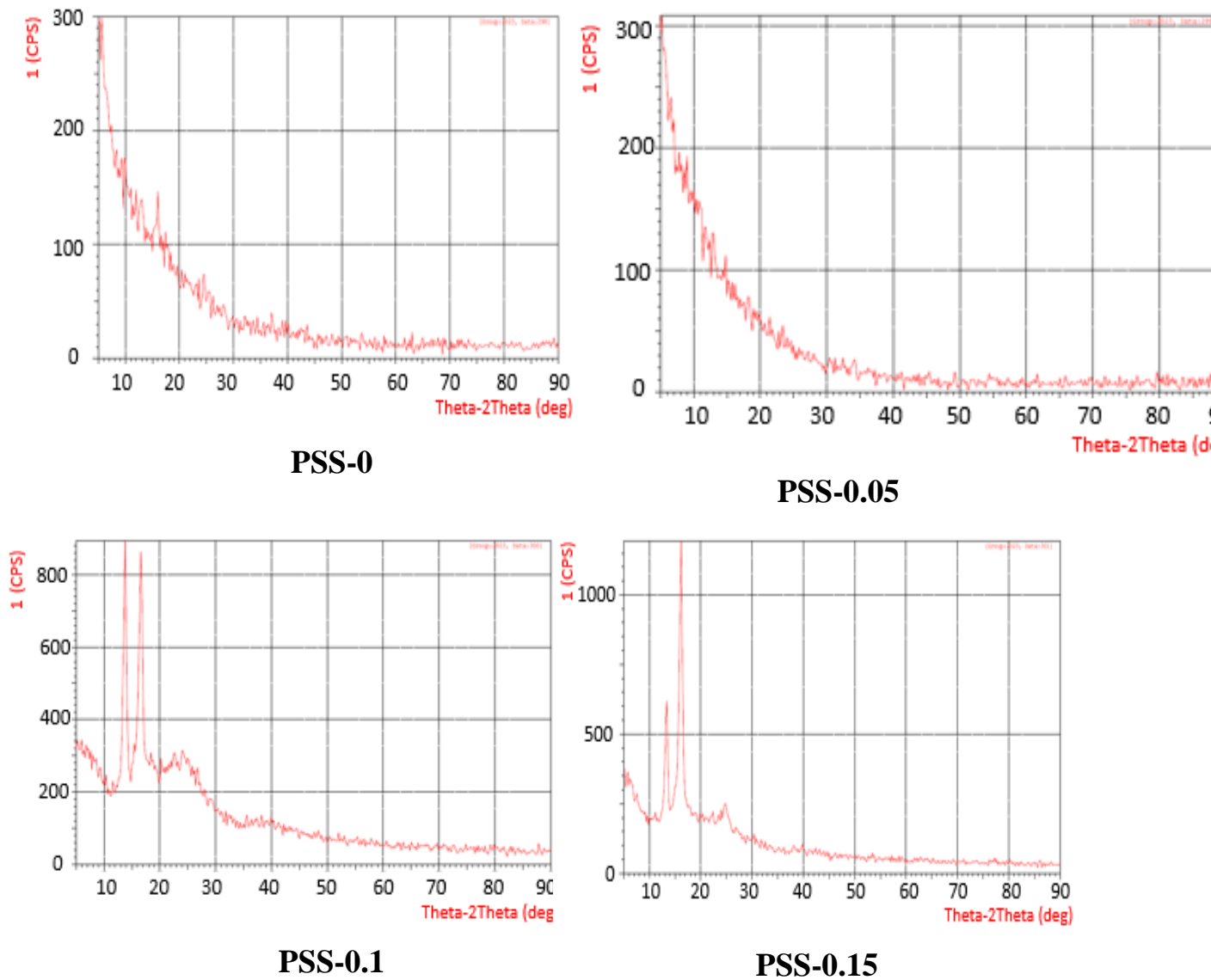
Figure 4.16 – FTIR of the pristine and MMMs

The FTIR spectrum of PSS-0 exhibits several bands characteristic of C–Cl, C–H, C=C and OH groups. As observed from Figure 4.16, the characteristic bands of pristine-PVC can be classified into three regions. The first is the C–Cl stretching region in the range of 800–600 cm<sup>-1</sup>. The second region is C–C stretching in the range from 1200–900 cm<sup>-1</sup>. The third region is C=C stretching in the range from 1425–1250 cm<sup>-1</sup> [124, 125].

Following the modification with SiO<sub>2</sub>-SDS NPs, the asymmetrical and symmetrical Si-O-Si stretching appeared at 1026 and 511 cm<sup>-1</sup>, respectively [126, 127]. Therefore, peaks at approximately 1026 cm<sup>-1</sup> confirmed the existence of Si-O-Si on the surface of modified membranes, which indicated the SiO<sub>2</sub>-SDS NPs were successfully incorporated. It can be noticed that the intensity peaks of Si-O-Si were enhanced progressively with an increase in the added concentration of SiO<sub>2</sub>-SDS NPs indicating that more SiO<sub>2</sub> NPs are accumulated in the membranes' surface. The peak at 2927 cm<sup>-1</sup> corresponds to the stretching vibration absorption of –OH groups. Remarkably, the intensity of this peak has

increased with an increase in the SiO<sub>2</sub>-SDS NPs addition indicating that more added SiO<sub>2</sub>-SDS NPs lead to an increase in the amount of –OH groups on the surface of the modified membranes which has a positive impact on improving their performance.

Figure 4.17, shows the XRD patterns of the synthesized membranes. As shown in the figure, the pristine and modified membrane with SiO<sub>2</sub>-SDS NPs 0.05 wt.% have amorphous structure. However, after increasing the SiO<sub>2</sub>-SDS NPs beyond 0.05 wt.% two sharp peaks at  $2\theta = 13^\circ$  (220) and  $16^\circ$  (311) (JCPDS card no. 19-0629) appeared while a smaller peak appeared at  $24^\circ$  (422) indicating a successful incorporating of SiO<sub>2</sub>-SDS NPs in the membrane surface [128, 129].



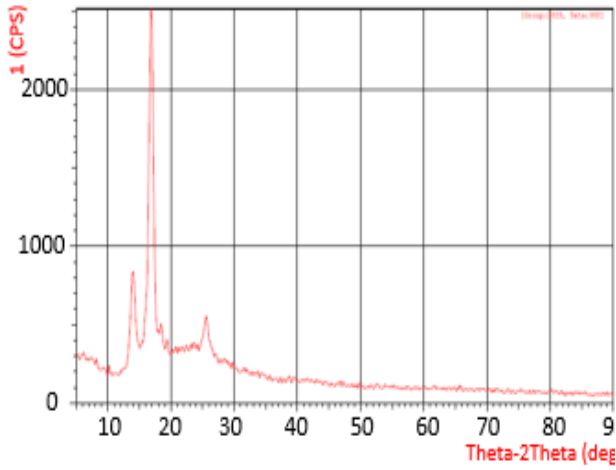
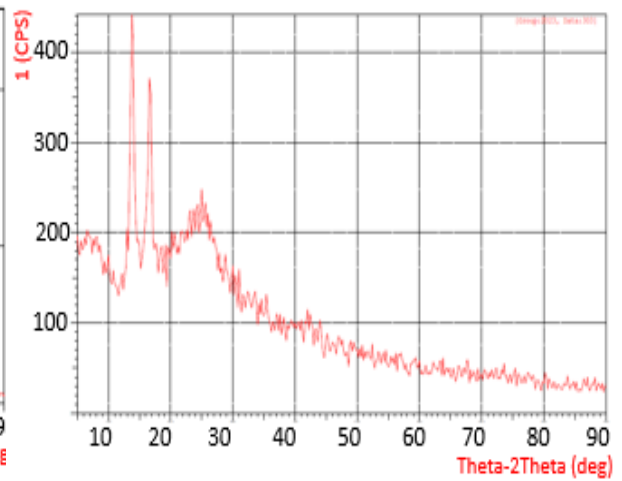
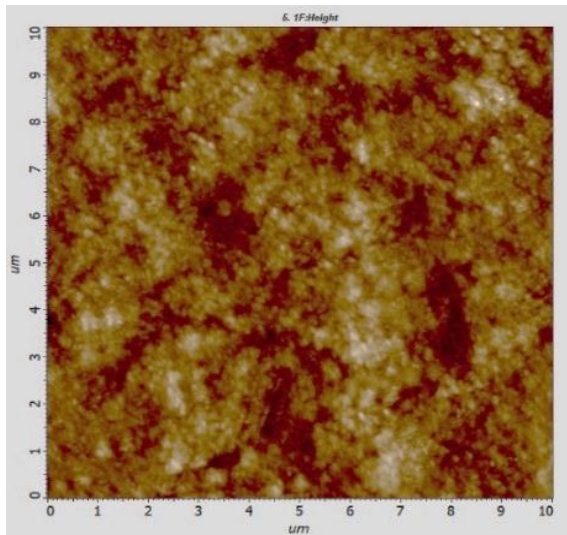
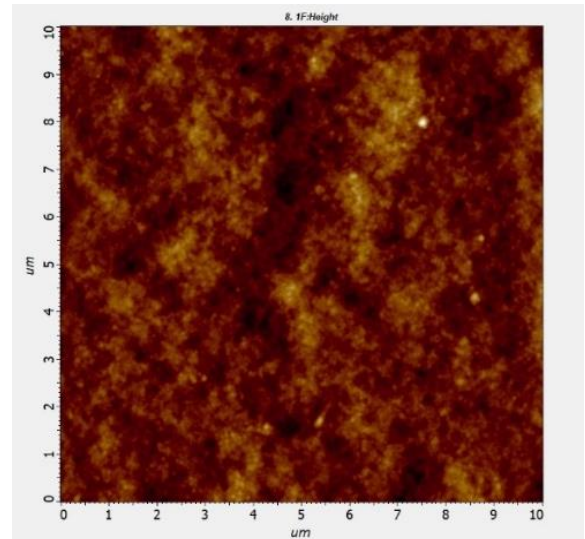
**PSS-0.2****PSS-0.25**

Figure 4.17 – XRD of the pristine and MMMs

Figures 4.18 and 4.19 show the two and three-dimensional surface AFM images of the top surfaces of the PVC membranes prepared at several  $\text{SiO}_2$ -SDS NPs amounts in the PVC casting solution. In these 2D and 3D images, the brightest regions present the highest area of the material's surface and the dark regions indicate the lowest areas of the membrane.

**PSS-0****PSS-0.05**



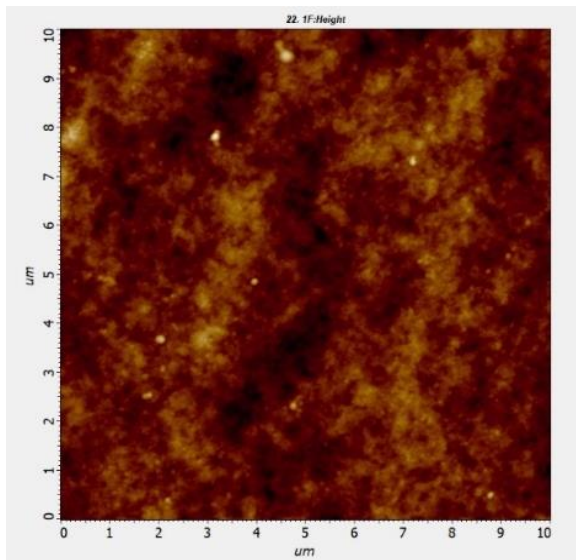
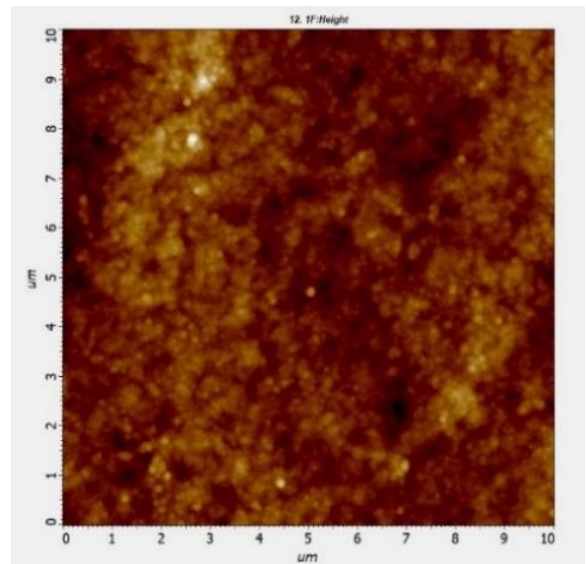
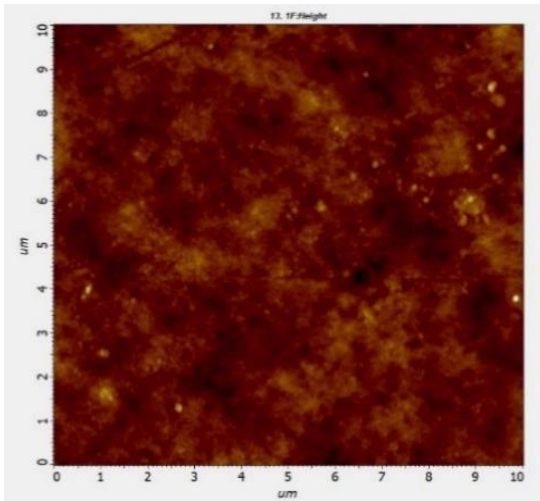
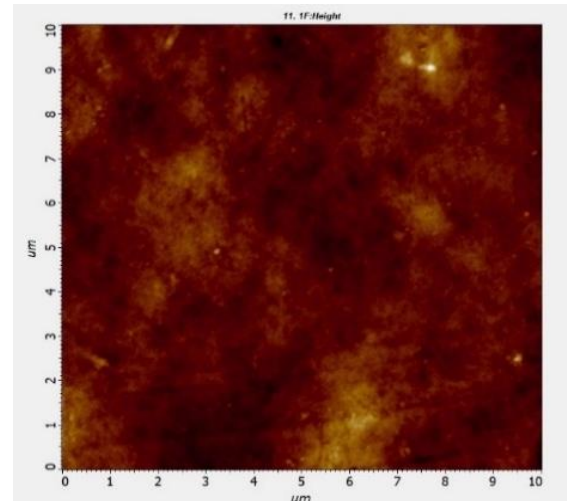
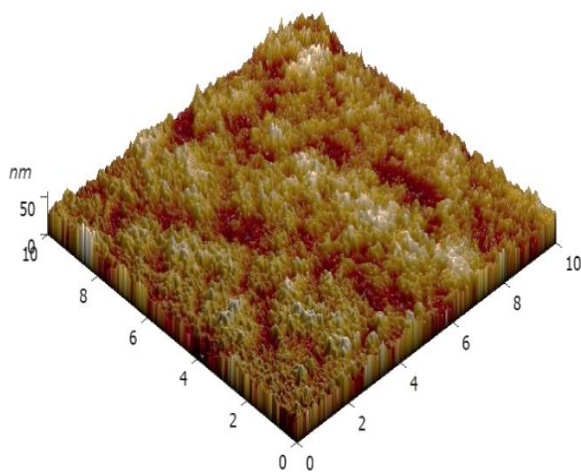
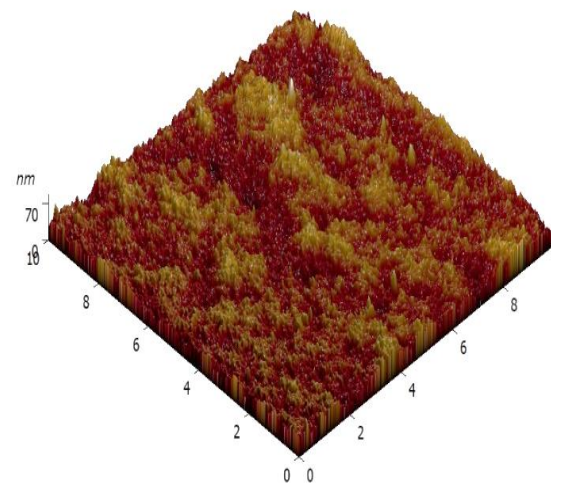
**PSS-0.1****PSS-0.15****PSS-0.2****PSS-0.25**

Figure 4.18 – 2D AFM images of the top surface of the pristine and MMMs

**PSS-0****PSS-0.05**

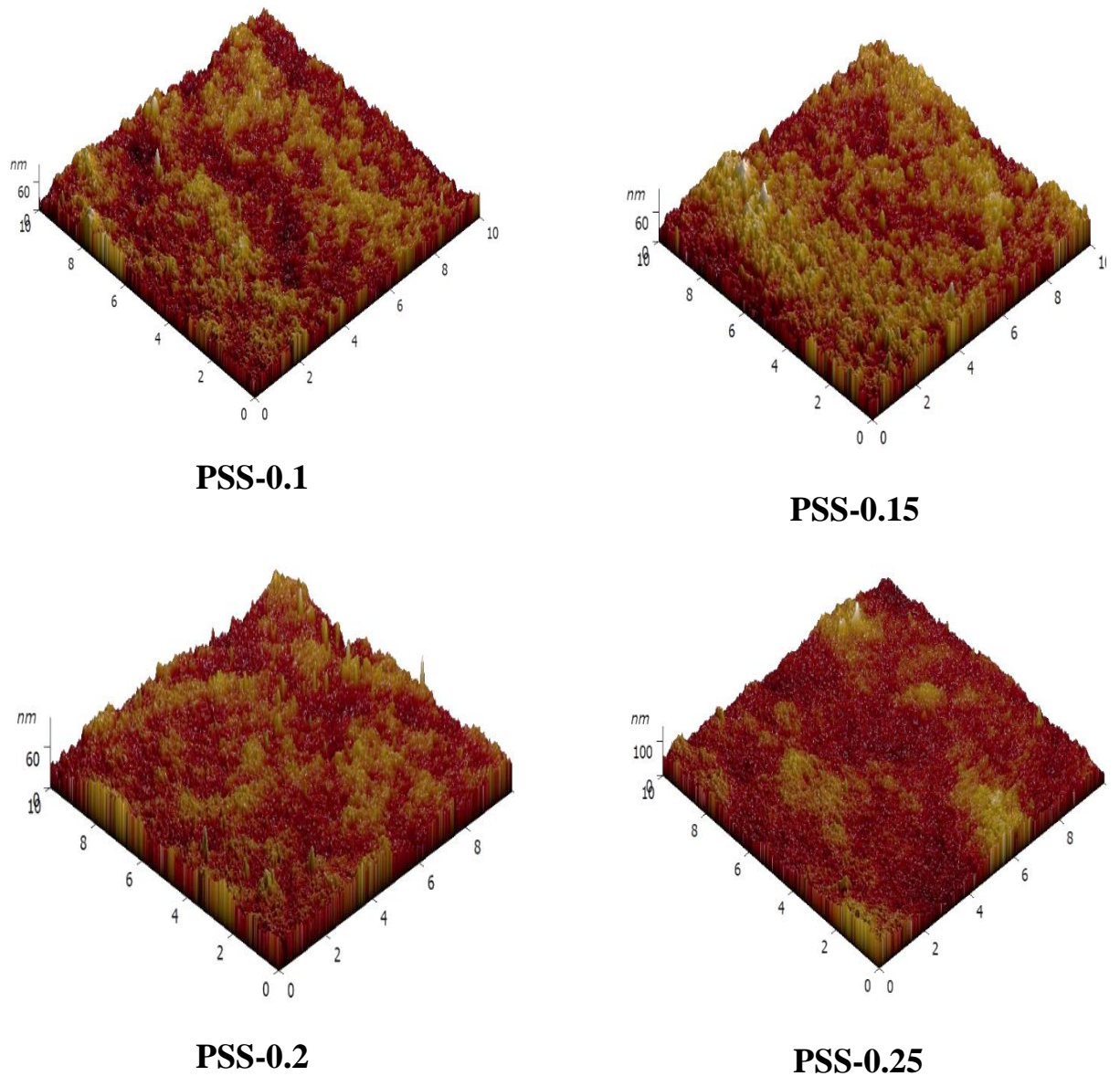


Figure 4.19 – 3D AFM images of the top surface of the pristine and MMMs

For the AFM images analysis, the roughness parameters were calculated for a scan area of  $10\text{ nm} \times 10\text{ nm}$ . Surface roughness is considered the most important factor for improving the antifouling ability of membranes [130, 131]. The surface roughness parameters of the membranes which are determined in terms of the average roughness (Ra), the root mean square (Rq), and the mean difference between the highest peaks and lowest valleys (Rz) are shown in Table 4.2.

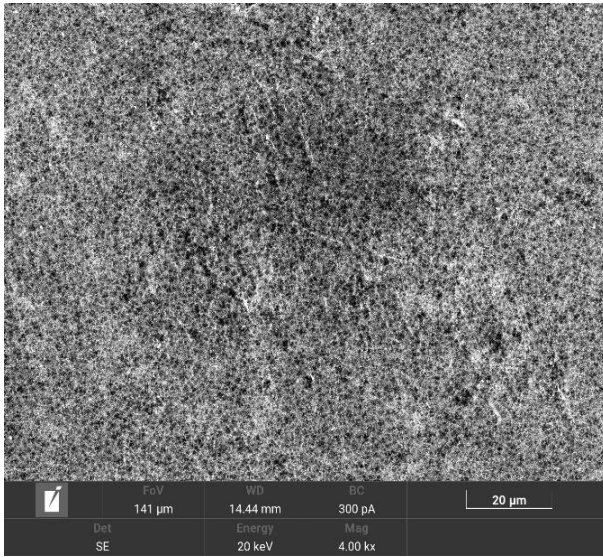
Table 4.2 – The surface roughness parameters from AFM images

Type of membranes	Average roughness (Ra), nm	Root mean square (Rq), nm	Distance between the highest peak and lowest valley (Rz), nm
PSS-0	<b>5.597</b>	<b>7.080</b>	<b>59.050</b>
PSS-0.05	7.023	8.873	89.939
PSS-0.10	8.248	10.403	100.325
PSS-0.15	8.364	10.662	109.499
PSS-0.20	6.143	7.833	102.962
PSS-0.25	9.580	12.455	146.930

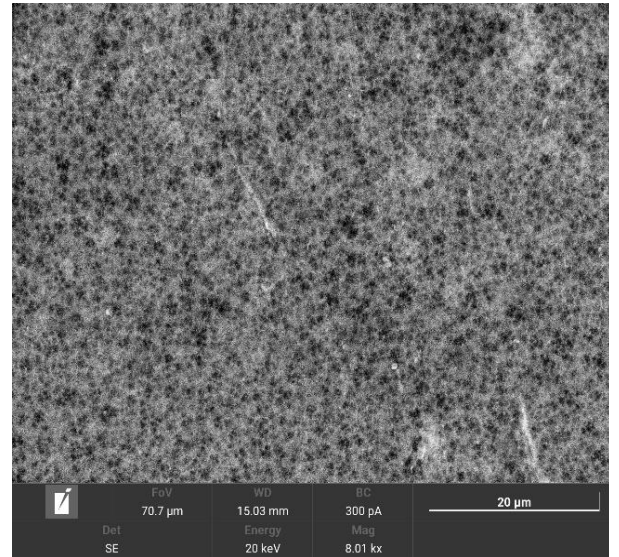
The membrane surface seems to be rougher after adding SiO<sub>2</sub>-SDS nanoparticles. As can be seen in Table 4.2, a growing trend in the roughness of the membrane surface could be observed by increasing the content of SiO<sub>2</sub>-SDS nanoparticles. When a 0.15 wt.% of SiO<sub>2</sub>-SDS NPs were added, the Ra value increased from 5.597 nm for pristine membrane (PSS-0) to 8.364 nm for (PSS-0.15), the Rq value increased from 7.080 nm (PSS-0) to 10.403 nm (PSS-0.15), and Rz value increased from 59.050 nm to 100.325 nm.

The increase in membrane roughness might be attributed to the incorporation of nanoparticles on the membrane surface. The membrane with a rougher surface has more tendency to deposition of particles on its surface. The particles accumulate in the valleys of the rough membrane surface. Subsequently, fouling becomes more severe for membranes with a rougher surface [132]; however, at the same time, the increase in roughness may increase the hydrophobicity of the membrane surface [133], leading to weaker interaction between foulants and the membrane surface. Whereas the addition of more NPs led to slight decreases in mean roughness to 6.143 nm for (PSS-0.2), but also is rougher than pristine membrane (PSS-0). This is mainly from the accumulation of more NPs on the surface of the membranes as shown in Figure 4.20. The mean pore size of a membrane can affect its roughness. Different studies have shown that membranes with larger pore sizes tend to have higher roughness values compared to membranes with smaller pore sizes [134]. The top surface SEM images of the pristine and MMMs

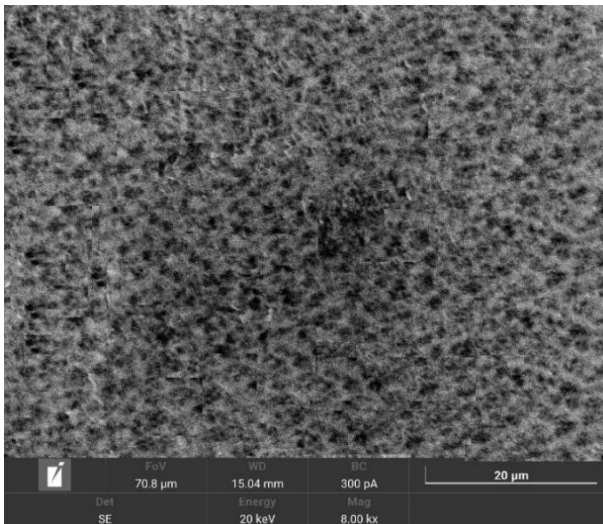
are presented in Figure 4.20.



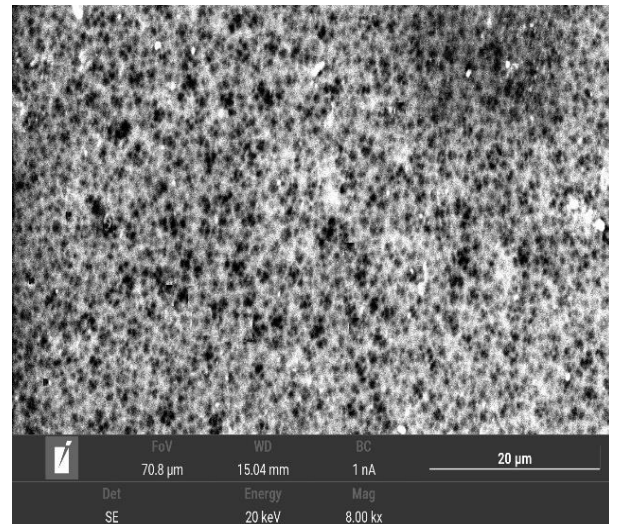
**PSS-0**



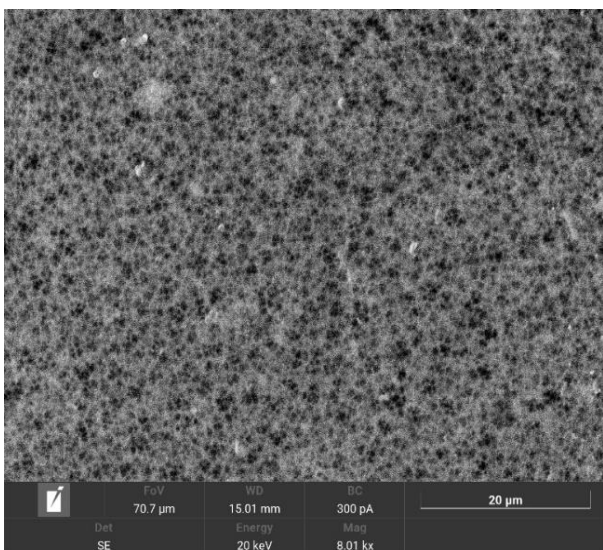
**PSS-0.05**



**PSS-0.1**



**PSS-0.15**



**PSS-0.25**

## PSS-0.2

Figure 4.20 – SEM of the top surface of the pristine and MMMs

As shown in this figure, the surface morphology of the PSS-0.0 presented a rough surface with some pores dispersed on the surface due to the higher amount of PVC at the film interface which results in fewer pores on the top layer of the membrane [115, 135]. After modification the surface became more porous due to the presence of SiO<sub>2</sub>-SDS NPs in the surface of the PSS-0.05, PSS-0.1, and PSS-0.15 membranes. However, an important increase in the amount of SiO<sub>2</sub>-SDS NPs may block the layers due to the accumulation of SiO<sub>2</sub> NPs on the surface of PSS-0.2 and PSS-0.25 membranes.

Figure 4.21 illustrates the SEM images of the cross-section structures of the pristine and modified membranes with SiO<sub>2</sub>-SDS NPs. The images confirm that the addition of SiO<sub>2</sub>-SDS NPs up to 0.15 wt.% did not affect the morphology and the asymmetric structures of the membranes' cross-sections. The SEM images revealed that a thin filtration layer on the top surface of the membrane appeared with a supporting layer with macro-voids at the bottom. The top layers of the membranes have significantly increased with an increase in the amount of SiO<sub>2</sub>-SDS NPs added. However, the cross-section structure of the PSS-0.2 and PSS-0.25 membranes seem to be affected by the addition of large amounts of SiO<sub>2</sub>-SDS NPs. The deformation of the cross-section structure of PSS-0.2 and PSS-0.25 membranes may be due to the accumulation of the NPs in their cross-section structure which block the layer.

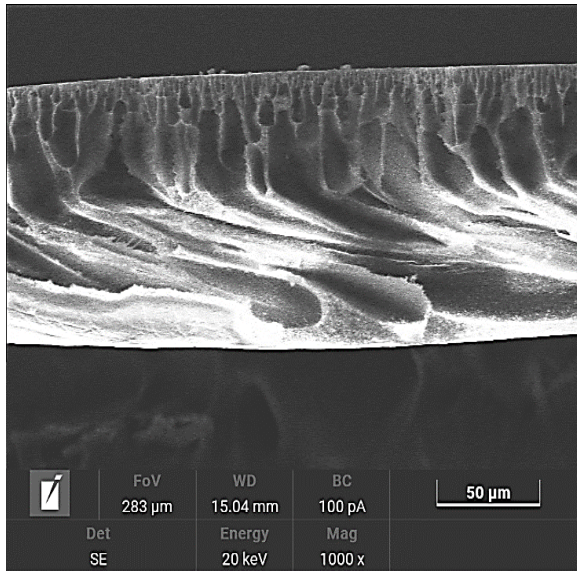
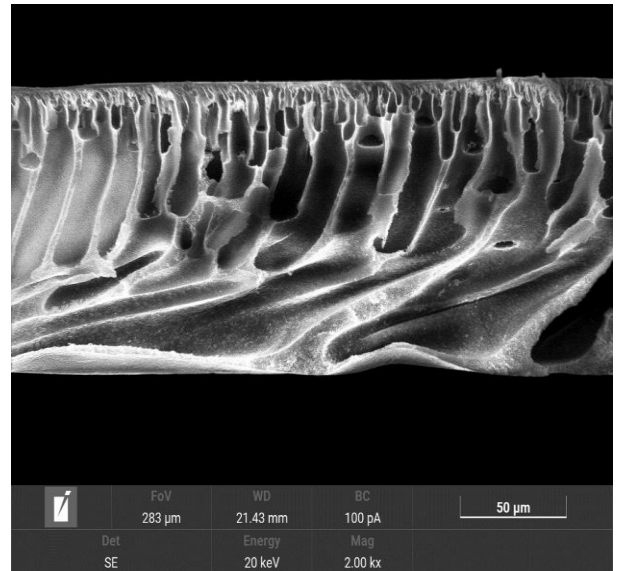
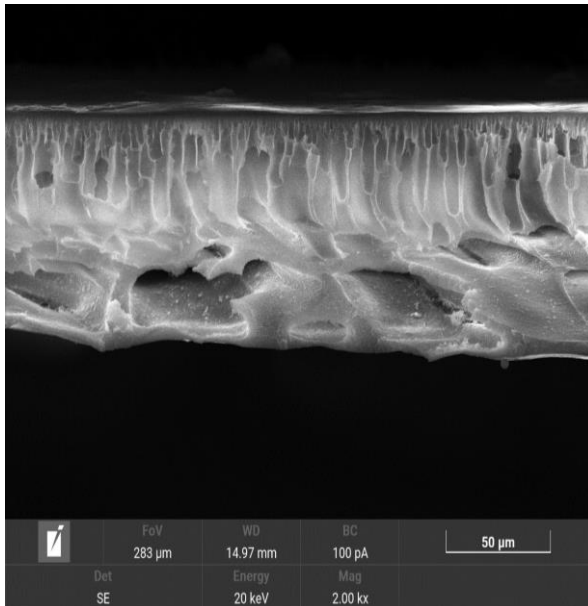
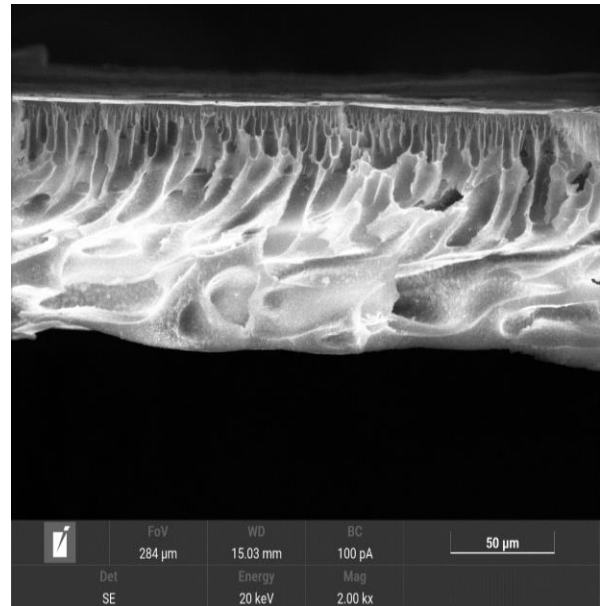
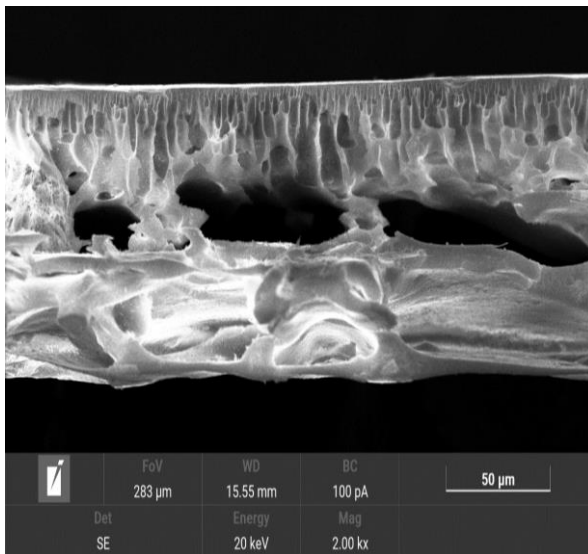
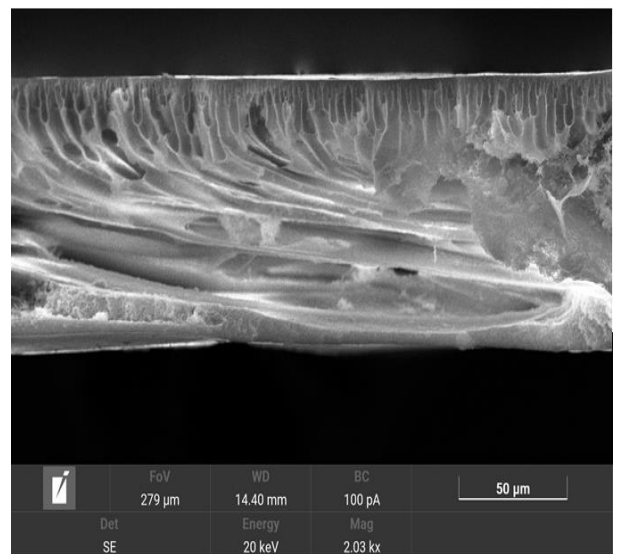
**PSS-0****PSS-0.05****PSS-0.1****PSS-0.15****PSS-0.2****PSS-0.25**

Figure 4.21– SEM of the cross-sectional of the pristine and MMMs

Figure 4.22, show the effect of SiO<sub>2</sub>-SDS NPs on the thickness and porosity of pristine and nanocomposite membranes.

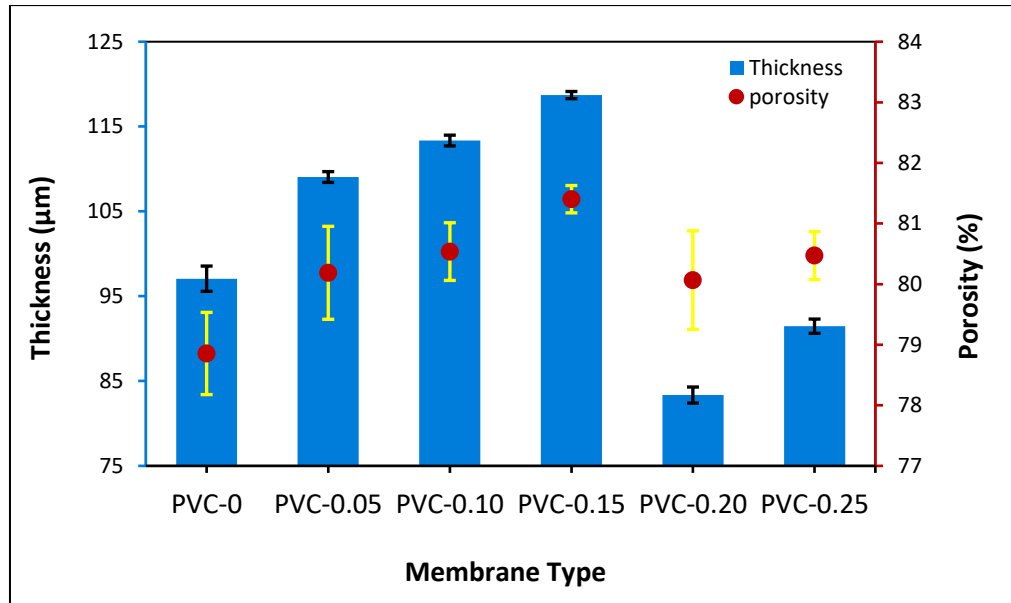


Figure 4.22 – PVC/SiO<sub>2</sub>-SDS membranes thickness and porosity compared with the pristine membrane

With the increase of the SiO<sub>2</sub>-SDS NPs concentration up to 0.15 wt.%, the membrane thickness and porosity increased. The highest thickness was  $118.71 \pm 0.42$  µm for (PSS-0.15) MMMs. The thickness of PSS-0 was  $100.21 \pm 0.76$  µm and increased to  $109.05 \pm 0.64$  µm, and  $113.35 \pm 0.64$  µm when the concentration of SiO<sub>2</sub>-SDS NPs in the casting solution were 0.05 and 0.1 wt.%, respectively. These results were likely due to the increase in the viscosity of the dope solution upon the addition of nanoparticles [42]. The measured porosity of the pristine membrane (PSS-0) was  $78.62 \pm 1.21$  %. Increasing the content of nano-additives increased porosity to around  $80.19 \pm 0.77$  % for the (PSS- 0.05) MMMs. This increase continued to the maximum porosity of  $81.40 \pm 0.23$ % for the (PSS-0.15) membrane. Similar results were reported in [136]. Adding 0.2 wt.% SiO<sub>2</sub>-SDS NPs decreased the porosity to  $80.07 \pm 0.81$  %. This drop could be due to the dope solution's viscosity increase which may function as a resistance, resulting in a delayed liquid-liquid demixing process.

The mean pore size is very important factor that affects the permeate flux of the UF membrane. The mean pore diameter of the pristine and MMMs are shown in Figure 4.23.

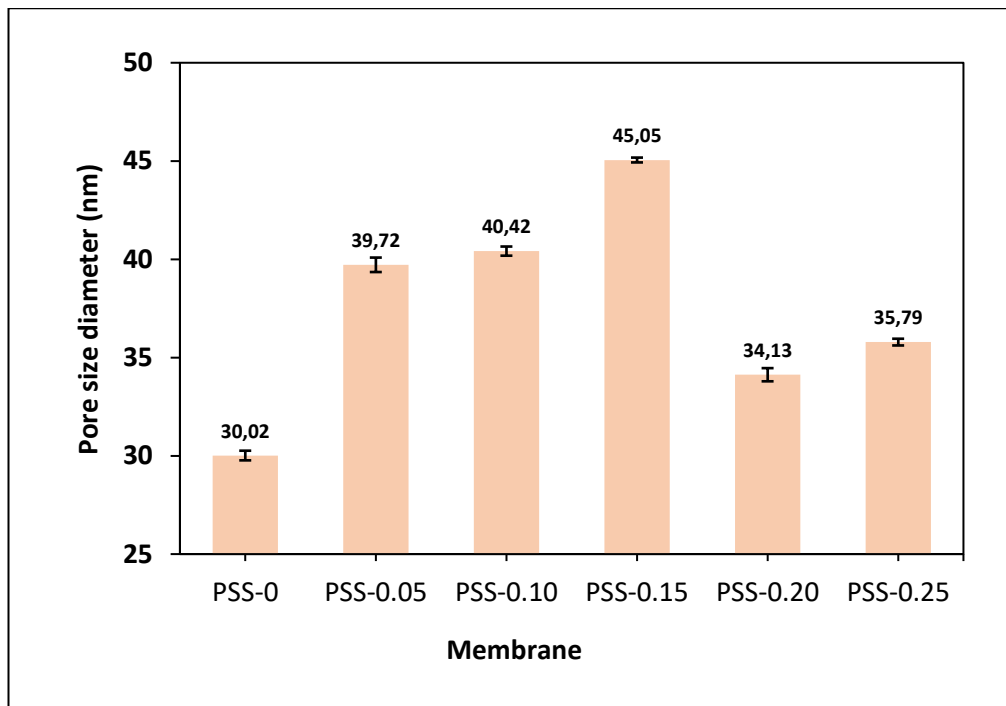


Figure 4.23 – PVC/SiO<sub>2</sub>-SDS membranes porosity, thickness and pore size compared with the pristine membrane.

It can be noticed from the figure that as the SiO<sub>2</sub>-SDS NPs amount increased, the mean pore diameter increased from 30 nm for pristine membrane (PSS-0) to 39 nm for (PSS-0.05), until it reached a maximum of 45 nm for (PSS-0.15). This increase could be a result of enhanced exchange rate between the solvent and non-solvent during the membranes formation induced by the addition of SiO<sub>2</sub>-SDS NPs to the casting solution [137, 138]. Further increase in SiO<sub>2</sub>-SDS NPs resulted in a drop in pore size probably due to NPs accumulation on the membrane surface.

#### 4.3.2 Membrane Performance Evaluation for Carwash Treatment

Figure 4.24 presents the effect of different concentrations of SiO<sub>2</sub>-SDS NPs on the pure water flux at room temperature, and a pressure of one bar. Generally, all modified membranes had a higher pure water flux.



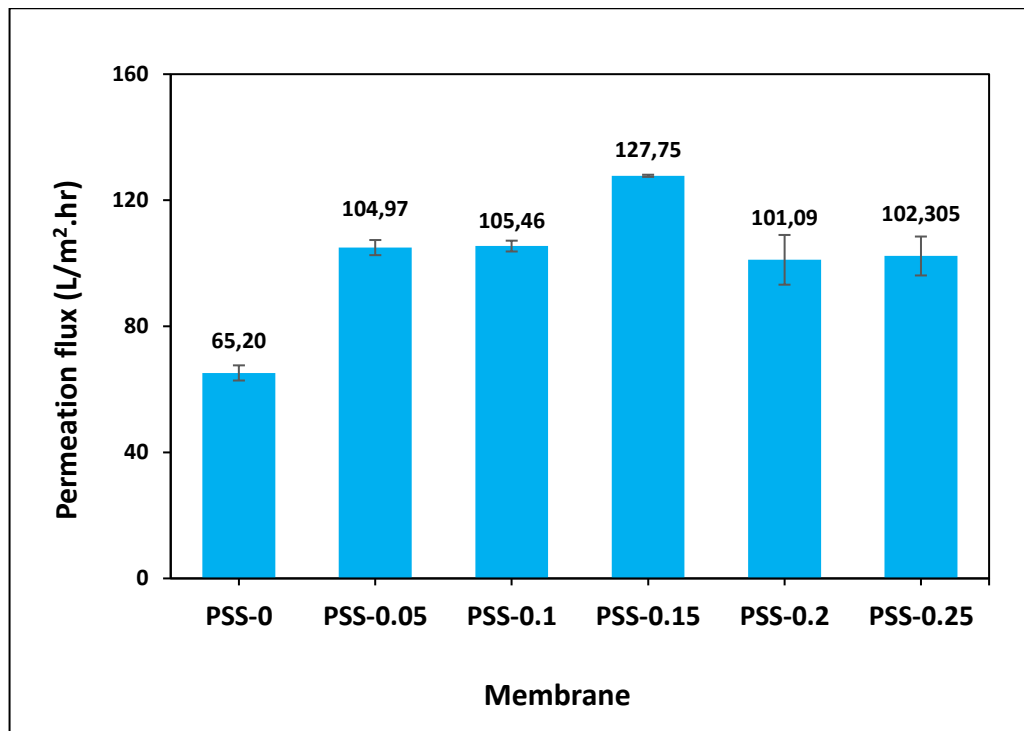


Figure 4.24 –Pure water flux of Pristine and nanocomposite membranes prepared with different concentrations of SiO<sub>2</sub>-SDS NPs

The results show that by adding 0.05 wt.% SiO<sub>2</sub>-SDS NPs (PSS-0.05), the pure water flux increased from 65.2±2.4 L/m<sup>2</sup>.h for PSS-0 to 104.97±2.4 L/m<sup>2</sup>.h. The pure water flux continued to show a significant increase after the addition of SiO<sub>2</sub>-SDS NPs, reaching its highest value at 0.15 wt.% with 127.75±1.72 L/m<sup>2</sup>.h. The increasing trend of pure water flux was consistent with pore size, porosity, membrane morphology and the structure of the supporting layer with macro-voids in the modified membranes as shown in earlier sections. However, the addition of 0.2, and 0.25 wt.% of SiO<sub>2</sub>-SDS NPs, resulted reduction in pure water flux to about 101.09 ±7.88 and 102.30±6.17 L/m<sup>2</sup>.h, respectively. This reduction could be attributed to pore blockage due to the agglomeration of the high content of SiO<sub>2</sub>-SDS NPs.

The TSS, surfactant, oil product and COD rejection of the prepared membranes was calculated and the results are presented in Figure 4. 25.

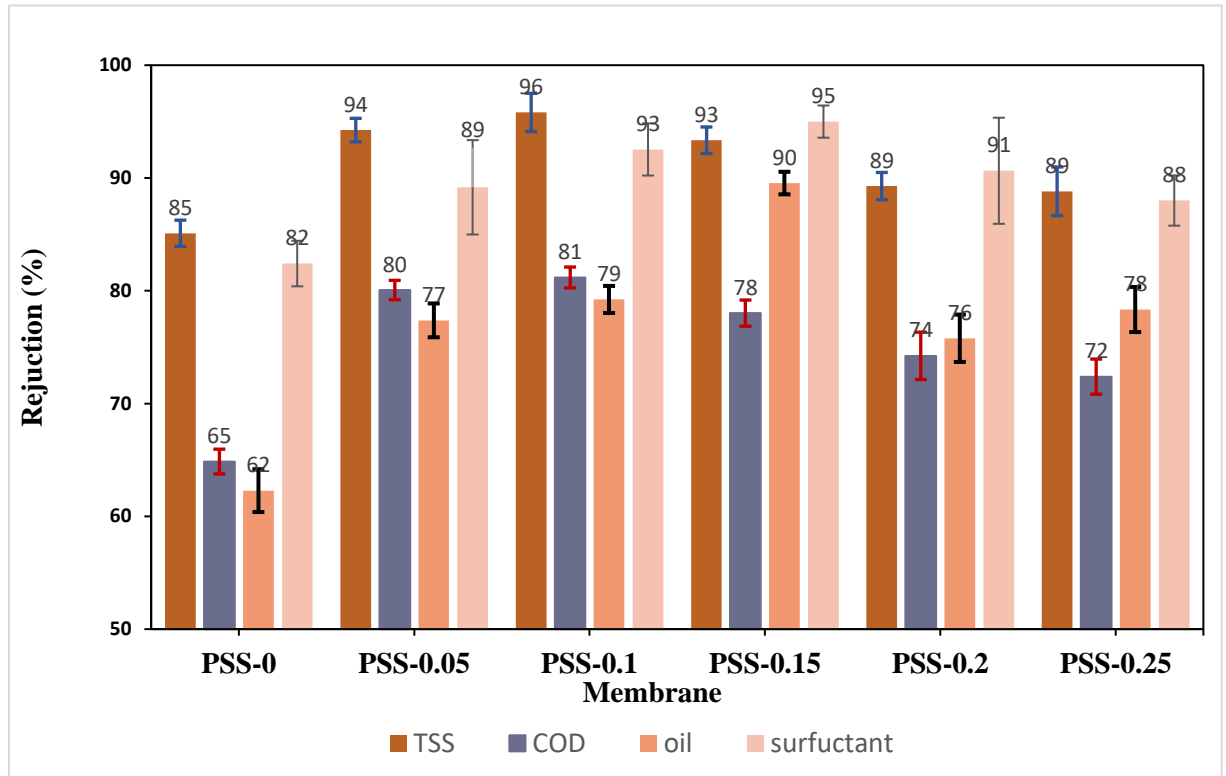


Figure 4.25 – Rejection, % for CWW of pristine and nanocomposite membranes ( $25\pm 1^\circ\text{C}$ , and 1 bar).

UF membranes possess the capacity to effectively remove pollutants due to their size exclusion mechanism [139, 140]. The removal of COD also may be explained by the fact that adsorption, in addition to exclusion mechanism, is the other mechanism for removing organic matter, where particles captured inside the membrane structure, which permits the removal of particles smaller than the membrane's pores [141]. As indicated in Figure 4.25, pollutants rejection of nanocomposite membranes was improved in comparison to the pristine membrane. Although the pristine membrane has the smallest pore size which should have the highest rejection, the possible explanation for this deviation is the contribution of surface roughness for hosting TSS and organic matter which in turn could change the pore size profile for the modified membrane leading to a better rejection compared to the pristine membrane. The other factor that might have played a role is the increase in porosity is accompanied by an increase in tortuosity and the longer path for small particles might led to their entrapment and consequently increased rejection.

The PSS-0.05 and PSS-0.1 have a close TSS rejection% were  $94.25 \pm 1.04\%$  and  $95.81 \pm 1.69\%$ , respectively, in comparison with the other samples, and the rejection value declined by about 1–2.3 % for PSS-0.15 in comparison with PSS-0.05 and PSS-0.1 due to the membrane's surface having a percentage of large pores that were in agreement with the results of AFM. Additionally, the PSS-0.1 membrane demonstrated the highest COD rejection of  $81.18 \pm 1.09\%$ . It was observed that the pristine membrane had a COD rejection of approximately  $64.85 \pm 1.16\%$ , while all MMMs prepared with different concentrations of SiO<sub>2</sub>-SDS NPs exhibited a COD rejection rate of over 72 %. The ultrafiltration system effectively eliminated suspended solids, as evidenced by the TSS test results. Organic matter in the wastewater existed in soluble form, colloidal particles, or adhered to the outer surface of the suspended solids. By removing the suspended solids, the organic matter was partially eliminated, which contributed to the improvement in COD rejection.

On the other hand, the ultrafiltration membrane retained some organic material larger than its pore size, resulting in a reduction of organic material in the permeate. Nanocomposite membranes provide a sufficiently high in rejection degree of anionic surfactants as (MBAS) in the range from 88 to 95 %, as shown in Figure 4.25, the maximum rejection at PSS-0.15 which reach to  $95 \pm 1.4\%$  compared to pristine membrane PSS-0.

Furthermore, it has been established that the rejection of oil product for carwash wastewater increases for membrane (PSS-0.15) from  $62 \pm 1.9\%$  to  $90 \pm 1\%$ , as shown in Figure 4.25. This is attributed to the anionic surfactant (SDS) which are long molecules that have head hydrophilic on one end and tail oleophilic on the other, this property allows the tail to interact with oil molecules and form stable structures in oily environments. Therefore, the addition of 0.15 wt.% of SiO<sub>2</sub>-SDS NPs raises rejection of oil product to the maximum where the anionic surfactants (SDS) reach across the oil-water boundary and lowers the tension that keeps the two substances separate, and then grab an oil molecule with its end of the oleophilic.

After the membranes are used with wastewater, they need to be able to regain their water flux which is crucial for their effectiveness. If the membranes cannot regain their

water flux, it can lead to reduced filtration performance and lower quality of treated water. Therefore, it is imperative to assess and compare the water flux of membranes before and after fouling to ensure their functionality and reliability. Following the ultrafiltration test, the membranes were cleaned, and the pure water fluxes were measured once more, as shown in Figure 4.26.

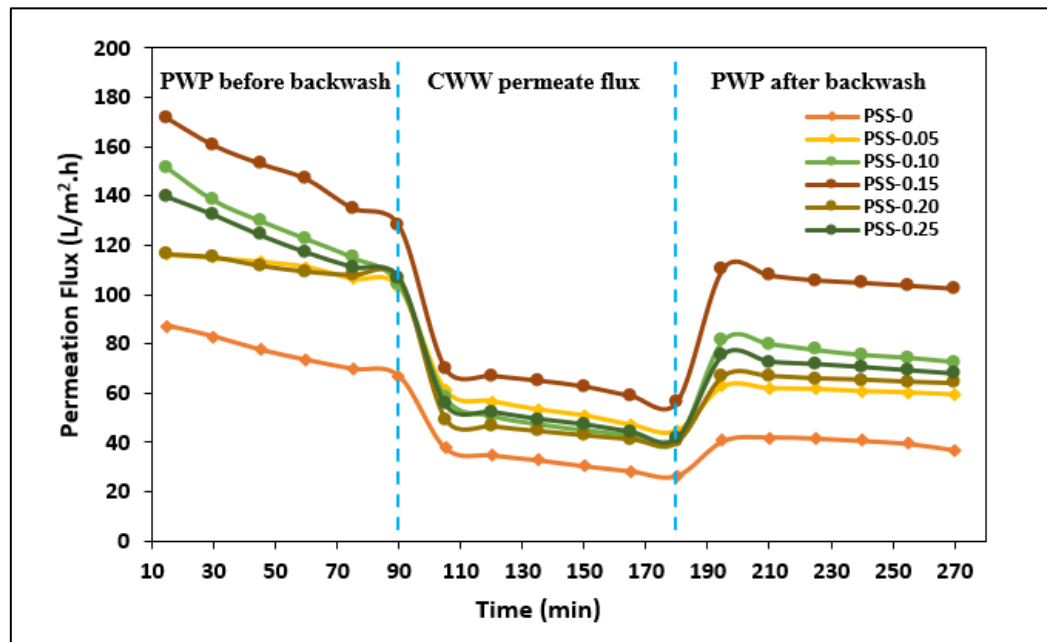


Figure 4.26 – The dependence of membrane permeability on the composition of the studied waters at the same transmission time

The first 90 minutes for clean water flow, the second 90 minutes for flow CWW and the third 90 minutes for clean water flow after the contaminated membranes have been backwashed with clean water for one hour.

After backwashing, pure water flux was lower than before backwashing and the membranes are unable to recover their water flux as a result of the irreversible fouling. This decrease in pure water flux can be attributed to the contaminants that are entrapped into membrane pores or strongly adhered to the surface of the membrane even after backwashing. Figure 4.26 shows that the PSS-0.15 membrane showed of the highest capacity for flux restoration compared to the PSS-0 and other membranes which suffer earnest irreversible fouling.

The membrane fouling resistance is typically conducted by analyzing the flux recovery ratio (FRR). Increased values of FRR signify enhanced membrane performance in terms of mitigating fouling effects during the operation of UF processes. Values of

FRR for all nanocomposite membranes were noticeably higher than those of the virgin PVC membrane (Figure 4.27).

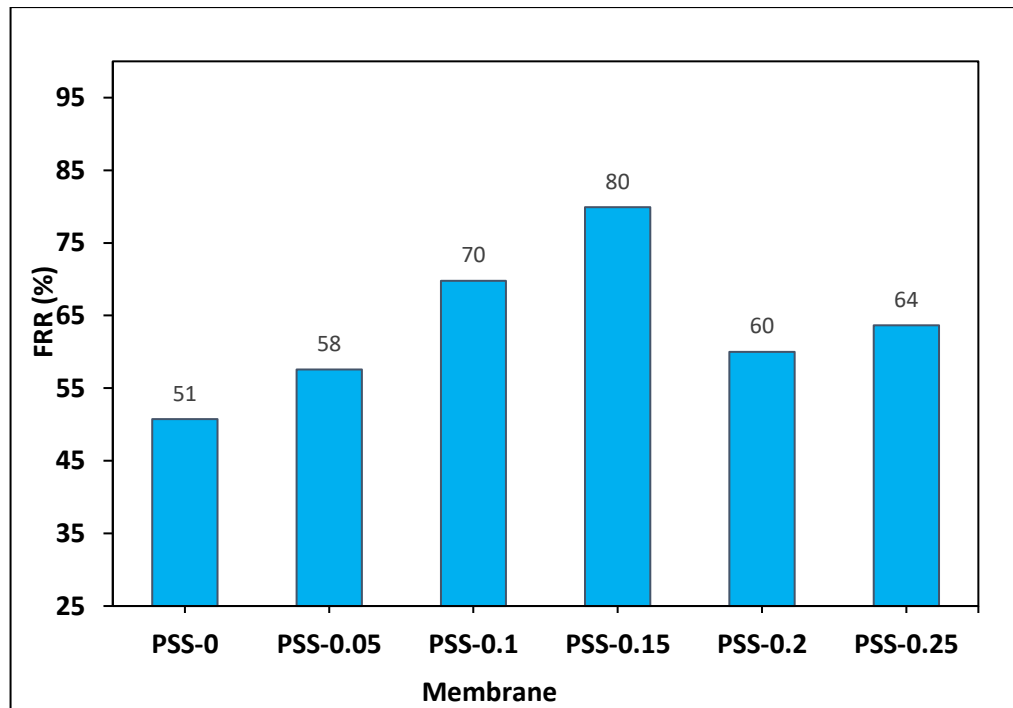


Figure 4.27 – The flux recovery ratio (FRR) of the pristine and nanocomposite membranes

The highest FRR observed was 80 % for the PSS-0.15 membrane, in comparison to the unmodified membrane with an FRR of 51 %. The low fouling tendency of the modified membranes could be due to the presence of large amounts of  $\text{OH}^-$  groups in the modified membranes with  $\text{SiO}_2$ -SDS NPs that interacted with Cl atoms of PVC chains through hydrogen bonds forming a hydrophilic layer in the surface and within the structure of the membranes (Figure 4.28) preventing the hydrophobic substance from adsorption or attachment onto the membranes. Subsequently, the FRR decreased for the PSS-0.2 and PSS-0.25 membranes, which contained 0.2 and 0.25 wt.% of  $\text{SiO}_2$ -SDS nanoparticles due to an increase in pore blockage.

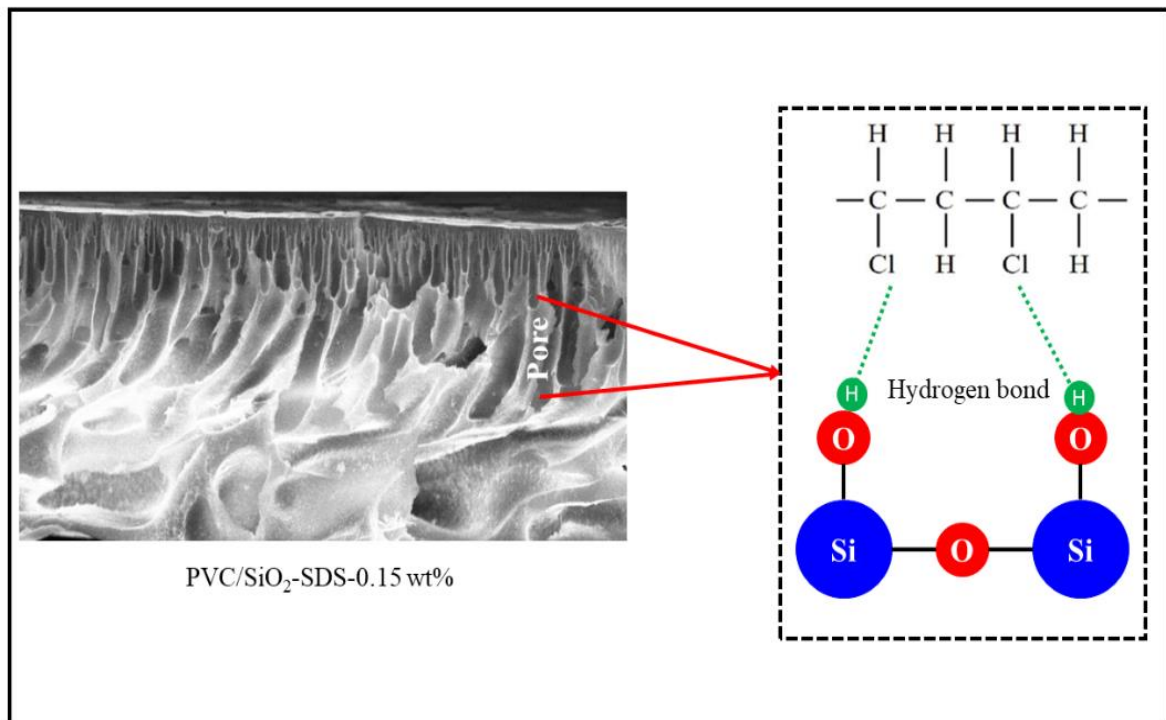


Figure 4.28 – Antifouling mechanism of the modified membranes by SiO<sub>2</sub>-SDS NPs

#### 4.4 Discussion and Explanation of the Obtained Results of Experimental Studies Based on the Data Analysis of the Prepared Membranes

Figure 4.29 presents the results of determining the following membrane characteristics in the form of graphs.

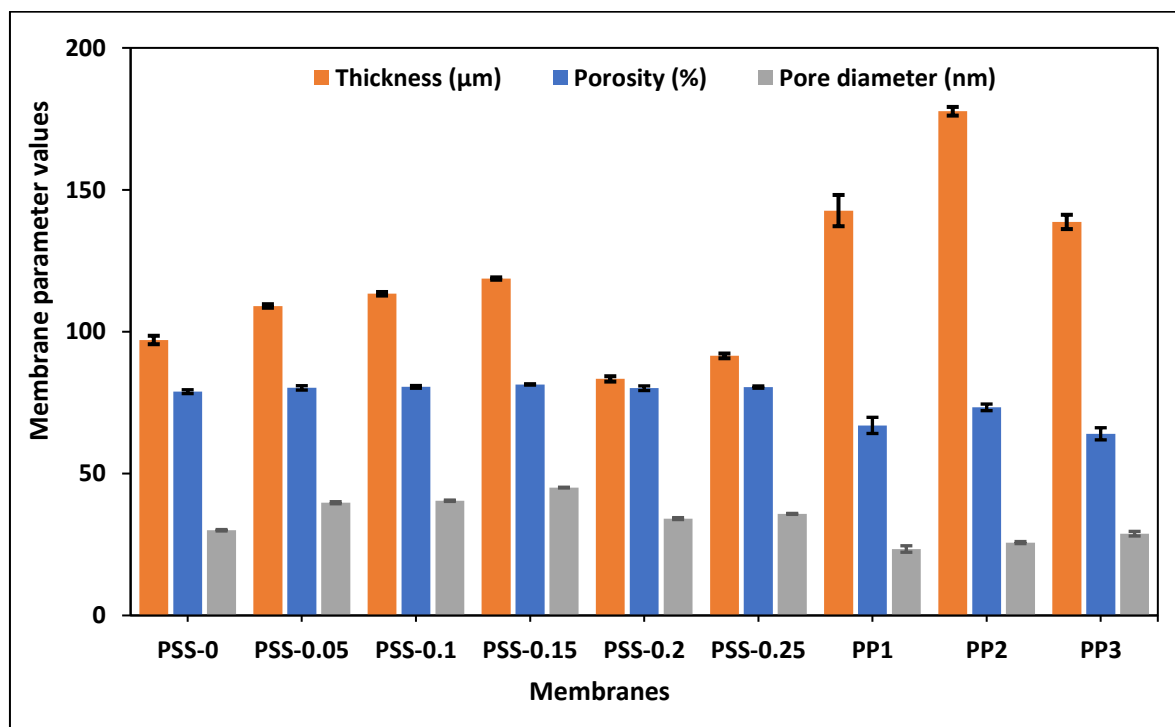


Figure 4.29 – Influence of membrane modification methods on their characteristics

From a comparison of these graphs, it can be seen that the highest porosity among the studied membranes was shown by membranes PSS-0.05, PSS-0.1 and PSS-0.15, the smallest - close to the porosity of the control membrane PSS-0 - was shown by membranes PP1–PP3. A significant decrease in the porosity of membranes obtained from PVC and its derivatives modified with thiophenols can be explained by the observed change in the consistency (viscosity) of the casting solution compared to a solution containing only PVC. As is known, an increase in viscosity, as well as the concentration of a polymer solution, can interfere with and cause a delay in the exchange between solvent/non-solvent during the process of phase inversion of the forming membrane. This leads to a decrease in the proportion of macrovoids in the membrane, it becomes denser and, as a result, its porosity decreases. This conclusion is confirmed by both the much greater thickness of these membranes and the smaller size of their pores compared to other membranes.

Figure 4.30 shows graphs that allow to compare the resulting membranes according to one of their most important characteristics - permeability.

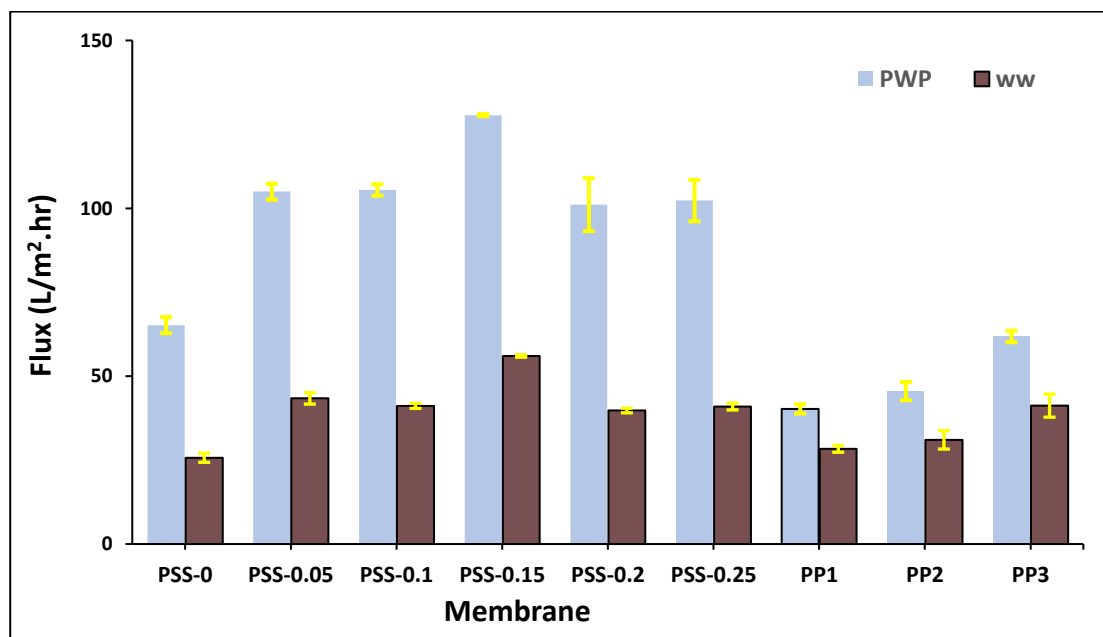


Figure 4.30 – Influence of membrane modification methods on the permeability of pure water and WW of a car wash in Yekaterinburg

From the significant increase (by 38–49%) in the permeability of membranes modified with  $\text{SiO}_2$ -SDS NPs compared to the NP-0 membrane when using pure water, as well as a comparison of the thickness, porosity and pore size with other membranes,

it can be concluded that the addition of NPs into the casting solution contributed to the hydrophilization of the surface and pores of the membrane, which, however, had little effect on the permeability of the membrane when filtering the WW of a car wash. PP1-PP3 membranes, obtained by modifying PVC with its functionalized derivatives, showed a decrease in permeability when filtering pure water by 5–38%, compared to the control membrane PSS-0, while compared to membranes modified with NPs, the decrease in their permeability was 2.5–3 times. That is, a decrease in the pore size and overall porosity of PP1-PP3 membranes, compared to other membranes, leads to a natural decrease in permeability when the used transmembrane pressure within 1–2 bar is no longer sufficient to push even DI.

Figure 4.31 shows the results of a study of membranes on the rejection of pollutants from a car wash.

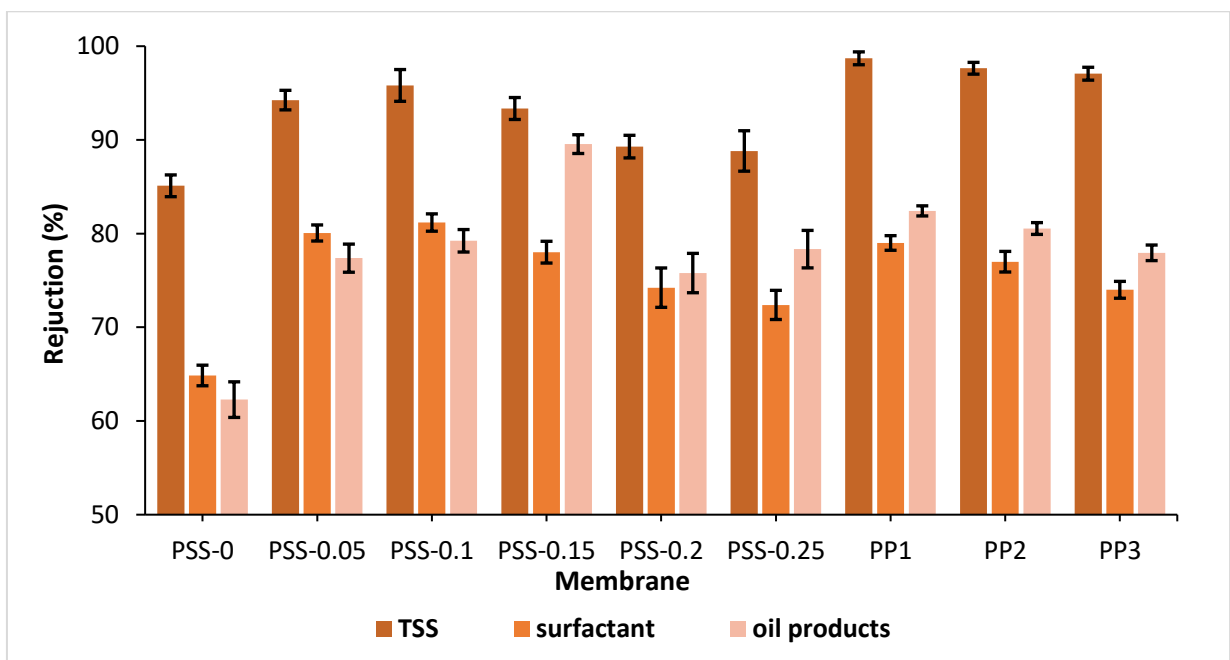


Figure 4.31 – Influence of membrane modification methods on the degree of purification of WW car washes in Yekaterinburg

It is clear from the figure that all types of modified membranes with respect to suspended solids, surfactant and petroleum products showed a higher degree of rejection compared to the control unmodified PSS-0 membrane. Moreover, as one would expect, taking into account the obtained values of porosity and pore size (Figure 4.31), membranes PP1–PP3 were more effective in terms of complete rejection of suspended solids compared to others.



#### **4.5 Investigation and Evaluation of Biodegradation of Pollutants from Car Washes Contained in The Retentate of Used UF Membranes**

Despite the relatively small consumption of WW at one car wash, the presence of many them and the specific contamination of wastewater leads to a significant load on biological urban treatment facilities. This is due to the fact that most car washes have only sedimentation tanks designed to clean suspended solids, after which wastewater is discharged into the sewer.

The ecological situation is no better with deep cleaning of the WW using membrane cleaning technology. That is, by reducing the volume of discharge WW due to purification and reuse, we obtain a concentrate (retentant) containing all the original pollutants in a smaller volume. Taking into account this problem, the possibility of biological treatment of the retentant before discharge into the city sewage system from impurities causing COD WW was investigated. Taking into account the specifics of WW car washes, such impurities include detergents, or rather organic surfactants that make up them.

Given that a number of detergents are characterized by a low degree of biooxidation, the first part of the study was devoted to assessing the biodegradation of two selected detergents used in car wash technology, (1. Active Foam, a means for contactless car wash of the Russian Federation and 2. Car Wash (Amway), contact car wash, USA). Evaluation of the effectiveness of biodegradation was carried out to reduce the COD of model solutions. It was found that by biochemical oxidation it is possible to reduce the COD of detergent-based model solutions by ~ 85 %.

The obtained adapted biocenosis to model solutions was used in experiments for cleaning the retentants of WW car washes. As a result of experiments with bio-purification of retentants, which are concentrates of industrial CWW of a car wash with a multiplicity of 2.5 times in relation to the initial volume of CWW, it was shown that it was possible to reduce their COD by 85–90 %. Thus, it is proposed to supplement the technological scheme for cleaning CWW, including the reuse of WW, with biological treatment of the retentant before discharging it into the sewer (Figure 4.32).

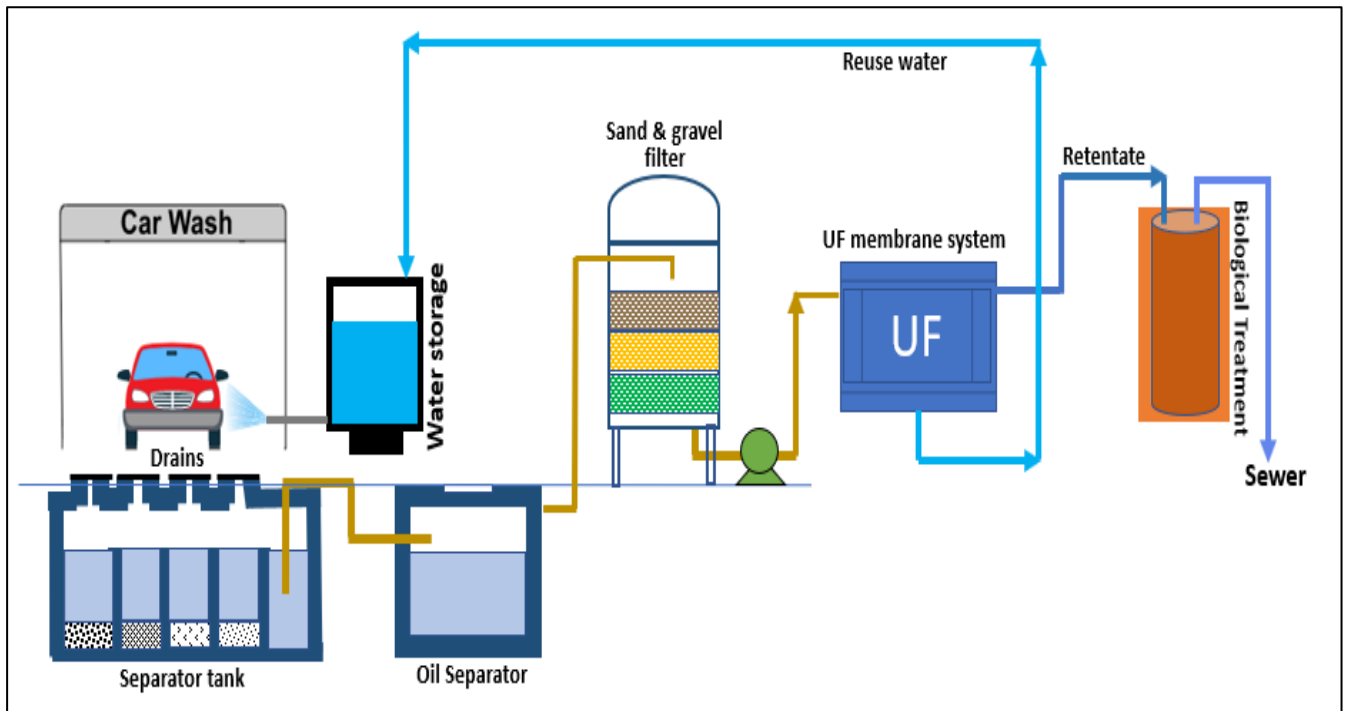


Figure 4.32 – The technological scheme for cleaning the WW of a car wash, including the reuse of WW, with biological treatment of the retentant

#### Conclusion to the chapter 4

The results of experiments were discussed in details for each type of prepared membranes by finding the morphology and topology and different characteristics, as well as the efficiency of the membranes through clarified the permeability, the rejection of wastewater from car wash stations and fouling resistance.

Discussing the reasons for the high or low rejection for each type of obtained membranes and the antifouling properties through analyzing the flux recovery ratio (FRR).

A scheme was also proposed for the process of treating car wash wastewater and including the reuse of WW, with biological treatment of the retentant before discharging it into the sewer.

## CONCLUSION

As part of this work, a representative series of experimental studies was carried out, the main results of which are the following:

1. Of the three synthesized membrane samples with a PVC concentration of 14, 15, and 16 wt.%, the UF membrane with 14 wt.% PVC concentration has the highest permeability, so this concentration in DMAc dope solution is optimal and suitable for treatment of carwash wastewater from the main pollutants.

2. A natural decrease in the permeation flux of UF membranes by 57.7 % for pure water and by 68.9 % for carwash wastewater (CWW) was established as the concentration of PVC in the dope solution increased from 14 to 16 wt. %.

3. Pure water permeability decreased at higher PVC concentration, while the oil and greases rejection increased up to 75.1% when treated through the membrane with a PVC concentration of 16 wt.%. This result confirmed that the permeation flux and efficiency are related to the pore size and porosity of the membranes, which depend on the polymer concentration in the dope solution.

4. From SEM images, the size of the macrovoids decreased and spongy elements formed into finger-like structures appeared, as the PVC concentration in the dope solution was increased.

5. The porosity of PVC membranes decreased with increasing PVC concentration due to the strong entanglement of the polymer chains and the higher viscosity of more concentrated polymer solutions, which slowed down diffusion non-solvent through the phase separation polymer solution.

6. The roughness and thickness of the membranes were increased by adding a higher concentration of PVC to the dope solution.

7. The 14 wt.% PVC membrane significantly has anti-fouling resistance in long-term operation more than other membranes. For 14 wt.% PVC membrane, FRR is about 55.45 % after 3 cycles carwash wastewater, which is greater than 15, and 16 wt.% of PVC membranes.

8. As a result of this work, and in order to improve the performance of PVC-based UF membranes used in car wash wastewater treatment, we recommend modifying the

membrane by using nanomaterials with polymer to improve the permeability and performance of the membrane and achieve better results.

9. Under mechanical synthesis conditions, a number of known and new post-modified PVC derivatives functionalized with *N*- and *S*-nucleophiles were obtained and studied; A reasonable selection was made from among them of polymers suitable for the manufacture of UV membranes (PVC-OTF, PVC-BTF and PVC-TF).

10. Using the phase inversion method, new types of PVC membranes and composite membranes obtained from casting solutions of the following composition were obtained and studied:

11. PVC 14, 15, 16 % (wt.) in DMAA (3 types of membranes);

12. PVC 14 % (wt.) in a mixture of two solvents NMP and THF and 4% (wt.) polymer additives in the form of PVC-OTF, PVC-BTF PVC-TF (3 types of membranes);

13. PVC 14 % (wt.) in DMAA and a modifying additive of SIO<sub>2</sub>-SDS NPs in an amount, % (wt.) of 0.05, 0.1, 0.15, 0.2 and 0.25 (5 types of membranes).

14. It has been established that all samples of PVC membranes and composite membranes are porous ultrafiltration membranes, differing to a greater extent from each other in thickness (within 83–178 μm), pore size (within 23–45 nm) and, to a lesser extent, with porosity (within 64–81%).

15. It was established that modification of the structure of PVC membranes with the additives PVC-OTF, PVC-BTF and PVC-TF contributed, in comparison with the PVC 14 membrane and other membranes, to densification of their structure, reduction of porosity and pore size. Therefore, it was natural to slightly increase the degree of purification of car wash wastewater from suspended solids compared to other membranes.

16. It has been proven that modification of the structure of PVC membranes with silicon dioxide nanoparticles (SIO<sub>2</sub>-SDS NPs) led to an increase in the hydrophilicity of their surface, which affected a twofold increase in their permeability for DI, but turned out to be insignificant for the permeability of SW car washes.

17. Based on the morphological and topological characteristics of membranes obtained using SEM, AFM and FTIR, patterns have been identified that allow us to assess the effectiveness and performance of the manufactured membranes depending on the

concentration in the casting solution of PVC, SIO<sub>2</sub>-SDS NPs and modified PVC additives (PVC- OTF, PVC-BTF and PVC-TF).

18. PVC derivatives obtained for the first time by mechanosynthesis, including fragments of the following known chemical substances: a) azoloazines; b) antidiabetic drug AB-19 (diethyl ester of 4-oxo-1,4-dihydropyrazolo[5,1-c]-1,2,4-triazine-3,8-dicarboxylic acid); c) the antiviral drug TRIAZID (5-methyl-6-nitro-7-oxo-triazolo[1,5-a]pyrimidinide), d)  $\alpha$ -aminophosphonates and e) triazatriptycene, are objects for continued research and the search for their applicability. Of these, PM polymers b) and c) are of interest for studying their properties as possible polymer drugs.

19. Thus, as a result of the experimental studies carried out, the goal of this work was achieved. Based on the available raw material source - PVC and its modified structures, new types of flat UV membranes have been obtained that are effective for purifying wastewater from car wash pollutants, including petroleum products.

**Prospects for further development of the research topic.** As part of further development of the research topic, it is possible to consider the use of the resulting PVC-containing azoloazines as polymer drugs. PVC derivatives of triazatriptycene can find their application as materials for gas separation/storage. Polymeric Schiff bases can be used as materials for the supramolecular extraction of metal cations. Other materials based on modified PVC obtained in this work can also be used to produce UF membranes.

## LIST OF ABBREVIATIONS AND CONVENTIONS

The dissertation is prepared in accordance with GOST R 7.0.11-2011.

All symbols and abbreviations are deciphered directly in text of the dissertation, and are also given below.

2D	Two dimensions
3D	Three dimensions
ABS	acrylonitrile-butadiene-styrene
AFM	atomic force microscopy
BOD	biological oxygen demand
CA	cellulose acetate
COD	chemical oxygen demand
COSOCE	Camellia oleifera seed-oil-based cyclohexyl ester
CWW	carwash wastewater
DI	DI-IONIZ WATER
DMAc	N,N-dimethylacetamide
DMF	Dimethylformamide
dmPz	dimethylpyrazole
DMSO	dimethyl sulfoxide
DOP	dioctyl-phthalate
DPVC	dehydrochlorination of polyvinyl chloride
DR <sub>ir</sub>	irreversible fouling ratio
DR <sub>r</sub>	reversible fouling ratio
DR <sub>t</sub>	total fouling ratio
EG	ethylene glycol
ELSD	erosol light scattering detector
FER	federal environmental regulations
FFV	fractional free volume
FRR	flux recovery ratio
FTIR	Fourier-Transform Infrared spectroscopy

GPC	gel permeation chromatography
HMDI	hexamethylene diisocyanate
IR	Infrared spectroscopy
Isocy-PVC	isocyanate-PVC
J	permeation flux
$J_{w1}$	pure water flux
<i>m</i> -CPBA	<i>m</i> -chlorobenzoic acid
MF	microfiltration
MWCO	molecular weight cut-off
MMM <sub>S</sub>	mixed matrix membrane
NF	nanofiltration
NIPS	Non-Solvent Induced Phase Inversion
NMP	N-methyl-2-pyrrolidone
PAN	polyacrylonitrile
PES	petroleum ether
PES	polyethersulfone
PSf	polysulfone
PTC	cross thermal clustering
PVC	Polyvinyl chloride
PVDF	polyvinylidene fluoride
Pyr-PVC	pyridinated PVCs
Pz	pyrazole
R%	Rejection %
RO	reverse osmosis
SDBS	Sodium dodecylbenzene sulfonate
SDS	sodium dodecyl sulfate
SEM	Scanning Electron Microscopy
SiO <sub>2</sub> NPs	Silicon dioxide NANOPARTICLE
SPEEK	sulfonated poly ether ketone
SWW	waste water from car washes

TAC	triallyl cyanurate
t-BuOOH	tert-butylhydroperoxide
TEPA-PVC	PVC-supported tetraethylenepentamine
T <sub>g</sub>	glass transition temperature
THF	tetrahydrofuran
TSS	total suspended solids
UF	ultrafiltration
WW	wastewater



## REFERENCES

1. Yordanova S. Thermal investigation of calixarene-containing PVC composites / Yordanova S., Miloshev S. // Journal of the University of Chemical Technology and Metallurgy – 2006. – T. 41 – № 4 – C.397–402.
2. Starnes W.H. Structural defects in poly(vinyl chloride) / Starnes W.H. // Journal of Polymer Science Part A: Polymer Chemistry – 2005. – T. 43 – № 12 – C.2451–2467.
3. Endo K. Synthesis and structure of poly(vinyl chloride) / Endo K. // Progress in Polymer Science – 2002. – T. 27 – № 10 – C.2021–2054.
4. Kameda T. Chemical modification of poly(vinyl chloride) by nucleophilic substitution / Kameda T., Ono M., Grause G., Mizoguchi T., Yoshioka T. // Polymer Degradation and Stability – 2009. – T. 94 – № 1 – C.107–112.
5. Carey F.A. Advanced organic chemistry: part A: structure and mechanisms / F. A. Carey, R. J. Sundberg – Springer Science & Business Media, 2007.
6. Williams A. Free energy relationships in organic and bio-organic chemistry / A. Williams – Royal Society of Chemistry, 2019.
7. Yoshinaga T. Alkaline dechlorination of poly(vinyl chloride) in organic solvents under mild conditions / Yoshinaga T., Yamaye M., Kito T., Ichiki T., Ogata M., Chen J., Fujino H., Tanimura T., Yamanobe T. // Polymer Degradation and Stability – 2004. – T. 86 – № 3 – C.541–547.
8. Moulay S. Trends in chemical modification of poly (vinyl chloride) / Moulay S. // Khimiya (Chemistry) – 2002. – T. 11 – C.217–244.
9. Pi Z. Allylated PVC / Pi Z., Kennedy J.P. // Journal of Polymer Science Part A: Polymer Chemistry – 2001. – T. 39 – № 2 – C.307–312.
10. Percec V. Functionalization of the active chain ends of poly (vinyl chloride) obtained by single-electron-transfer/degenerative-chain-transfer mediated living radical polymerization: Synthesis of telechelic  $\alpha$ ,  $\omega$ -di (hydroxy) poly (vinyl chloride) / Percec V., Popov A. V // Journal of Polymer Science Part A: Polymer Chemistry – 2005. – T. 43 – № 6 – C.1255–1260.
11. Bicak N. Merrifield-like resin beads by acid catalyzed incorporation of benzyl chloride into dehydrochlorinated PVC / Bicak N., Karagoz B. // European polymer

journal – 2007. – T. 43 – № 11 – C.4719–4725.

12. Shmakova N.A. IR spectroscopic study of chemical transformations upon irradiation of the poly (vinyl chloride)–triallyl cyanurate system / Shmakova N.A., Feldman V.I., Sukhov F.F. // High Energy Chemistry – 2001. – T. 35 – C.224–228.

13. Abdelaal M.Y. Chemical modification of PVC into polymer-supported oxazolinones and triazoles / Abdelaal M.Y., Sobahi T.R. // Journal of applied polymer science – 2007. – T. 104 – № 4 – C.2304–2309.

14. Kruglova V.A. Synthesis of N-vinylazole polymers via chemical modification of poly(vinyl halides) / Kruglova V.A., Dobrynina L.M., Vereshchagin L.I. // Polymer Science Series A – 2007. – T. 49 – № 4 – C.407–411.

15. Shaglaeva N.S. Nucleophilic substitution of chlorine atoms in polyvinyl chloride / Shaglaeva N.S., Sultangareev R.T., Zabanova E.A., Lebedeva O. V., Trofimova K.S. // Russian Journal of Applied Chemistry – 2008. – T. 81 – № 1 – C.131–134.

16. Sacristán J. Surface modification of PVC films in solvent–non-solvent mixtures / Sacristán J., Reinecke H., Mijangos C. // Polymer – 2000. – T. 41 – № 15 – C.5577–5582.

17. Lakshmi S. Bacterial adhesion onto azidated poly (vinyl chloride) surfaces / Lakshmi S., Kumar S.S.P., Jayakrishnan A. // Journal of Biomedical Materials Research: An Official Journal of The Society for Biomaterials, The Japanese Society for Biomaterials, and The Australian Society for Biomaterials and the Korean Society for Biomaterials – 2002. – T. 61 – № 1 – C.26–32.

18. Herrero M. Bacterial adhesion to poly (vinyl chloride) films: Effect of chemical modification and water induced surface reconstruction / Herrero M., Quéméner E., Ulve S., Reinecke H., Mijangos C., Grohens Y. // Journal of adhesion science and technology – 2006. – T. 20 – № 2–3 – C.183–195.

19. Navarro R. Modification of poly(vinyl chloride) with new aromatic thiol compounds. Synthesis and characterization / Navarro R., Bierbrauer K., Mijangos C., Goiti E., Reinecke H. // Polymer Degradation and Stability – 2008. – T. 93 – № 3 – C.585–591.

20. Herrero M. PVC modification with new functional groups. Influence of hydrogen bonds on reactivity, stiffness and specific volume / Herrero M., Tiemblo P., Reyes-Labarta J., Mijangos C., Reinecke H. // Polymer – 2002. – T. 43 – № 9 – C.2631–2636.

21. García N. The grafting of luminescent side groups onto poly (vinyl chloride) and the identification of local structural features / García N., Hoyos M., Teyssedre G., Navarro R., Reinecke H., Tiemblo P. // *Polymer degradation and stability* – 2007. – T. 92 – № 12 – C.2300–2307.
22. Teyssedre G. Study of secondary relaxations in poly (vinyl chloride) by phosphorescence decay: Effect of the chemical structure and the concentration of luminescent probes / Teyssedre G., Reinecke H., Corrales T., Navarro R., García N., Tiemblo P. // *Journal of Photochemistry and Photobiology A: Chemistry* – 2007. – T. 187 – № 2–3 – C.222–232.
23. Szakács T. Epoxidation of thermally degraded poly(vinyl chloride) / Szakács T., Iván B. // *Polymer Degradation and Stability* – 2004. – T. 85 – № 3 – C.1035–1039.
24. Bicak N. Epoxide containing spherical beads from PVC / Bicak N., Senkal B.F., Gazi M. // *Polymer Bulletin* – 2003. – T. 51 – № 3 – C.231–236.
25. Mekki H. Preparation of vinyl chloridevinyl ether copolymers via partial etherification from PVC / Mekki H., Belbachir M. // *Express Polymer Lett* – 2007. – T. 1 – C.495–498.
26. Belbachir M. Composition and method for catalysis using bentonites // – 2006.
27. Yoshioka T. Dechlorination of poly(vinyl chloride) using NaOH in ethylene glycol under atmospheric pressure / Yoshioka T., Kameda T., Imai S., Okuwaki A. // *Polymer Degradation and Stability* – 2008. – T. 93 – № 6 – C.1138–1141.
28. Bahaffi S.O.S. Chemical Modification of Poly(Vinyl Chloride) with Ethylene Glycol and its Application in Ion-Chromatography / Bahaffi S.O.S., Abdelaal M.Y., Assirey E.A. // *International Journal of Polymeric Materials* – 2006. – T. 55 – № 7 – C.477–484.
29. Takacs L. Temperature of the milling balls in shaker and planetary mills / Takacs L., McHenry J.S. // *Journal of materials science* – 2006. – T. 41 – C.5246–5249.
30. Al-AbdulRazzak S. End-group determination in poly (ethylene terephthalate) by infrared spectroscopy / Al-AbdulRazzak S., Lofgren E.A., Jabarin S.A. // *Polymer International* – 2002. – T. 51 – № 2 – C.174–182.
31. Capuano R. Valorization and mechanical recycling of heterogeneous post-consumer polymer waste through a mechano-chemical process / Capuano R., Bonadies I., Castaldo

- R., Cocca M., Gentile G., Protopapa A., Avolio R., Errico M.E. // *Polymers* – 2021. – T. 13 – № 16 – C.2783.
32. Cavalieri F. Development of composite materials by mechanochemical treatment of post-consumer plastic waste / Cavalieri F., Padella F. // *Waste management* – 2002. – T. 22 – № 8 – C.913–916.
33. Baheti V. Ball milling of jute fibre wastes to prepare nanocellulose / Baheti V., Abbasi R., Militky J. // *World Journal of Engineering* – 2012. – T. 9 – № 1 – C.45–50.
34. Mottillo C. Advances in Solid-State Transformations of Coordination Bonds: From the Ball Mill to the Aging Chamber / Mottillo C., Friščić T. // *Molecules* – 2017. – T. 22 – № 1 – C.144.
35. Rubin Pedrazzo A. Mechanochemical synthesis of  $\beta$ -Cyclodextrin Polymers Based on Natural Deep Eutectic Solvents / Rubin Pedrazzo A., Cecone C., Trotta F., Zanetti M. // *ACS Sustainable Chemistry & Engineering* – 2021. – T. 9 – № 44 – C.14881–14889.
36. Cho H.Y. Atom Transfer Radical Polymerization in the Solid-State / Cho H.Y., Bielawski C.W. // *Angewandte Chemie* – 2020. – T. 132 – № 33 – C.14033–14039.
37. Yoo K. Mechanochemical solid-state vinyl polymerization with anionic initiator / Yoo K., Lee G.S., Lee H.W., Kim B.-S., Kim J.G. // *Faraday Discussions* – 2023. – T. 241 – C.413–424.
38. Vogt C.G. Direct mechanocatalysis: palladium as milling media and catalyst in the mechanochemical Suzuki polymerization / Vogt C.G., Grätz S., Lukin S., Halasz I., Etter M., Evans J.D., Borchardt L. // *Angewandte Chemie International Edition* – 2019. – T. 58 – № 52 – C.18942–18947.
39. Grätz S. Mechanochemical Suzuki polycondensation—from linear to hyperbranched polyphenylenes / Grätz S., Wolfrum B., Borchardt L. // *Green chemistry* – 2017. – T. 19 – № 13 – C.2973–2979.
40. Nirmani L.P.T. Mechanochemical Suzuki polymerization for the synthesis of polyfluorenes / Nirmani L.P.T., Pary F.F., Nelson T.L. // *Green Chemistry Letters and Reviews* – 2022. – T. 15 – № 4 – C.863–868.
41. Abhari A.R. Synthesis and characterization of surface-modified PVC/NanoClay/Tween60 as a super hydrophilic membrane: application in the

- nanofiltration of organic dyes from aqueous solution / Abhari A.R., Abhari F.M., Jannat B., Mahmoodi Z., Farrokhzadeh S. // *Polymer Bulletin* – 2021. – C.1–23.
42. Al-Ani F.H. Experimental investigation of the effect of implanting tio<sub>2</sub>-nps on pvc for long-term uf membrane performance to treat refinery wastewater / Al-Ani F.H., Alsahy Q.F., Raheem R.S., Rashid K.T., Figoli A. // *Membranes* – 2020. – T. 10 – № 4 – C.77.
43. Skórczewska K. Modification of Poly (vinyl chloride) with Bio-Based Cassia Oil to Improve Thermo-Mechanical and Antimicrobial Properties / Skórczewska K., Szulc J., Lewandowski K., Ligocka A., Wilczewski S. // *Materials* – 2023. – T. 16 – № 7 – C.2698.
44. Liu Jinying In-situ modified PVC resin and application thereof in waterproof roll / Liu Jinying – 2020.
45. Rabie S.T. Synthesis and characterization of functionalized modified PVC-chitosan as antimicrobial polymeric biomaterial / Rabie S.T., Abdel-Monem R.A., Darwesh O.M., Gaballah S.T. // *Polymer Bulletin* – 2023. – T. 80 – № 8 – C.8899–8918.
46. Beveridge J.M. Covalent functionalization of flexible polyvinyl chloride tubing / Beveridge J.M., Chenot H.M., Crich A., Jacob A., Finn M.G. // *Langmuir* – 2018. – T. 34 – № 35 – C.10407–10412.
47. Mao C. A photochemical method for the surface modification of poly(vinyl chloride) with O-butyrylchitosan to improve blood compatibility / Mao C., Zhao W.B., Zhu A.P., Shen J., Lin S.C. // *Process Biochemistry* – 2004. – T. 39 – № 9 – C.1151–1157.
48. Balakrishnan B. Chemical modification of poly (vinyl chloride) using poly (ethylene glycol) to improve blood compatibility / Balakrishnan B., Jayakrishnan A. // *Trends in Biomaterials and Artificial Organs* – 2005. – T. 18 – № 2 – C.230–236.
49. Ahamed I.S. Synthesis and characterization of some polymers for removing of some heavy metal ions of industrial wastewater / Ahamed I.S., Ghonaim A.K., Abdel Hakim A.A., Moustafa M.M., KAMAL E. // *J. Appl. Sci. Res* – 2008. – T. 4 – № 12 – C.1946–1958.
50. Dong F. Knoevenagel condensation catalysed by poly(vinyl chloride) supported tetraethylenepentamine (PVC-TEPA) / Dong F., Li Y.Q., Dai R.F. // *Chinese Chemical Letters* – 2007. – T. 18 – № 3 – C.266–268.

51. Tiemblo P. The gas transport properties of PVC functionalized with mercapto pyridine groups / Tiemblo P., Guzman J., Riande E., Mijangos C., Reinecke H. // *Macromolecules* – 2002. – T. 35 – № 2 – C.420–424.
52. Duvall T.C. Synergistic blend of a metal-based stabilizer or lewis acid and a free mercaptan for enhanced pvc stabilization // – 2002.
53. AISUENI, F.A., OGUON, E., HASHIM, I. and GOBINA E. Characterization and evaluation of nanoparticles ceramic membrane for the separation of oil-in- water emulsion . , 2021. – 17–26c.
54. Awad E.S. Membrane techniques for removal of detergents and petroleum products from carwash effluents: a review // *Chim. Techno Acta.* – 2023. – T. 10. – № 1. – 1–12c.
55. Wenten I.G. MEMBRANE IN WATER AND WASTEWATER TREATMENT , 2008.
56. Pronk W. Gravity-driven membrane filtration for water and wastewater treatment: a review / Pronk W., Ding A., Morgenroth E., Derlon N., Desmond P., Burkhardt M., Wu B., Fane A.G. // *Water research* – 2019. – T. 149 – C.553–565.
57. Bopape M.F. Numerical modelling assisted design of a compact ultrafiltration (UF) flat sheet membrane module / Bopape M.F., Geel T. Van, Dutta A., Bruggen B. Van der, Onyango M.S. // *Membranes* – 2021. – T. 11 – № 1 – C.54.
58. Richardson J.F. Coulson and Richardson's chemical engineering: Particle technology and separation processes / J. F. Richardson, J. H. Harker, J. R. Backhurst – Butterworth-Heinemann, 2002.
59. Nazif A. Effective parameters on fabrication and modification of braid hollow fiber membranes: A review / Nazif A., Karkhanechi H., Saljoughi E., Mousavi S.M., Matsuyama H. // *Membranes* – 2021. – T. 11 – № 11 – C.1–29.
60. Awad E.S. A mini-review of enhancing ultrafiltration membranes (Uf) for wastewater treatment: Performance and stability / Awad E.S., Sabirova T.M., Tretyakova N.A., Alsahy Q.F., Figoli A., Salih I.K. // *ChemEngineering* – 2021. – T. 5 – № 3.
61. Leos J.Z. Microfiltration and ultrafiltration: principles and applications / J. Z. Leos, A. L. Zydney – New York: Routledge, 2017. Вып. 1st Editio.
62. Jin L. Comparison of fouling characteristics in different pore-sized submerged

ceramic membrane bioreactors / Jin L., Ong S.L., Ng H.Y. // *Water research* – 2010. – T. 44 – № 20 – C.5907–5918.

63. Abuhabib A.A. Nanofiltration membrane modification by UV grafting for salt rejection and fouling resistance improvement for brackish water desalination / Abuhabib A.A., Mohammad A.W., Hilal N., Rahman R.A., Shafie A.H. // *Desalination* – 2012. – T. 295 – C.16–25.

64. Qu X. Applications of nanotechnology in water and wastewater treatment / Qu X., Alvarez P.J.J., Li Q. // *Water research* – 2013. – T. 47 – № 12 – C.3931–3946.

65. Gao B. Studies on adsorption property of novel composite adsorption material PEI/SiO<sub>2</sub> for uric acid / Gao B., Jiang P., Lei H. // *Materials Letters* – 2006. – T. 60 – № 28 – C.3398–3404.

66. Lalia B.S. A review on membrane fabrication: Structure, properties and performance relationship / Lalia B.S., Kochkodan V., Hashaiekh R., Hilal N. // *Desalination* – 2013. – T. 326 – C.77–95.

67. Zahid M. A comprehensive review on polymeric nano-composite membranes for water treatment / Zahid M., Rashid A., Akram S., Rehan Z.A., Razzaq W. // *J. Membr. Sci. Technol* – 2018. – T. 8 – № 1 – C.1–20.

68. Jung J.T. Understanding the non-solvent induced phase separation (NIPS) effect during the fabrication of microporous PVDF membranes via thermally induced phase separation (TIPS) / Jung J.T., Kim J.F., Wang H.H., Nicolo E. Di, Drioli E., Lee Y.M. // *Journal of Membrane Science* – 2016. – T. 514 – C.250–263.

69. Hashim N.H. Pollutants characterization of car wash wastewater / Hashim N.H., Zayadi N. // *MATEC Web of Conferences* – 2016. – T. 47 – C.4–9.

70. Chukwu, O., Segi, S., & Adeoye P.A. Effect of Car-wash effluent on the Quality of Receiving Stream / Chukwu, O., Segi, S., & Adeoye P.A. // *Journal of Engineering and Applied Sciences* – 2008. – T. 3 – № 7 – C.607–610.

71. Zaneti R.N. Car wash wastewater treatment and water reuse—a case study / Zaneti R.N., Etchepare R., Rubio J. // *Water science and technology* – 2013. – T. 67 – № 1 – C.82–88.

72. Nekoo S.H. Experimental study and adsorption modeling of COD reduction by

- activated carbon for wastewater treatment of oil refinery / Nekoo S.H., Fatemi S. // *Iranian Journal of Chemistry and Chemical Engineering (IJCCE)* – 2013. – T. 32 – № 3 – C.81–89.
73. Rai R. Assessment of environmental impacts of vehicle wash centres at Olakha , Thimphu Bhutan / Rai R., Sharma S., Gurung D.B., Sitaula B.K., Raut N. // *International Research Journal of Environmental Sciences* – 2018. – T. 7 – № 1 – C.1–10.
74. Sasi Kumar N. Treatment of car washing unit wastewater—a review / Sasi Kumar N., Chauhan M.S. // *Water Quality Management* – 2018. – C.247–255.
75. Janik H. Trends in modern car washing / Janik H., Kupiec A. // *Polish Journal of Environmental Studies* – 2007. – T. 16 – № 6 – C.927–931.
76. Zaneti R. Car wash wastewater reclamation. Full-scale application and upcoming features / Zaneti R., Etchepare R., Rubio J. // *Resources, Conservation and Recycling* – 2011. – T. 55 – № 11 – C.953–959.
77. Bruggen B. Der Van Industrial process water recycling: Principles and examples / Bruggen B. Der Van, Boussu K., Vreese I. De, Baelen G. Van, Willemse F., Goedemé D., Colen W. // *Environmental Progress* – 2005. – T. 24 – № 4 – C.417–425.
78. Boussu K. Technical and economical evaluation of water recycling in the carwash industry with membrane processes / Boussu K., Baelen G. Van, Colen W., Eelen D., Vanassche S., Vandecasteele C., Bruggen B. Van Der // *Water Science and Technology* – 2008. – T. 57 – № 7 – C.1131–1135.
79. Boussu K. Applicability of nanofiltration in the carwash industry / Boussu K., Kindts C., Vandecasteele C., Bruggen B. Van der // *Separation and Purification Technology* – 2007. – T. 54 – № 2 – C.139–146.
80. Istirokhatun T. Treatment of car wash wastewater by UF membranes / Istirokhatun T., Destianti P., Hargianintya A., Oktiawan W., Susanto H. // *AIP Conference Proceedings* – 2015. – T. 1699.
81. Lau W.J. Car wash industry in Malaysia: Treatment of car wash effluent using ultrafiltration and nanofiltration membranes / Lau W.J., Ismail A.F., Firdaus S. // *Separation and Purification Technology* – 2013. – T. 104 – C.26–31.
82. Uçar D. Membrane processes for the reuse of car washing wastewater / Uçar D. //



Journal of Water Reuse and Desalination – 2018. – T. 8 – № 2 – C.169–175.

83. Sadiq A.J. Comparative study of embedded functionalised MWCNTs and GO in Ultrafiltration (UF) PVC membrane: interaction mechanisms and performance / Sadiq A.J., Awad E.S., Shabeeb K.M., Khalil B.I., Al-Jubouri S.M., Sabirova T.M., Tretyakova N.A., Majdi H.S., Alsahy Q.F., Braihi A.J. // International Journal of Environmental Analytical Chemistry – 2020. – T. 00 – № 00 – C.1–22.

84. Kiran S.A. Influence of bentonite in polymer membranes for effective treatment of car wash effluent to protect the ecosystem / Kiran S.A., Arthanareeswaran G., Thuyavan Y.L., Ismail A.F. // Ecotoxicology and Environmental Safety – 2015. – T. 121 – C.186–192.

85. Kamelian F.S. Preparation of acrylonitrile-butadiene-styrene membrane: Investigation of solvent/nonsolvent type and additive concentration / Kamelian F.S., Mousavi S.M., Ahmadpour A., Ghaffarian V. // Korean Journal of Chemical Engineering – 2014. – T. 31 – № 8 – C.1399–1404.

86. Ermakova T.G. Modification of poly(vinyl chloride) with sodium salts of triazoles / Ermakova T.G., Kuznetsova N.P., Prozorova G.F., Arbuzov A.B., Talzi V.P., Kryazhev Y.G., Likholobov V.A. // Doklady Chemistry – 2017. – T. 474 – № 1 – C.109–112.

87. Baklykov A. V Method of determination of 5-methyl-6-nitro-7-oxo-1, 2, 4-triazolo [1, 5-a] pyrimidinide l-argininy-the active component of drug «triazid» by hplc method / Baklykov A. V, Tumashov A.A., Kotovskaya S.K., Ulomsky E.N., Rusinov G.L., Rusinov V.L., Artem'ev G.A., Kopchuk D.S., Charushin V.N. // Drug development & registration – 2018. – № 2 – C.78–83.

88. Rusinov V.L. Synthesis and Evaluation of Novel [1,2,4]Triazolo[5,1- c ][1,2,4]-triazines and Pyrazolo[5,1- c ][1,2,4]triazines as Potential Antidiabetic Agents / Rusinov V.L., Sapozhnikova I.M., Bliznik A.M., Chupakhin O.N., Charushin V.N., Spasov A.A., Vassiliev P.M., Kuznetsova V.A., Rashchenko A.I., Babkov D.A. // Archiv der Pharmazie – 2017. – T. 350 – № 5.

89. Azam M.A. Biological Activities of 2-Mercaptobenzothiazole Derivatives: A Review / Azam M.A. // Scientia Pharmaceutica – 2012. – T. 80 – № 4 – C.789–823.

90. Weidman J.R. The Use of Iptycenes in Rational Macromolecular Design for Gas

Separation Membrane Applications / Weidman J.R., Guo R. // *Industrial & Engineering Chemistry Research* – 2017. – T. 56 – № 15 – C.4220–4236.

91. Association A.P.H. Standard methods for the examination of water and wastewater. 22nd / Association A.P.H. // Washington, DC: American Public Health Association – 2012.

92. Lu K.-J. Novel PVDF membranes comprising n-butylamine functionalized graphene oxide for direct contact membrane distillation / Lu K.-J., Zuo J., Chung T.-S. // *Journal of Membrane Science* – 2017. – T. 539 – C.34–42.

93. Gayatri R. Preparation and Characterization of PVDF–TiO<sub>2</sub> Mixed-Matrix Membrane with PVP and PEG as Pore-Forming Agents for BSA Rejection / Gayatri R., Fizal A.N.S., Yuliwati E., Hossain M.S., Jaafar J., Zulkifli M., Taweepreda W., Ahmad Yahaya A.N. // *Nanomaterials* – 2023. – T. 13 – № 6 – C.1023.

94. Bhran A. Preparation of PVC/PVP composite polymer membranes via phase inversion process for water treatment purposes / Bhran A., Shoaib A., Elsadeq D., Elgendi A., Abdallah H. // *Chinese Journal of Chemical Engineering* – 2018. – T. 26 – № 4 – C.715–722.

95. Bagheripour E. Novel nanofiltration membrane with low concentration of polyvinylchloride: Investigation of solvents' mixing ratio effect (Dimethyl acetamide/Tetrahydrofuran) / Bagheripour E., Moghadassi A.R., Hosseini S.M. // *Arabian Journal of Chemistry* – 2017. – T. 10 – C.S3375–S3380.

96. Stanley R. Effect of Surfactants on the Wet Chemical Synthesis of Silica Nanoparticles / Stanley R., Nesaraj a S. – 2014. – № October 2013 – C.9–21.

97. A. K. Ghosh Carbon based Nanofillers Embedded Fouling Resistant Polyvinyl Chloride Nanocomposite Membranes for Oil-water Separation / A. K. Ghosh, S. Mamtani V., A. K. Adak // *International Journal of Scientific Research in Science, Engineering and Technology* – 2023. – C.394–398.

98. Elfiky A.A.E.A. Novel nanofiltration membrane modified by metal oxide nanocomposite for dyes removal from wastewater / Elfiky A.A.E.A., Mubarak M.F., Keshawy M., Sayed I.E.T. El, Moghny T.A. // *Environment, Development and Sustainability* – 2023.

99. Al-Ani D.M. Preparation and characterization of ultrafiltration membranes from PPSU-PES polymer blend for dye removal / Al-Ani D.M., Al-Ani F.H., Alsahy Q.F., Ibrahim S.S. // *Chemical Engineering Communications* – 2021. – T. 208 – № 1 – C.41–59.
100. Belmont J.A. Porous membrane having a fluorinated copolymer as surface treatment // – 2021.
101. Xu Z. Organosilane-functionalized graphene oxide for enhanced antifouling and mechanical properties of polyvinylidene fluoride ultrafiltration membranes / Xu Z., Zhang J., Shan M., Li Y., Li B., Niu J., Zhou B., Qian X. // *Journal of Membrane Science* – 2014. – T. 458 – C.1–13.
102. Alsahy Q.F. Poly (vinyl chloride) hollow-fiber membranes for ultrafiltration applications: Effects of the internal coagulant composition / Alsahy Q.F., Rashid K.T., Noori W.A., Simone S., Figoli A., Drioli E. // *Journal of applied polymer science* – 2012. – T. 124 – № 3 – C.2087–2099.
103. Saljoughi E. Effect of preparation variables on morphology and pure water permeation flux through asymmetric cellulose acetate membranes / Saljoughi E., Sadrzadeh M., Mohammadi T. // *Journal of Membrane Science* – 2009. – T. 326 – № 2 – C.627–634.
104. Antony A. Removal Efficiency and Integrity Monitoring Techniques for Virus Removal by Membrane Processes / Antony A., Blackbeard J., Leslie G. // *Critical Reviews in Environmental Science and Technology* – 2012. – T. 42 – № 9 – C.891–933.
105. Titchou F.E. Removal of organic pollutants from wastewater by advanced oxidation processes and its combination with membrane processes / Titchou F.E., Zazou H., Afanga H., Gaayda J. El, Ait Akbour R., Nidheesh P.V., Hamdani M. // *Chemical Engineering and Processing - Process Intensification* – 2021. – T. 169 – C.108631.
106. Yong M. Properties of polyvinyl chloride (PVC) ultrafiltration membrane improved by lignin: Hydrophilicity and antifouling / Yong M., Zhang Y., Sun S., Liu W. // *Journal of Membrane Science* – 2019. – T. 575 – № September 2018 – C.50–59.
107. Strathmann H. The formation mechanism of phase inversion membranes / Strathmann H., Kock K. // *Desalination* – 1977. – T. 21 – № 3 – C.241–255.

108. Alsahy Q.F. A study of the effect of embedding ZnO-NPs on PVC membrane performance use in actual hospital wastewater treatment by membrane bioreactor / Alsahy Q.F., Al-Ani F.H., Al-Najar A.E., Jabuk S.I.A. // *Chemical Engineering and Processing - Process Intensification* – 2018.
109. Alsahy Q.F. A new Sponge-GAC-Sponge membrane module for submerged membrane bioreactor use in hospital wastewater treatment / Alsahy Q.F., Al-Ani F.H., Al-Najar A.E. // *Biochemical Engineering Journal* – 2018. – T. 133 – C.130–139.
110. Rajesh S. Preparation, morphology, performance, and hydrophilicity studies of poly (amide-imide) incorporated cellulose acetate ultrafiltration membranes / Rajesh S., Shobana K.H., Anitharaj S., Mohan D.R. // *Industrial & Engineering Chemistry Research* – 2011. – T. 50 – № 9 – C.5550–5564.
111. Bakeri G. Effect of polymer concentration on the structure and performance of polyetherimide hollow fiber membranes / Bakeri G., Ismail A.F., Shariaty-Niassar M., Matsuura T. // *Journal of membrane science* – 2010. – T. 363 – № 1–2 – C.103–111.
112. Akbari A. Study on the impact of polymer concentration and coagulation bath temperature on the porosity of polyethylene membranes fabricated via TIPS method / Akbari A., Yegani R. // *Journal of Membrane and Separation Technology* – 2012. – T. 1 – № 2 – C.100.
113. Torrestiana-Sanchez B. Effect of nonsolvents on properties of spinning solutions and polyethersulfone hollow fiber ultrafiltration membranes / Torrestiana-Sanchez B., Ortiz-Basurto R.I., Brito-De La Fuente E. // *Journal of Membrane Science* – 1999. – T. 152 – № 1 – C.19–28.
114. Aani S. Al Investigation of UF membranes fouling and potentials as pre-treatment step in desalination and surface water applications / Aani S. Al, Wright C.J., Hilal N. // *Desalination* – 2018. – T. 432 – № December 2017 – C.115–127.
115. Alsahy Q. Hollow fiber ultrafiltration membranes from poly(vinyl chloride): Preparation, morphologies, and properties / Alsahy Q., Algebory S., Alwan G.M., Simone S., Figoli A., Drioli E. // *Separation Science and Technology* – 2011. – T. 46 – № 14 – C.2199–2210.
116. Park H.B. Maximizing the right stuff: The trade-off between membrane permeability

and selectivity / Park H.B., Kamcev J., Robeson L.M., Elimelech M., Freeman B.D. // *Science* – 2017. – T. 356 – № 6343.

117. Mohammed T.J. Effect of settling time, velocity gradient, and camp number on turbidity removal for oilfield produced water / Mohammed T.J., Shakir E. // *Egyptian Journal of Petroleum* – 2018. – T. 27 – № 1 – C.31–36.

118. Tchobanoglous G. Wastewater engineering: treatment and reuse / Tchobanoglous G., Burton F., Stensel H.D. // *American Water Works Association. Journal* – 2003. – T. 95 – № 5 – C.201.

119. Vatanpour V. Highly antifouling polymer-nanoparticle-nanoparticle/polymer hybrid membranes / Vatanpour V., Jouyandeh M., Mousavi Khadem S.S., Paziresh S., Dehqan A., Ganjali M.R., Moradi H., Mirsadeghi S., Badieli A., Munir M.T., Mohaddespour A., Rabiee N., Habibzadeh S., Mashhadzadeh A.H., Nouranian S., Formela K., Saeb M.R. // *Science of The Total Environment* – 2022. – T. 810 – C.152228.

120. Hosseini S.M. Mixed matrix PES-based nanofiltration membrane decorated by (Fe<sub>3</sub>O<sub>4</sub>–polyvinylpyrrolidone) composite nanoparticles with intensified antifouling and separation characteristics / Hosseini S.M., Afshari M., Fazlali A.R., Koudzari Farahani S., Bandehali S., Bruggen B. Van der, Bagheripour E. // *Chemical Engineering Research and Design* – 2019. – T. 147 – C.390–398.

121. Alqaheem Y. Microscopy and Spectroscopy Techniques for Characterization of Polymeric Membranes / Alqaheem Y., Alomair A.A. // *Membranes* – 2020. – T. 10 – № 2 – C.33.

122. Ren H. Preparation of Cross-Sectional Membrane Samples for Scanning Electron Microscopy Characterizations Using a New Frozen Section Technique / Ren H., Zhang X., Li Y., Zhang D., Huang F., Zhang Z. // *Membranes* – 2023. – T. 13 – № 7 – C.634.

123. Cao X. Effect of TiO<sub>2</sub> nanoparticle size on the performance of PVDF membrane / Cao X., Ma J., Shi X., Ren Z. // *Applied Surface Science* – 2006. – T. 253 – № 4 – C.2003–2010.

124. Reddeppa N. AC conduction mechanism and battery discharge characteristics of (PVC/PEO) polyblend films complexed with potassium chloride / Reddeppa N., Sharma A.K., Rao V.V.R.N., Chen W. // *Measurement* – 2014. – T. 47 – C.33–41.

125. Saleh T.A. Synthesis and characterization of alumina nano-particles polyamide membrane with enhanced flux rejection performance / Saleh T.A., Gupta V.K. // Separation and Purification Technology – 2012. – T. 89 – C.245–251.
126. Yu H. Development of a hydrophilic PES ultrafiltration membrane containing SiO<sub>2</sub>@ N-Halamine nanoparticles with both organic antifouling and antibacterial properties / Yu H., Zhang X., Zhang Y., Liu J., Zhang H. // Desalination – 2013. – T. 326 – C.69–76.
127. Yu S. Effect of SiO<sub>2</sub> nanoparticle addition on the characteristics of a new organic–inorganic hybrid membrane / Yu S., Zuo X., Bao R., Xu X., Wang J., Xu J. // Polymer – 2009. – T. 50 – № 2 – C.553–559.
128. Wang H. Novel proton-conductive nanochannel membranes with modified SiO<sub>2</sub> nanospheres for direct methanol fuel cells / Wang H., Li X., Feng X., Liu Y., Kang W., Xu X., Zhuang X., Cheng B. // Journal of Solid State Electrochemistry – 2018. – T. 22 – № 11 – C.3475–3484.
129. Abedini R. A novel cellulose acetate (CA) membrane using TiO<sub>2</sub> nanoparticles: Preparation, characterization and permeation study / Abedini R., Mousavi S.M., Aminzadeh R. // Desalination – 2011. – T. 277 – № 1–3 – C.40–45.
130. Lee C.-W. Membrane roughness as a sensitive parameter reflecting the status of neuronal cells in response to chemical and nanoparticle treatments / Lee C.-W., Jang L.-L., Pan H.-J., Chen Y.-R., Chen C.-C., Lee C.-H. // Journal of Nanobiotechnology – 2016. – T. 14 – № 1 – C.9.
131. Mao Y. Roughness-enhanced hydrophobic graphene oxide membrane for water desalination via membrane distillation / Mao Y., Huang Q., Meng B., Zhou K., Liu G., Gugliuzza A., Drioli E., Jin W. // Journal of Membrane Science – 2020. – T. 611 – C.118364.
132. Kebria M.R.S. SiO<sub>2</sub> modified polyethyleneimine-based nanofiltration membranes for dye removal from aqueous and organic solutions / Kebria M.R.S., Jahanshahi M., Rahimpour A. // Desalination – 2015. – T. 367 – № July 2020 – C.255–264.
133. Zheng Q. Size Effects of Surface Roughness to Superhydrophobicity / Zheng Q., Lü

C. // *Procedia IUTAM* – 2014. – T. 10 – C.462–475.

134. Johnson D. Polymer membranes–Fractal characteristics and determination of roughness scaling exponents / Johnson D., Hilal N. // *Journal of Membrane Science* – 2019. – T. 570 – C.9–22.

135. Darvishmanesh S. Novel polyphenylsulfone membrane for potential use in solvent nanofiltration / Darvishmanesh S., Jansen J.C., Tasselli F., Tocci E., Luis P., Degreève J., Drioli E., Bruggen B. Van der // *Journal of Membrane Science* – 2011. – T. 379 – № 1–2 – C.60–68.

136. Al-timimi D.A.H. Novel polyether sulfone / polyethylenimine grafted nano-silica nanocomposite membranes : Interaction mechanism and ultrafiltration performance / Al-timimi D.A.H., Alsahy Q.F., Abdulrazak A.A., Drioli E. // *Journal of Membrane Science* – 2022. – T. 659 – № May – C.120784.

137. Kosiol P. Determination of pore size distributions of virus filtration membranes using gold nanoparticles and their correlation with virus retention / Kosiol P., Hansmann B., Ulbricht M., Thom V. // *Journal of Membrane Science* – 2017. – T. 533 – C.289–301.

138. Arkhangelsky E. Maximal pore size in UF membranes / Arkhangelsky E., Duek A., Gitis V. // *Journal of Membrane Science* – 2012. – T. 394–395 – C.89–97.

139. Jarma Y.A. Field Evaluation of UF Filtration Pretreatment Impact on RO Membrane Scaling / Jarma Y.A., Thompson J., Khan B.M., Cohen Y. // *Water* – 2023. – T. 15 – № 5 – C.847.

140. Siddique A. Potential use of ultrafiltration (UF) membrane for remediation of metal contaminants Elsevier, 2023. – 341–364c.

141. Zielińska M. Use of Ceramic Membranes in a Membrane Filtration Supported by Coagulation for the Treatment of Dairy Wastewater / Zielińska M., Galik M. // *Water, Air, & Soil Pollution* – 2017. – T. 228 – № 5 – C.173.

## APPENDIX (A)

## IR-Spectra for obtained post modified PVC derivatives

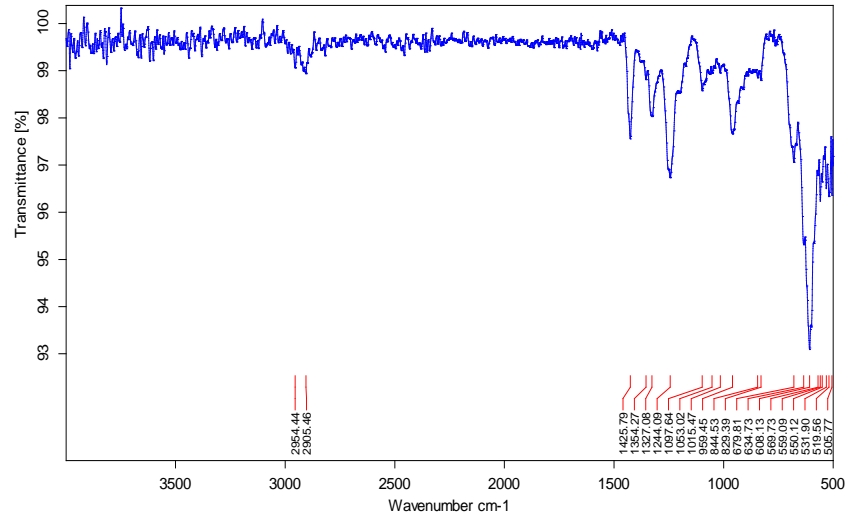


Figure 1 – IR data of PVC 2.1

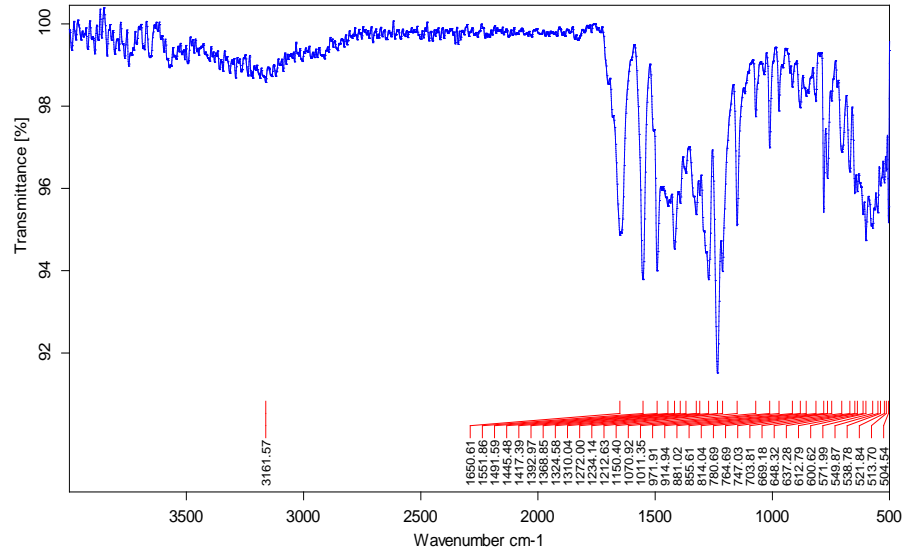


Figure 2 - IR data of polymer 2-9

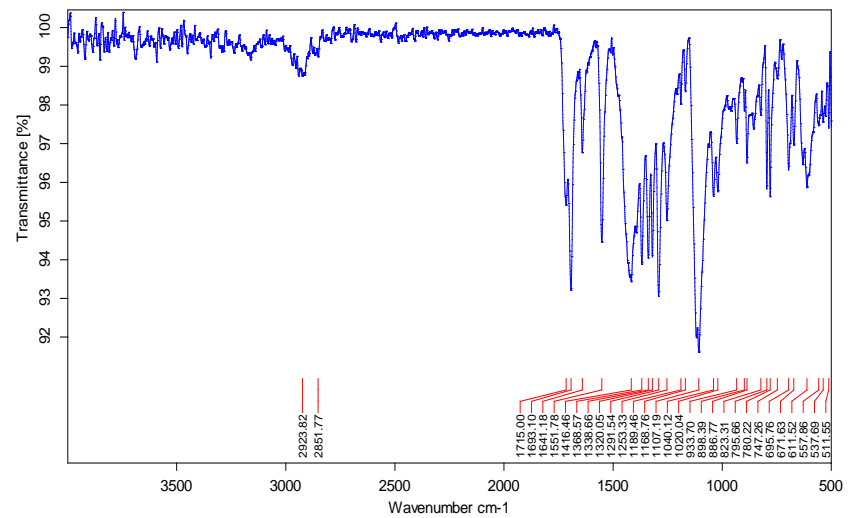


Figure 3 - IR data of polymer 2-10



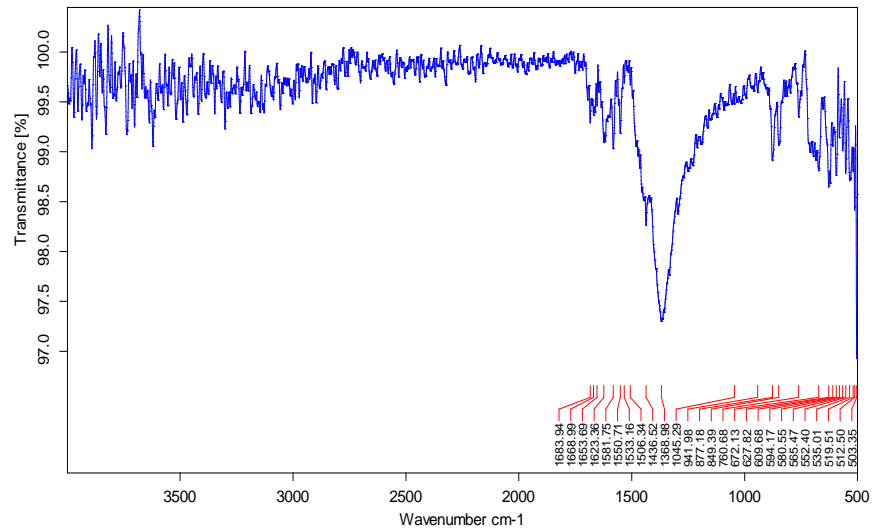


Figure 4 - IR data of polymer 2-12

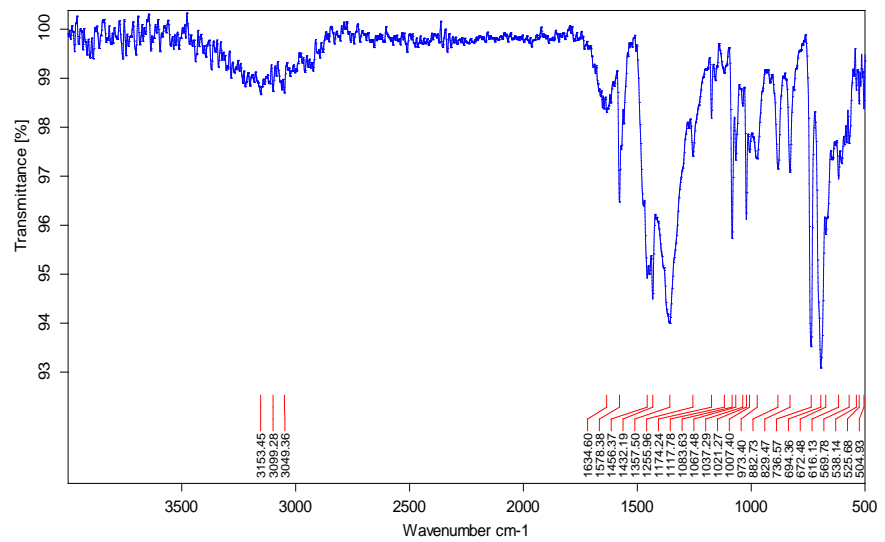


Figure 5 - IR data of polymer 2-23

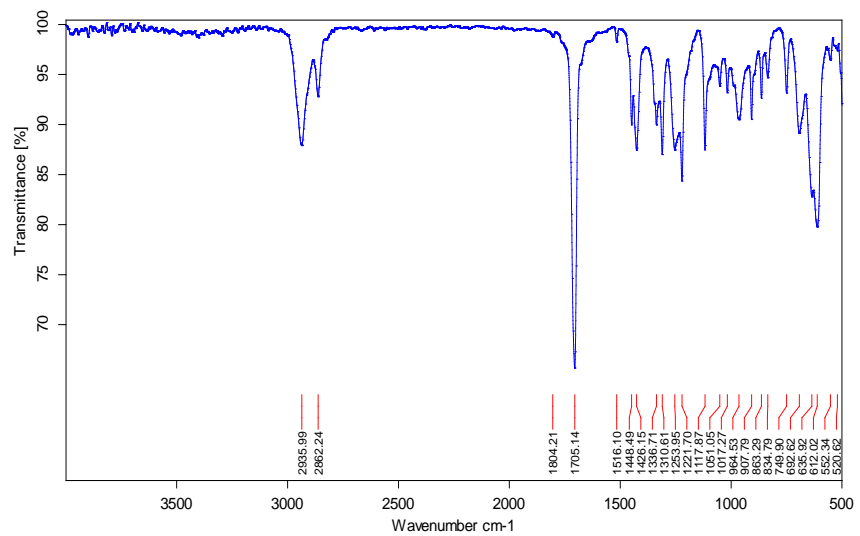


Figure 6 - IR data of polymer 2-24

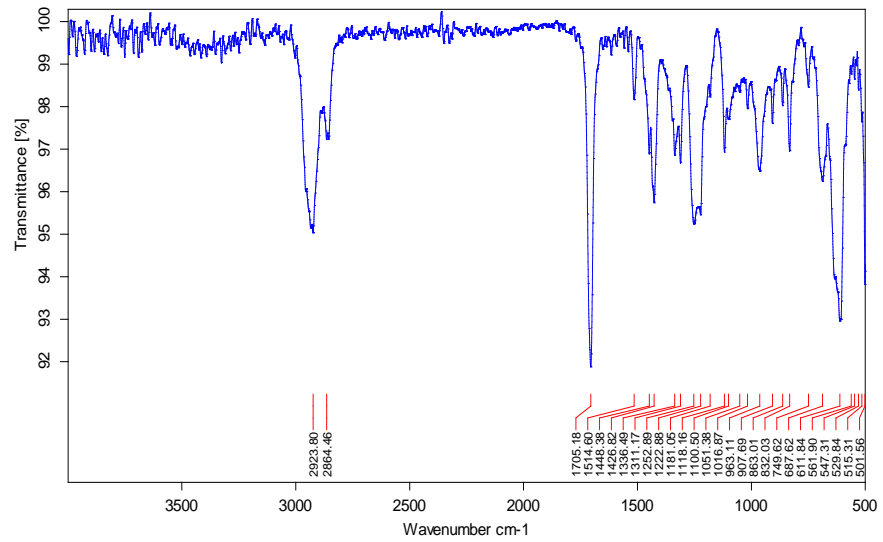


Figure 7 - IR data of polymer 2-25

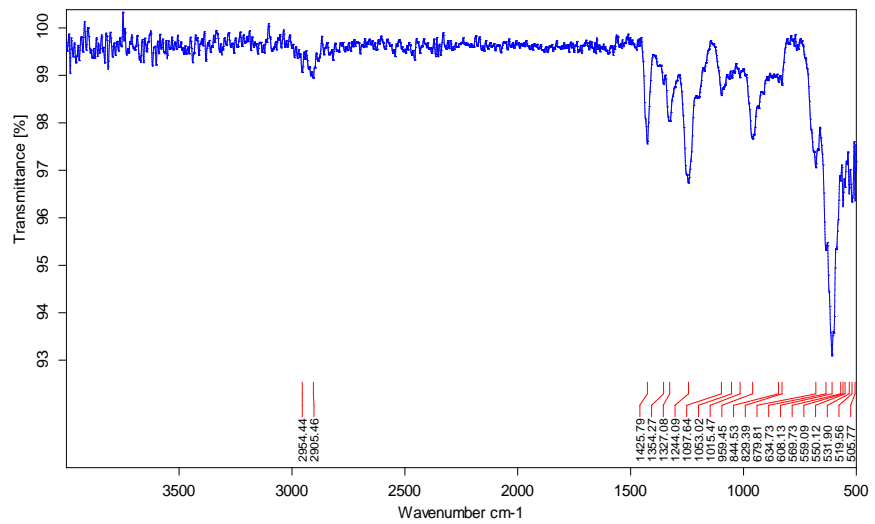


Figure 8 - IR data of polymer 2-26

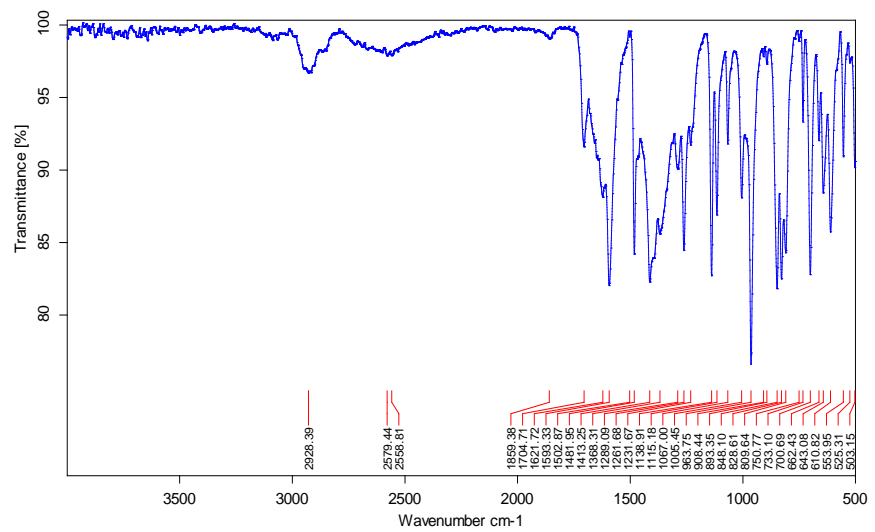


Figure 9 - IR data of polymer 2-27

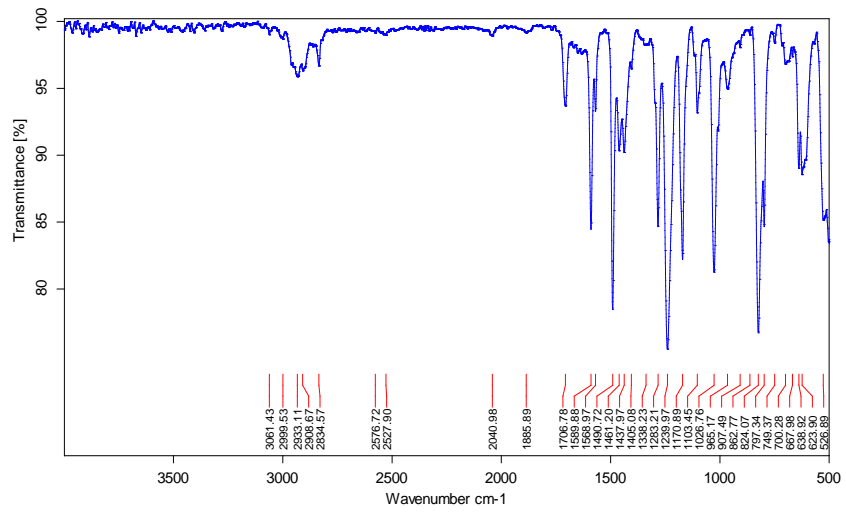


Figure 10 - IR data of polymer 2-28

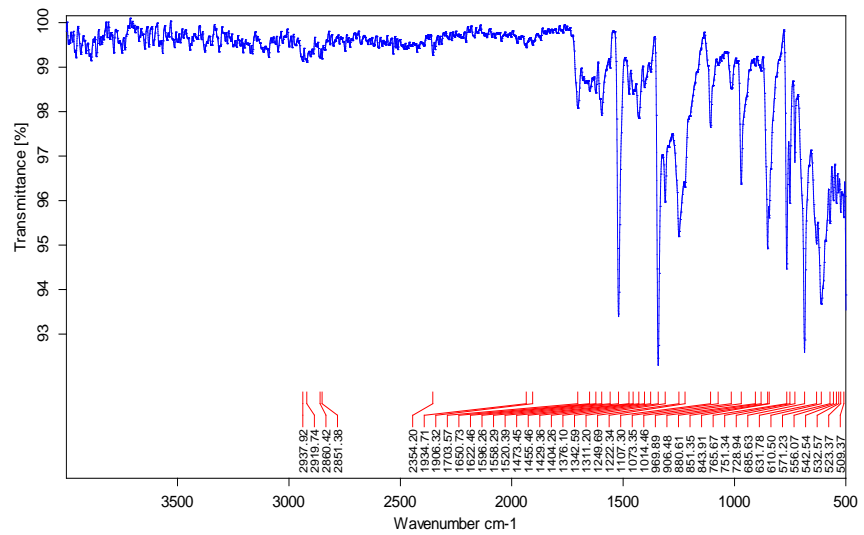


Figure 11 - IR data of polymer 2-32

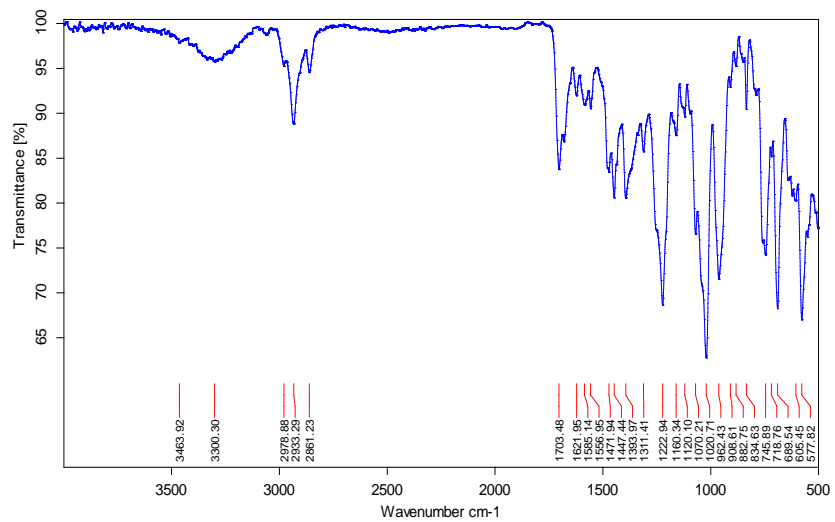


Figure 12 - IR data of polymer 2-35

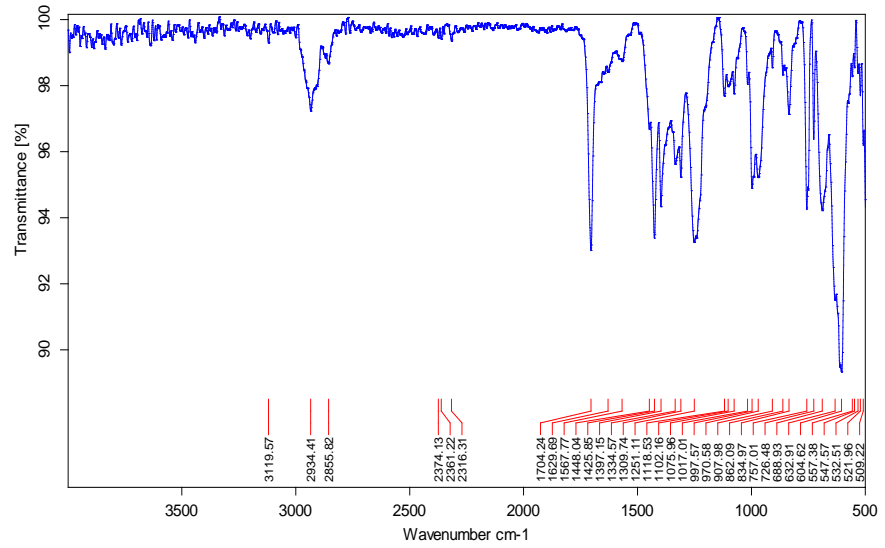


Figure 13 - IR data of polymer 2-39

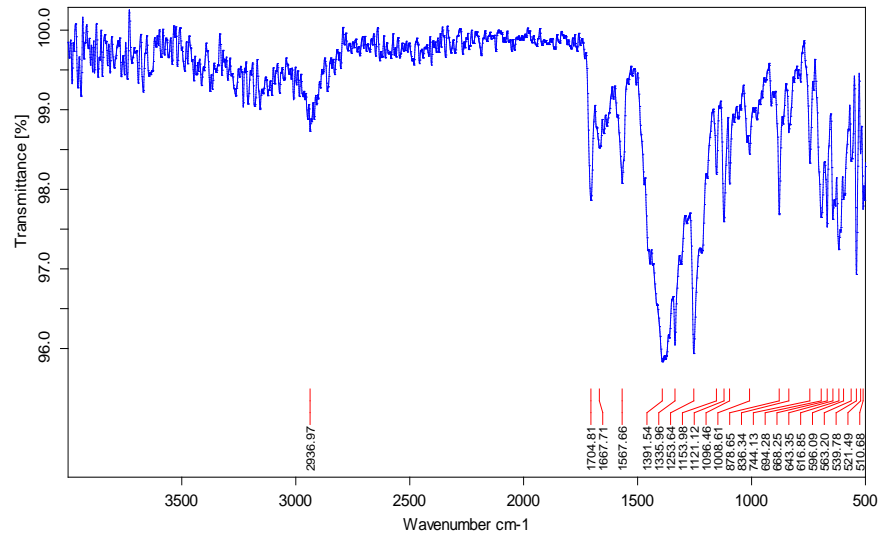


Figure 14 - IR data of polymer 2-41